CO hydrogenation on reduced solid solution catalysts

Rennison, A. J.

Award date:
1987

Awarding institution:
University of Bath

CO HYDROGENATION ON

REDUCED SOLID SOLUTION CATALYSTS

submitted by A.J. Rennison

for the degree of Ph.D. of the

University of Bath

1987

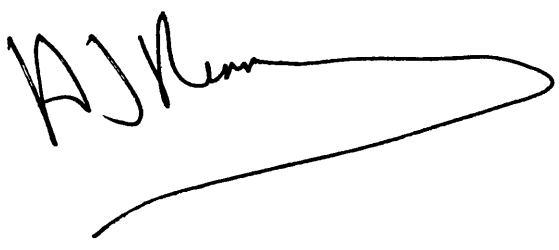

ProQuest LLC
789 East Eisenhower Parkway
P.O. Box 1346
Ann Arbor, MI 48106-1346

To

Marion

Paul

Naomi

Jenny

Simon

MEMORANDUM

The work described in this thesis was conducted in the School of Chemistry at the University of Bath* during the period October 1981 to September 1984 and has not been submitted for any other degree. All the work described is the original work of the author except where specially acknowledged.

* The high pressure work on $Os_3(CO)_{12}$ was carried out at I.C.I. Runcorn during 1982 and 1983.

Acknowledgements

The author would like to thank the following for their assistance and advice during the preparation of this thesis.

Professor F.S. Stone, my supervisor, for his encouragement and advice throughout this work.

Dr R. Sampson, my industrial supervisor, particularly for discussion of the osmium work.

Ms L. Lancaster, for great assistance in the preparation of the final draft.

Mr J. Stainer and Mr M. Lock for technical assistance.

Mr A. Carver for assistance with XRD and AA.

The Science and Engineering Research Council and I.C.I. Plc for a CASE award.

Past members of Lab 4W 0.5 for a happy and relaxed working environment.

SUMMARY

Oxide solid solutions of the NiO-MgO, CoO-MgO and cobalt-spinel types have been prepared in high surface area form and studied in two specially designed and constructed pieces of equipment.

(a) a high vacuum catalysis and chemisorption system;

(b) a 1 atm laboratory flow reactor.

Reduction of the solid solutions in carbon monoxide and/or hydrogen has yielded catalysts which are active in CO hydrogenation. Catalysts consisting of osmium carbonyl have also been prepared and studied for CO hydrogenation activity.

Chemisorption characterization has revealed that whilst the quantities of metal produced by reduction of NiO-MgO or CoO-MgO are very small, cobalt-spinel-derived catalysts contain larger amounts of metal comparable with conventional metal catalysts. This is presumed to be due to the harsh reduction conditions necessarily used with the spinel catalysts.

Selectivity to non-methane products is superior for the cobalt-spinel-derived catalysts but the specific activity (turnover frequency) is very much less than that reported for conventional cobalt catalysts. It was not possible to measure the specific activity of the MgO-based catalysts.

The osmium catalysts studied produced mainly methane at 1 atm but higher hydrocarbons were seen at 10 and 100 atm. Some evidence has been found that the support pre-treatment affects subsequent catalytic activity.

CONTENTS

1. INTRODUCTION

1.1. The Need for Alternative Energy Sources

1.1.1. The Energy Problem

It has been realised for some time that the consumption of crude oil and its products is still rising worldwide, albeit at a slower rate than before the oil crisis of 1973, despite rising costs and a greater awareness of the need to conserve non-renewable energy resources.

It has been estimated[1] that at the rate of consumption prevalent in the early 1970's crude oil reserves would be exhausted by the middle of the next century. Even if the lower rate of consumption seen after the oil crisis is maintained, the most optimistic forecasts would not extend reserves by more than 50 years.

It is difficult to find a substitute for crude oil, because although it is only one of the major energy-providing resources available in the modern world it is used in many different ways. The four major uses are:

(1) as a fuel for transportation;

(2) as a feedstock for the petrochemical industry;

(3) as a source of heat;

(4) electricity generation.

In the two latter cases it would appear to be relatively easy to limit usage by substituting nuclear energy and developing energy conservation technology. However, the need for an alternative to satisfy the former two requirements is overwhelming.

Various processes and technologies have been put forward to satisfy these needs and they fall into two main categories. The first involves the utilization of renewable energy resources derived from living material, i.e. biomass. The second involves the use of oil and petroleum residues such as those found in tar and shale sands and the utilization of substances derived from coal.

1.1.2. Renewable Energy Resources

Renewable energy resources can be used in two distinct ways:

(1) the conversion of organic material to methane, hydrocarbons, alcohols or syngas ($CO + H_2$) using biocatalytic or catalytic processes;

(2) combustion and subsequent generation of electricity.

Both of these processes are important and clearly any technology which employs a renewable raw material is highly desirable. However, both processes are hampered by a raw material which tends to be bulky and can be unhygienic (animal waste to methane).

It seems likely that bio-engineering techniques will play their part in providing a significant contribution to energy and chemical feedstock needs in the future.

1.1.3. Shale and Tar Sands and Petroleum Residues

Petroleum residues left after the refining of crude oil and natural shale and tar sands contain high molecular weight carbon compounds which can be converted

to useful fuels and chemical feedstocks. These materials represent another possible source of energy to supplement crude oil. Relatively large amounts of sulphur-containing species are present in petroleum residues whereas natural oil shales and sands contain significant quantities of nitrogen-containing compounds. The removal of these contaminants by appropriate catalytic reactions complicates their use, but utilization of these substances to produce fuel appears to be viable, especially in those parts of the world where appreciable quantities of shales and oil sands can be found.

1.1.4. Coal

Coal reserves worldwide are about an order of magnitude larger than those of oil. For this reason it is a very important natural resource in the development of alternative energy sources to crude oil.

Wender[2] categorises five different processes by which coal may be treated. These are:

(1) gasification

(2) liquefaction

(3) oxidation

(4) carbonization

(5) production of acetylene (via calcium carbide or using a plasma arc)

Each of these processes is important in producing products of use to the chemical industry; for example, aliphatic alcohols and phenols can be made by the liquefaction of coal and oxidation produces aromatic

acids. However, for the present thesis the process of greatest interest is coal gasification.

The overall reaction of coal gasification can be described as[3]

$$\text{Coal} + O_2 + H_2 \longrightarrow CO + H_2 + CO_2 + CH_4 \qquad (1)$$

After removal of the CO_2 and CH_4 (the quantities of CH_4 and CO_2 can be reduced by increasing the temperature), a mixture of CO and H_2 (syngas) is left which is then used as a feedstock for further reaction. The ratio of CO to H_2 can be altered by means of the water gas shift reaction shown below:

$$CO + H_2O = CO_2 + H_2 \qquad (2)$$

Syngas is used for three main types of reaction; these are methanation, Fischer-Tropsch synthesis and methanol synthesis. All of these reactions involve the use of catalysts.

1.2. Catalysis

The term catalysis was first used by Berzelius in 1836. It was said to occur if a chemical process is speeded up by entities which ideally are not themselves consumed.[4]

Catalysis allows a chemical process to proceed via a route of lower activation energy than is otherwise possible. Many reactions, although thermodynamically possible, will not proceed at any measurable rate without the aid of catalysts.

Catalysis can be divided into two major types:

(1) heterogeneous catalysis, where the catalyst is present in a different phase from the reactant molecules;

(2) homogeneous catalysis, where the catalyst is in the same phase as the reactant molecules.

Although the chief reaction of interest in this work (CO hydrogenation to hydrocarbons) can be homogeneously catalysed, in this thesis only heterogeneous catalysis where the catalyst is in the solid phase and the reactants initially in the gas phase will be considered.

1.3. Methanation

Methanation, the reaction of oxides of carbon to methane using heterogeneous catalysis, is a reaction of considerable industrial importance, for example in the production of substitute natural gas (SNG).[5] The overall process is described by the equation:

$$CO + 3H_2 = CH_4 + H_2O \qquad (3)$$

although other stoichiometries are possible under certain circumstances. Over a wide range of temperature the thermodynamics of the above reaction are favourable.[6]

Nickel is the catalyst which is most often cited as a good methanation catalyst as under most operating conditions it produces very small amounts of C_2 and higher products. Typical operating conditions for a commercial nickel methanation catalyst are 523 - 723 K

and 1 - 7 MPa. Many catalyst systems based on nickel have been investigated and described in the literature.[7-12]

The mechanism of the reaction of CO and hydrogen to methane has received less attention than the reaction to higher hydrocarbons (the Fischer-Tropsch synthesis) but much of the work which has been carried out is relevant to both types of reaction.

An early theory put forward for hydrocarbon synthesis by Fischer and Tropsch[13] has also been used to explain methanation. They proposed that CO was adsorbed and reduced to carbide. This carbide was then considered to be hydrogenated to methylene groups, followed by further hydrogenation of the methylene groups to methane. The carbide theory was subsequently modified by various workers, including Craxford and Rideal[14,15] who refined the theory to refer to a surface carbide being involved rather than the bulk carbide proposed by Fischer and Tropsch. This mechanism[16] is shown schematically in Scheme 1.

This theory lost popularity because it failed to explain various aspects of product selectivity in Fischer-Tropsch synthesis, in particular the type of branching observed experimentally and the formation of oxygenated products.[17]

Various other mechanisms have been proposed. The following account, although not exhaustive, indicates most of the mechanistic features described in

Scheme 1

The Carbide Theory of Methanation [14,16]

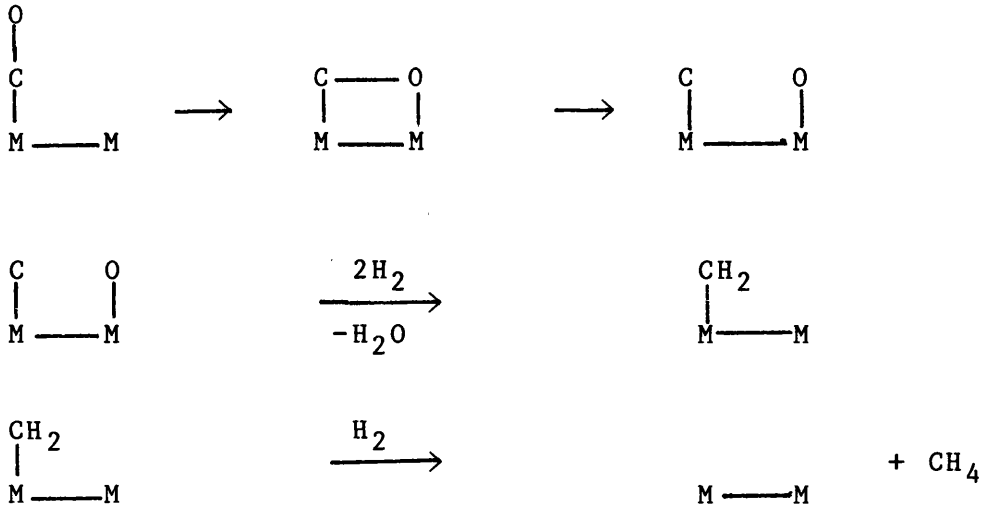

the literature.

Vlasenko, Rusov and Kozub[18] proposed a mechanism involving an adsorbed $[H_2]^-$ anion and an adsorbed $[CO]^+$ cation. The basic steps are shown in Scheme 2.

Scheme 2

Mechanism of Methanation Proposed by Vlasenko et al

$$M + e^- + H_2 \longrightarrow [\,M\text{-}H_2\,]^-$$

$$M + CO \longrightarrow [\,M\text{-}CO\,]^+ + e^-$$

$$[\,M\text{-}CO\,]^+ + [\,M\text{-}H_2\,]^- \longrightarrow [\,M\text{-}HCOH\,]^+ + e^- + M \quad \text{(RDS)}$$

$$[\,M\text{-}HCOH\,]^+ + [\,M\text{-}H_2\,]^- \longrightarrow M\text{-}CH_2 + H_2O + M$$

$$M\text{-}CH_2 + [\,M\text{-}H_2\,]^- \longrightarrow CH_4 + e^- + 2M$$

M represents a vacant metal site

Vannice[7] raises objections to this scheme on the grounds that for catalysis by iron the charges shown for the adsorbed CO and H_2 species are the opposite of those

normally assumed to exist[19] on Fe surfaces.

Mechanisms have also been proposed which involve an H_2CO adsorbed species,[20,21] and the one proposed by Vannice shown in Scheme 3 is typical.

Scheme 3

Mechanism of Methanation Proposed by Vannice[21]

$$H_2(g) + CO(g) \longrightarrow H_2CO_{(ads)}$$

$$H_2CO_{(ads)} + y/2\ H_{2(ads)} \longrightarrow CH_{y(ads)} + H_2O \quad \text{(RDS)}$$

$$CH_{y(ads)} + H_{2(ads)} \longrightarrow CH_4$$

RDS = rate determining step

The first step is an overall representation of the combination of initially gas phase H_2 and CO to adsorbed H_2CO and is presumed to occur via $H_{2(ads)}$ and $CO_{(ads)}$ species. Vannice developed his idea with a mathematical derivation of rate equations which he correlated with the standard form of power rate law shown below.

$$N(CH_4) = A(\exp -E_a/RT)\ [p_H]^x\ [p_{CO}]^y \qquad (4)$$

where

$N(CH_4)$ is the turnover frequency for methanation, A the pre-exponential factor, E_a the apparent activation energy, p_H the partial pressure of molecular hydrogen, p_{CO} the partial pressure of CO and x,y are experimentally derived numbers.

From a comparison of calculated and experimental values Vannice concluded that the CO bond-breaking in the CHOH adsorbed species is the rate determining step (Scheme 3) and the number of hydrogen atoms involved in

this step lies between 1 and 4 for the Group VIII metals.

Other mechanisms have been proposed,[22,23] although often they were primarily designed to explain the formation of higher carbon number products and will be discussed in a later section. In nearly all cases a CHOH adsorbed species is proposed and it is the subsequent breaking of the C-O bond which leads to methane formation.

Recently, more information about the nature of the adsorption of CO on Group VIII metals has been described in the literature[24,25] and clear evidence of the dissociation of the molecule is seen at temperatures greater than about 350 K. The situation has been reviewed by Ponec[26] who concluded that at temperatures of interest in methanation and Fischer-Tropsch synthesis, "CO can always be adsorbed and dissociated on the metal surface" (in this case nickel). Ponec concludes that, when considering methanation, surface adsorbed carbon is heavily involved. He cites evidence for this from ^{13}C studies carried out with Araki[27] which showed that when ^{13}C carbon was deposited on a nickel surface and then after evacuation $^{12}C/H_2$ was admitted, the catalyst initially produced methane containing ^{13}C at a greater rate than it produced ^{12}C containing methane. This was taken to imply that a mechanism similar to that proposed by Fischer involving an adsorbed carbon species was dominant and that the adsorbed CHOH species could only be of secondary

importance in methanation. Other work on the chemisorption of CO and hydrogen includes that of Wedler, Papp and Schroll,[28] who found evidence for the interaction of CO and hydrogen on surfaces by observing an increase in the heat of adsorption of hydrogen when CO was present. However, they could not find any direct evidence for a CHOH type complex, whereas Palazov, Kadinov, Bonev and Shopov[29] have obtained evidence for CO-hydrogen surface complexes of various stoichiometries based on IR reflectance studies.

Before leaving this topic it is important to note that the adsorption of hydrogen on most metallic surfaces is now generally considered to be activated. Bartholomew and Zowtiak[30] have carried out a comprehensive investigation and found that the activation energy for adsorption varied depending on the support used and the loading of the catalyst. This is relevant when using hydrogen to measure metal surface areas (see Section 4).

Many workers have measured kinetic parameters, but the study due to Vannice[31] of the Group VIII metals is probably the most comprehensive. Apparent activation energies were measured and fell into the range 70-115 kJ mol^{-1}, the lowest value being due to Pt and the largest due to Co. The dependence of the rate of reaction on the partial pressure of hydrogen (x in Equation 4) was in the range 0.77-1.60, the highest value being for Ru and the lowest for Ni. The corresponding CO dependent values (y in Equation 4)

ranged from -0.6 for Ru to +0.1 for Ir.

Turnover frequencies were in the range $2 - 200 \times 10^{-3}\ s^{-1}$, the order of activity being Ru > Fe> Ni > Co > Rh > Pd > Pt > Ir.

By comparison Reuel and Bartholomew[32] obtained values between 137 and 295 kJ mol^{-1} as the apparent activation energy for methanation over Co/Al_2O_3 catalysts of various loadings. They found turnover frequencies to be in the range $0.8 - 8 \times 10^{-3}\ s^{-1}$.

Many of the points raised concerning methanation also apply to the Fischer-Tropsch synthesis and this process will now be reviewed.

1.4. The Fischer-Tropsch Synthesis

1.4.1. Thermodynamics

When a syngas ($CO + H_2$) mixture is passed over a catalyst to produce hydrocarbons of C_2 and above the process is referred to as the Fischer-Tropsch synthesis. The name also covers the formation of oxygenated products such as alcohols. Typical reactions are:

$$nCO + (2n+1)H_2 \longrightarrow C_nH_{2n+2} + nH_2O \quad n>1 \quad (5)$$

$$nCO + 2nH_2 \longrightarrow C_nH_{2n} + nH_2O \quad n>1 \quad (6)$$

$$nCO + mH_2 \longrightarrow C_n\text{-oxygenates} \quad n>1 \quad (7)$$

although by incorporating the water gas shift reaction CO_2 can be shown as the by-product rather than water. This is relevant for those catalysts which facilitate this reaction.

The Fischer-Tropsch reaction has been of great commercial interest over many years. During World

War 2, Germany produced a large percentage of its petroleum requirements from operating Fischer-Tropsch plants. More recently, South Africa, a country where coal reserves are relatively large, has operated its SASOL plants to manufacture synthetic petroleum and a range of other products for the petrochemical industry.

Fig. 1.1 shows the free energy of formation of methane and higher hydrocarbons and is taken from a review by Denny and Whan.[6]

As can be seen the free energy of formation of CH_4 is negative up to about 900 K whereas the free energies of formation of all the other hydrocarbons are positive at this temperature. For this reason as the temperature is increased methane becomes the thermodynamically favoured product, lower temperatures tending to favour the production of C_2 and higher hydrocarbons.

Figure 1.1

Free Energy of Formation of CH_4 and Higher Hydrocarbons

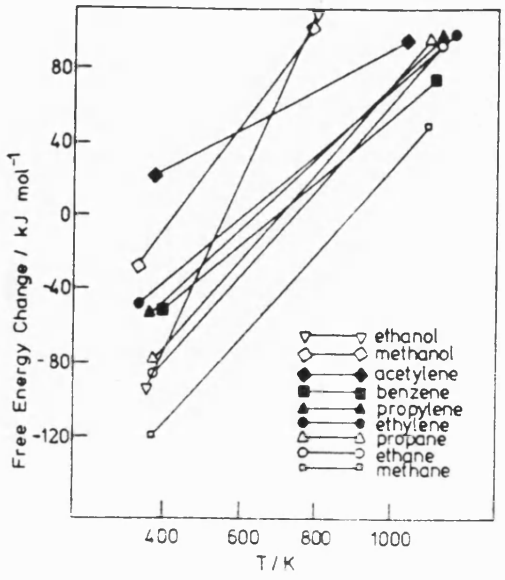

A catalyst is required to give an acceptable rate of reaction and also to improve selectivity towards a particular product or products.

1.4.2. Catalysts for Fischer-Tropsch Synthesis

The catalysts most effective in the Fischer-Tropsch synthesis are Group VIII metals.[33] These metals can be conveniently split into the platinum group metals (Ru, Rh, Pd, Os, Ir and Pt) and the three other important catalysts, Fe, Ni and Co.

1.4.2.1. Platinum Group Metals

Of this group ruthenium is the most active metal and it is also the most selective (under most conditions) towards non-methane products.

Ruthenium has been used for a considerable time to form waxes of very high molecular weight. The conditions of this synthesis are low temperature and high pressure and the reaction of CO and hydrogen over reduced ruthenium under these conditions is referred to as the polymethylene synthesis.[34] Ruthenium is also active as a catalyst under many other conditions of temperature and pressure. For example, Anderson[16] cites a catalyst composed of 0.5% ruthenium on alumina operated at 495 K ($CO:H_2=1:3$) which produced 40% (by weight) of methane and 47% of C_5 and above hydrocarbons. Kellner and Bell[35] investigated the effect of dispersion on the catalytic activity of Ru/Al_2O_3 catalysts. They found that when the dispersion (see later) was less than 0.7 the activity and higher hydrocarbon

selectivity fell with increasing dispersion. Under certain hydrogenation conditions (low temperature and high pressure) ruthenium catalysts form carbonyls which (unlike Fe carbonyls) are not active in Fischer-Tropsch synthesis. As far as is possible reaction conditions must be used which limit or eliminate the formation of these carbonyls. The method of pretreatment of the catalyst appears to have some effect on the rate of carbonyl formation.

All the other Pt group metals are less active than ruthenium in CO hydrogenation. Vannice[21] found that the turnover frequency for CO in CO hydrogenation at 548 K was about 20 times less for rhodium and palladium and approximately 100 times less for platinum and iridium. Quantities of methane in the products were also much greater. Iizuka, Tanaka and Tanabe studied CO hydrogenation over Rh/ZrO_2, Rh/Al_2O_3, Rh/SiO_2 and Rh/MgO and found the activity to be greatest on ZrO_2 and least on MgO supported rhodium.[36] Of the other metals in this group osmium is of particular interest since it has been studied in this work.

Deeba et al[37] have reported on a catalyst prepared from $Os_3(CO)_{12}$ supported on MgO which was active in CO hydrogenation both prior to and after oxidation in air. From infra-red studies the active sites appeared to be tri-nuclear and mononuclear osmium carbonyl species.

Other work on osmium includes that of Knözinger and Zhao[38] who prepared Os/Al_2O_3 catalysts from various osmium carbonyls. They found that whilst osmium was

less active than a comparable Ru catalyst by one order of magnitude the selectivity to C_2 and C_3 hydrocarbons was better.

Psaro, Ugo and Zanderighi[39] studied osmium catalysts derived from Os carbonyls supported on silica and alumina and found the resulting catalysts to be highly selective towards methane. Knözinger and others[40] used osmium catalysts derived from $Os(CO)_5$ supported on alumina and reported that those catalysts which were reduced to give Os metal aggregate, and gave better chain growth probability than previous work on ensembles of three or less atoms.

1.4.2.2. Iron

Iron is an important catalyst in the Fischer-Tropsch synthesis and much work has been reported in the literature. It is of note that the only commercially operating Fischer-Tropsch reactors, the SASOL plants in South Africa[41], use Fe catalysts.

Unlike Co and Ni where carbides are not effective catalysts, iron forms carbides easily at normal Fischer-Tropsch operating temperatures and these carbides are active in the production of products. Nitrides and other compounds such as borides are also active and the field has been reviewed by Anderson[16].

1.4.2.3. Nickel

As previously stated, nickel is primarily a methanation catalyst, although when used on certain supports non-methane products can be significant.

Vannice and Garten[42,43] supported Ni on TiO_2, SiO_2, Al_2O_3 and graphite and found the catalysts supported over TiO_2 to be the most active and have the best non-methane selectivity; a 10% w/w Ni/TiO_2 catalyst operating at 524 K ($CO:H_2$ 1:3, 1 atm) produced 50 mol% of C_2 and higher hydrocarbons.

Bartholomew, Pannel and Butler[44] used nickel on Al_2O_3, SiO_2 and TiO_2 and considered that the C_2 selectivity depended to some extent on the dispersion of the metal for those catalysts supported on silica and alumina.

Vannice[31] in testing all the Group VIII metals used a 5% Ni/Al_2O_3 catalyst, and achieved a non-methane selectivity of about 20 mol% when using a $CO:H_2$ ratio of 1.25:1. When larger amounts of hydrogen were present in the stream the amount of non-methane products fell. Vannice also showed that after Ru and Fe, nickel was the next most active metal for both the production of methane and in terms of molecules of CO reacted per active site.

1.4.2.4. Cobalt

Cobalt was one of the materials used extensively in early work on Fischer-Tropsch synthesis. A mixed Co/ThO_2/kieselguhr catalyst was the final choice for the Fischer-Tropsch plants operated in Germany during World War 2. More recently, cobalt has been less intensively investigated, but even so a number of relevant studies have been reported within the last ten years.

Palmer and Vroom[45] investigated the activity of Co (and nickel) foils and postulated that the temperature of final reduction had a very significant effect on the activity of the resultant catalyst. Vannice[31] has compared the activity of cobalt supported on Al_2O_3 with that of all the other Group VIII metals, except osmium, and found cobalt to be less active than nickel but more active than the Pt group metals except Ru; the C_2 and higher hydrocarbon selectivity was however superior to nickel, as expected.

Bartholomew and Reuel[32,46] have investigated cobalt catalysts supported on TiO_2, SiO_2, Al_2O_3 and MgO and found that the specific activity decreased in the order shown above. They also postulated that the specific activity of Co decreased with increasing dispersion.

Other recent papers include the work of Moon and Yoon[47] who have investigated the kinetics of CO hydrogenation over various Co/Al_2O_3 catalysts and have suggested that cobalt oxide present in the catalyst surface has an effect on the observed catalytic properties. Vanhove, Zhuyong, Makambo and Blanchard[48] have investigated the effect of support pore-size on hydrocarbon chain length. Agrawal, Katzer and Manogue[49] have studied the deactivation of cobalt catalysts as a function of time, although with special reference to methanation.

Of particular significance to the present work is the study by Highfield, Bossi and Stone[50] on reduced solid solutions containing cobalt, which will be

discussed later.

1.4.3. Mechanism of the Fischer-Tropsch Reaction

There are many similarities between the mechanism of the Fischer-Tropsch reaction and the simpler methanation reaction, the essential difference being that in the case of higher hydrocarbon formation carbon-carbon bonds are produced.

A number of reviews[6,16,26,51-53] summarizing the literature have been written and the information presented here is a brief outline of the proposed mechanisms.

As previously stated, Fischer[13] outlined the first proposed mechanism for the Fischer-Tropsch reaction and his ideas were subsequently modified and refined by Craxford and Rideal[14-15]. They proposed that hydrocarbons could be formed from surface arrangements of methylene groups as shown below:

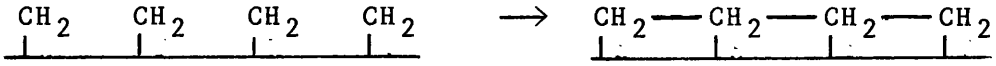

Methylene groups on surface

"Macromolecule" (only four groups shown but model suggested long chains of this type).

These adsorbed "macromolecules" could then be dislodged by interaction with hydrogen to give hydrocarbon chains of variable length. After this mechanism lost favour (Section 1.2), various mechanisms involving first molecularly adsorbed CO and subsequently hydrogenation to an adsorbed-CHOH species were proposed.[23,54]

Currently there are three main proposals for a mechanism for the Fischer-Tropsch synthesis and these are outlined below. Variations on these have also been proposed but they are not considered here as they do not significantly alter the basic reaction types.

(1) The Enol Mechanism

Although many variants exist the basic steps are shown in Scheme 4 and are generally ascribed to Storch, Golombic and Anderson,[23] although Eidus[54] has proposed a very similar mechanism.

Scheme 4

The Enol Mechanism for Fischer-Tropsch Synthesis

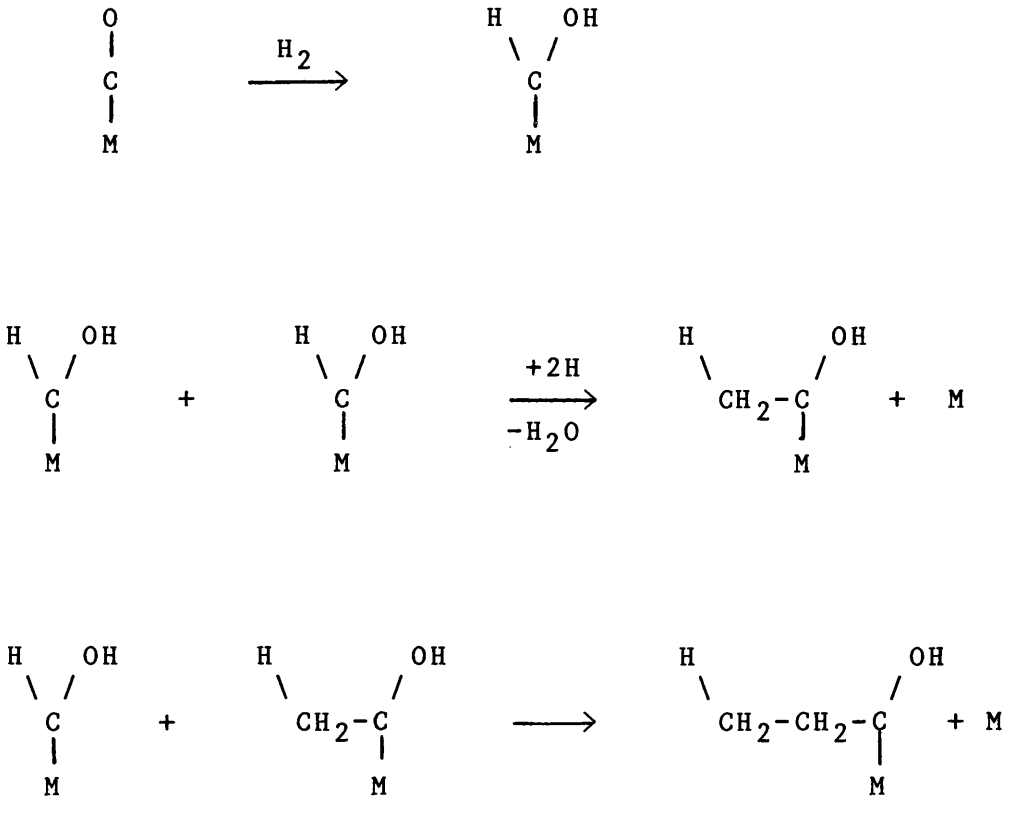

One of the problems of the above is that the adsorbed alcohols shown have seldom been observed to exist. Moreover, reactions of this type (condensation) do not occur in organometallic compounds, although similar reactions are seen in organic condensation reactions.[55]

(2) The CO Insertion Mechanism

This mechanism involves the insertion of a CO molecule between a surface metal atom and an adsorbed alkyl group or a hydrogen atom. The main proponents of this type of mechanism have been Pichler and Schulz.[56] The important steps are shown in Scheme 5, where the final product of the insertion reaction can again undergo insertion leading to the growth of the hydrocarbon chain. In Scheme 5, R represents either an alkyl group or a hydrogen atom.

Scheme 5

The CO Insertion Mechanism

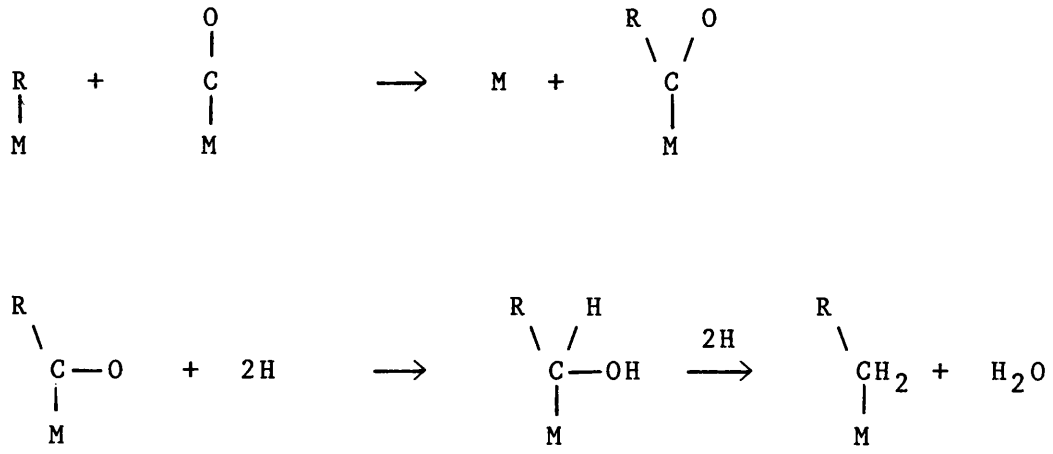

(3) The Mechanism Involving Dissociated CO

Certain of the catalysts widely used in the Fischer-Tropsch synthesis have the ability to dissociate CO to adsorbed carbon and oxygen atoms even at room temperature[51] and this has led to the development of an alternate mechanism which does not involve an oxygenated species directly in the formation of hydrocarbons. The main points are described in Scheme 6.

Scheme 6

The Dissociative Mechanism for the Fischer-Tropsch Reaction

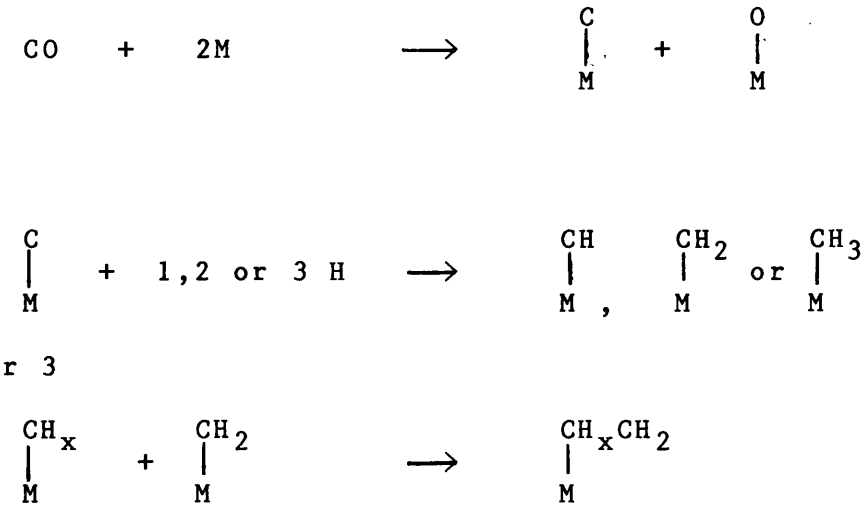

if x=1,2 or 3

If the two carbon atoms are adsorbed on the same site the process would be:

In many respects the mechanism is similar to that proposed much earlier by Fischer and by Craxford and Rideal.

Recently more evidence that a mechanism involving dissociated carbon is important has been reported both for methanation (see Section 1.2) and for the Fischer-Tropsch synthesis. Ponec[26] has suggested an inconsistency of the enol mechanism. In order to function the mechanism requires adjacent metal sites to be present on the catalyst surface. For this reason it would be expected that activity for non-methane production would be lower over alloys than on pure metal catalyst surfaces. From work carried out using nickel this is not found to be the case.[57] Ponec goes on to point out that if CO is removed from the reaction mixture while CO hydrogenation is being carried out the production of methane continues at an initially greater rate but the formation of any other products of higher carbon number ceases almost immediately. This second point, he proposes, indicates that CO must be important to the production of higher hydrocarbons. Bearing in mind these points, Ponec has put forward a mechanism which is a combination of previous ones. The main points are as follows.

(1) CO dissociates and the adsorbed carbon so produced is partially hydrogenated (the same steps as are shown in Scheme 6) to produce CH_x species.

(2) CH_x species grow into longer chains by a CO insertion step (as in Scheme 5) followed by partial hydrogenolysis. Oxygen can be lost prior to or during insertion.

(3) Chain growth is terminated by hydrogen. The mechanism as proposed appears to satisfy many of the experimental observations of the Fischer-Tropsch synthesis reaction, in particular the evidence for some CO dissociation on the surface and the fact that higher hydrocarbon formation is severely affected by removing CO from the gas stream.

The mechanism which Ponec suggests is supported to a greater or lesser extent by a number of papers which support the view that the dissociation of CO is an important mechanistic step[58-63] although workers differ on the nature of the steps after hydrogenation of adsorbed carbon to CH_x species.

In summary there is still some considerable disagreement on the mechanism of the Fischer-Tropsch reaction and the true mechanism covering all possible products is likely to be a complex mixture of possible surface reactions. It does seem probable that the mechanistic steps as described do play their part, in particular the dissociative adsorption of CO (the Boudouard reaction $2CO = CO_2 + C$ occurs at high temperatures over most of the catalysts mentioned) but much work remains to be done in this area before any definitive conclusions can be reached.

1.5. Solid Solutions as Catalysts

A solid solution has been defined as "a homogeneous mixture of two solids which is not a compound because its composition may vary within certain

limits".[64] Thus all alloys are solid solutions as are all carbon steels. However, in this work interest is directed at one particular type of solid solution, specifically those where a transition metal oxide is dissolved in a suitable inert oxide.

Oxide solid solutions have been studied extensively and have been proposed as ideal model catalysts for oxide catalysed reactions by Stone.[65] The catalytic properties of oxide solid solutions have been reviewed by Vickerman,[66] who lists MgO, corundum-phase Al_2O_3, and ZnO amongst the most commonly used solvent oxides for catalytically active metal oxides. These three oxides are used owing to their lack of inherent chemical activity. Other oxides which have been used as solvents include structures of the spinel type, TiO_2 and SnO_2. Work carried out on MgO solid solutions containing Ni and Co ions will be reviewed first.

1.5.1. CoO-MgO and NiO-MgO Solid Solutions

Characterization studies of NiO-MgO and CoO-MgO have been carried out by workers in the U.K., Italy, U.S.S.R. and Poland. Cimino, Lo Jacono, Porta and Valigi[67,68] carried out work on NiO-MgO and CoO-MgO solid solutions and showed by X-ray and magnetic measurements that true solid solutions were formed by these systems, i.e. incorporation of Ni^{2+} and Co^{2+} ions into the MgO lattice had taken place and no separate NiO or CoO phase was present.

Determination of the surface concentration of the

transition metal ions (in future TM will be used to represent transition metal) was compared to the concentration in the bulk using a variety of techniques. The reported conclusions of different workers tend to contradict. Bunina and Sazonova[69] using NO adsorption concluded that the concentration of Ni^{2+} ions in NiO-MgO was the same in the bulk as on the surface, whereas Kluz and Jagiello[70,71], using a chemical method, concluded that the surface concentration of Ni^{2+} was substantially less than the concentration in the bulk[72,73]. However, Cimino et al.[72,73] have applied photo-electron spectroscopy to this problem, and their conclusions agree essentially with Bunina and Sazonova.

Much of the work on NiO-MgO and CoO-MgO solid solutions has been carried out on low surface area samples, typically less than 20 m^2g^{-1}. Hagan, Lofthouse, Stone and Trevethan[74] prepared high surface area NiO-MgO and CoO-MgO solid solutions (40-300 m^2g^{-1}) and characterised them. They showed that true solid solutions with Ni^{2+} and Co^{2+} in octahedral coordination had been formed. They did however note the presence of Co^{2+} in tetrahedral coordination near the surface of the crystallites. Their work fully characterised the surface towards adsorption by CO_2, O_2 and H_2O vapour. Dyrek and Sojka have reported Co^{2+} in tetrahedral coordination within the bulk of the solid solution[75].

1.5.2. Reactions Catalysed by Solid Solutions

Various reactions can be catalysed by oxide solid solutions and by varying the concentration of the transition metal ion electronic effects between cations can be recognised. The decomposition of N_2O[76,77] over NiO-MgO and CoO-MgO was studied by Cimino and co-workers, and an increase in the activity per TM ion was seen when the concentration of either Ni or Co was reduced in the solid solution. Cimino, Pepe and Indovina[78] have investigated the oxidation of CO over CoO-MgO and found in this case the activity per metal ion remained constant and was independent of concentration. Kluz and Wojtaszczyk[79] reporting experiments using the same reaction over a similar solid solution catalyst found that varying the percentage of Co^{2+} in a tetrahedral environment in the solid solution (Schottky defects) had no effect on the activity.

Other reactions reported in the literature include the decomposition of isopropanol[80] and the oxidation of hydrogen.[81,82] Interpretations of the behaviour of oxide solid solutions as catalysts have been put forward by Kung[83] and Pomonis and Vickerman.[84]

1.5.3.Spinel Solid Solutions

Far less work has been reported on systems where spinel is the solvent. Characterisation of Ni-$MgAl_2O_4$ has been reported by Porta, Stone and Turner[85] and more

recently Angeletti, Pepe and Porta[86,87] have characterised the cation distribution in Co-$MgAl_2O_4$ and its activity for N_2O decomposition. The general conclusions reached indicate that in Ni-Spinel systems, the nickel ions are predominantly octahedrally distributed, with the fraction of Ni^{2+} ions in tetrahedral sites being between 0.22 and 0.10. For cobalt spinels the reverse is the case, with the fraction of Co^{2+} ions in tetrahedral sites lying between 0.75 and 0.82. Cimino and Schiavello have reported on the activity of Ni-Mg Al_2O_9 and the decomposition of N_2O.[88]

1.6. Reduced Solid Solutions as Supported Metal Catalysts

In contrast to the large amount of work published in the literature concerning catalysis by oxide solid solutions, very little work has been carried out on reduced solid solutions, the only published work to date being that of Stone, Highfield and Bossi[50] using NiO-MgO and CoO-MgO. The use of reduced solid solutions as metallic catalysts was proposed as an alternative route to highly dispersed supported metal catalysts.

In a solid solution such as CoO-ZnO, CoO-MgO or Co-$MgAl_2O_4$ the catalytically active metal exists as ions in either tetrahedral, octahedral or both types of site depending on the nature of the lattice used. A solid solution with a large concentration of solute ions (normally TM ions) will on reduction yield a correspondingly large quantity of surface metal

supported on the depleted solid solution. The resulting catalyst will be similar to a conventionally supported metal catalyst on an inert oxide support.

The situation is altered when the concentration of the TM ions in the solid solution is low. The surface of the solid solution contains only a relatively small number of TM ions interspersed between oxygen anions and solvent cations. On reduction the metal atoms formed are dispersed on the depleted oxide solid solution surface and although at reduction temperatures some mobility and aggregation will take place, the resulting supported metal catalyst will tend to be much more highly dispersed than one prepared by conventional impregnation methods.

By reducing the concentration of TM ions to a low level it was hoped that atomically dispersed metal atoms could be produced which might have quite different catalytic activity and selectivity to larger metal particles. If very small particles were produced metal support interactions would be easier to investigate in detail. By varying the concentration of the original solid solution and paying careful attention to controlling the reduction it was hoped that the particle size of the metal might be varied and its effect on catalytic activity might be determined.

Fig. 1.2 schematically compares a conventional supported metal catalyst with one produced by reduction of a TM-containing oxide solid solution. Although Fig. 1.2 indicates some of the differences between a

solid-solution-derived catalyst and a conventional one, another factor which has to be taken into consideration in the case of the reduced solid solution is the nature of the reduction conditions applied to the catalyst precursor.

From results obtained by Highfield and Stone[89] it would appear that solid solutions which are dilute in TM ions (<5 mol %) are considerably more difficult to reduce than those which are more concentrated, owing to the very significant stabilization of the TM ions in the inert oxide lattice. In order to reduce dilute solid solutions, relatively harsh conditions must be employed, but these very conditions give the reduced metal formed greater surface mobility with a greater chance of aggregation into larger metallic particles taking place. The reverse is true with more concentrated solid solutions which behave more like bulk metal.

In order to produce small particles of metal on the surface of the depleted solid solution, a balance must be achieved between using too low a concentration of TM in the solid solution (and hence the need to employ harsh reduction conditions) and using too high a concentration of TM, as the relatively large amounts of metal at or near the surface will tend to result in formation of large particles).

It should be noted that Highfield et al. do not assume that all the metal reduced is removed from the lattice of the solid solution. They suggest that some reduced material remains embedded in the surface of the

Figure 1.2

Schematic Representation of the Surface of Conventional and Solid Solution Derived Supported Metal Catalysts

(a) Conventional Supported Catalyst

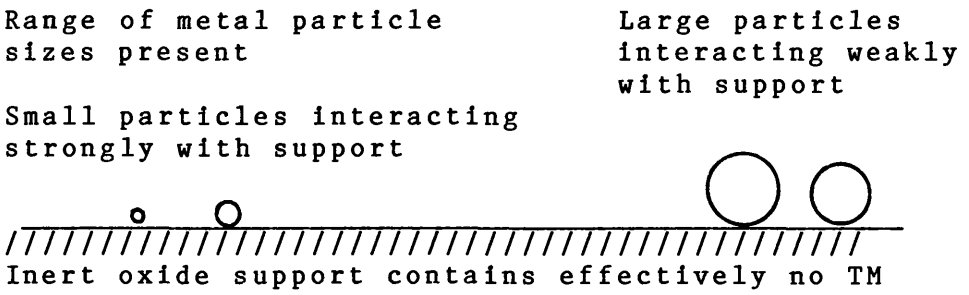

(b) Catalyst Derived from a Solid Solution

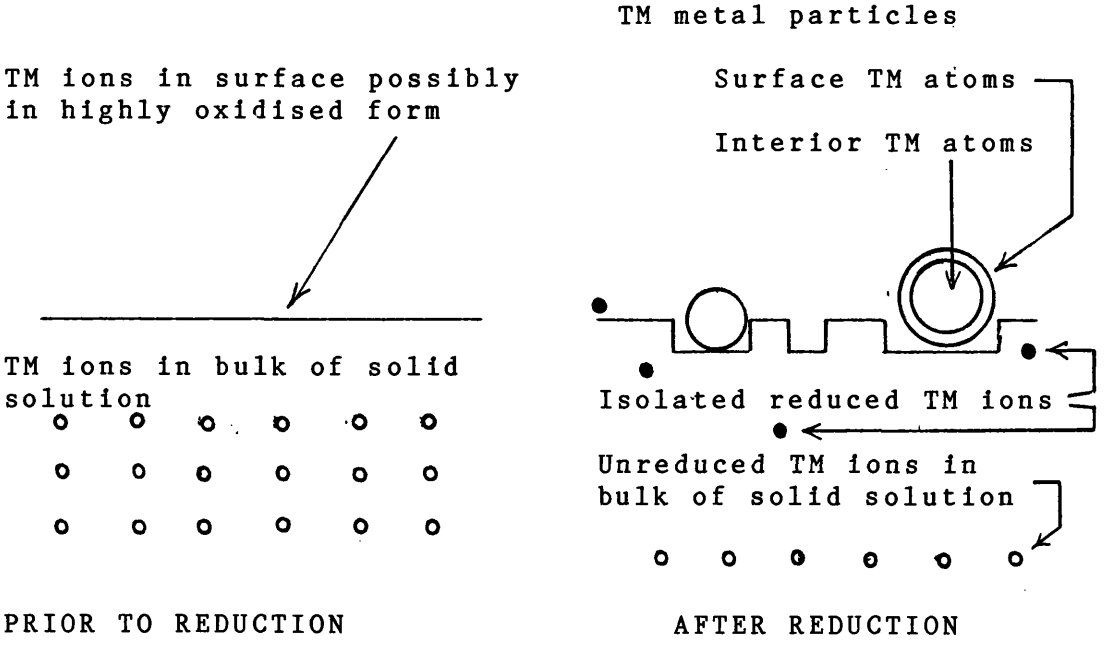

solid as isolated atoms. These may well have their own catalytic properties.

1.6.1. Measurement of Dispersion

This topic will be treated in a quantitative fashion later (Section 4.1.3.) but the concept of dispersion is of fundamental importance in supported metal catalysis as a method of estimating the average size of the metal particles present.

The dispersion of a metal catalyst can be defined as the ratio of the surface metal atoms to the total metal atoms present. Clearly, if for a conventional supported metal catalyst the particles are large, only a relatively small amount of the metal is available as surface atoms to act as catalytically active sites. If, other other hand, the particles of metal are small, a relatively larger amount of metal atoms are available to act as active sites and hence the specific activity (on a weight basis as distinct from a turnover frequency) for the catalyst is larger.

The situation is different for a supported metal catalyst derived from a solid solution, as a significant proportion of the TM remains in the lattice of the solid solution, the amount depending on the degree of reduction. In order to make useful comparisons with conventional catalysts, a different definition of dispersion is required, and the one chosen as most relevant is the ratio of the metal in the surface of the metal particles produced on the surface of the solid solution to the total quantity of metal in these

particles. This concept is further developed in Section 4.1.3.

In concluding it should be stressed that the measurement of dispersion only gives information on the average particle size of the metal present, and unusual distributions of particle size can give misleading results.[90]

1.6.2. Catalytic Results Obtained on Reduced Solid Solution Catalysts

The only results so far available for catalysis over reduced oxide solid solutions have been obtained for CO hydrogenation over reduced NiO-MgO and CoO-MgO.[50,89]

The nickel catalysts, as expected, have given methane as the major product of CO hydrogenation. The cobalt catalysts gave a range of products up to C_4 and the preliminery kinetic experiments carried out[89] indicate kinetic parameters similar to those reported by Vannice[31] for a conventionally supported cobalt catalyst, suggesting that the basic mechanism of CO hydrogenation is probably similar in both cases.

2. EXPERIMENTAL

2.1 Nomenclature

Various methods of describing the concentration of the transition metal in solid solutions have been utilized.

In this work the designation 10NiO-MgO means that ten per cent of the magnesium ions have been replaced with nickel ions. Another method of describing the above solid solution is to denote it $Ni_{0.1}Mg_{0.9}O$

Using the nomenclature of Cimino et al.[77,91] the above solid solution would be designated MN 10. However, strictly this would refer to a nickel ion concentration of 10 nickel ions per 100 magnesium ions, i.e. 10 in 110 rather than 10 in 100.

Spinel solid solutions can be designated in a similar way. A system comprised of magnesium aluminate where 10 per cent of the magnesium ions have been replaced by cobalt will be $Co_{0.1}Mg_{0.9}Al_2O_4$ and will be denoted 10CoSpinel.

Conventional osmium/alumina or osmium/silica catalysts are described, for example, as 2% Os/Al_2O_3 which means that the material contains 2% osmium by weight supported on alumina.

2.2. Preparation of Catalysts

2.2.1. CoO-MgO Solid Solutions

The preparation of the solid solutions took place in two stages, namely

(1) the preparation of the precursor mixture;

(2) firing of the mixture in a high temperature vacuum oven.

The precursor mixture was prepared by dissolving an appropriate quantity of cobalt nitrate (Analar) in distilled water and adding to this magnesium hydroxide (produced from the reaction of ammonium hydroxide and magnesium nitrate) and evaporating the mixture to dryness with gentle heating under vacuum in a rotary evaporator, after which more water was added and the evaporation was repeated twice more. After drying, this precursor mixture was subjected to analysis by atomic absorption spectroscopy (AAS). Typically between 1 and 5 g of material was prepared in this way.

The firing of the mixture took place in a high temperature vacuum oven which is shown schematically in Fig. 2.1. Approximately 1.0-1.5 g of precursor mixture was weighed out and placed in a platinum boat. This boat was then introduced into the apparatus at the large flange F and pushed along the mullite tube into the position shown in the diagram.

The system was sealed by clamping at F, and the apparatus was then pumped out via the bypass line. This process was carried out with extreme care over a period of 0.5 to 1 h to avoid dispersal of the powder.

Once the system was evacuated, a liquid nitrogen trap was placed at position T_1 and the mercury diffusion

A to diffusion pump, rotary pump and bypass line
B furnace
C Thermocouple
D Stopcocks
E Mullite Tube
F O-ring seal
G copper block
H sample boat (platinum)
I trolley for furnace
J digital temperature display
K rails for trolley
L ionization gauge head

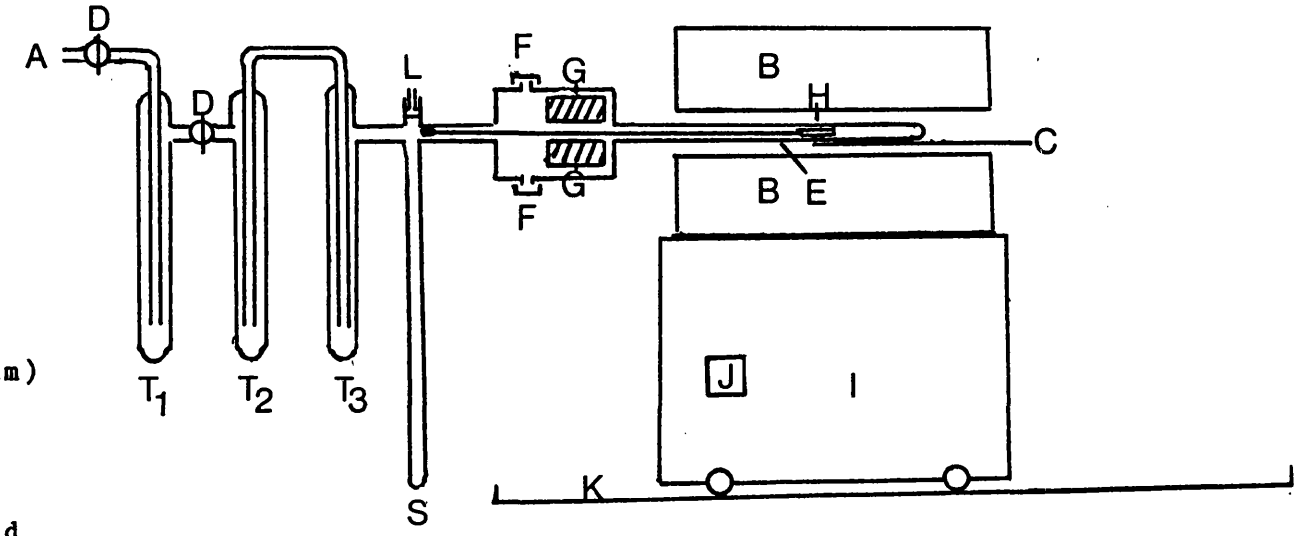

Fig. 2.1 The High Temperature Vacuum Oven

pump was switched on. The system was left to attain a vacuum of at least 10^{-3} torr. The furnace was then switched on and the temperature was raised in stages to the decomposition temperature of the hydroxide (625 K) and maintained at this level for at least 24 hours. A second liquid nitrogen trap was placed on the system at point T_2 when this temperature was achieved.

After this isothermal period the temperature was raised in stages to approx. 1275 K and maintained at this temperature for at least 48 hours. A third trap was placed on the system at point T_3 when the temperature of the furnace was in the region of 775-825 K.

When the thermal treatment was complete the sample was withdrawn to the copper block by pulling the follower attached by wire to the sample holder into the tube S by means of a magnet. After an appropriate period to allow cooling of the sample (3-4 h), the pumps were switched off, the traps were removed, and the system was brought up to atmospheric pressure.

After removal from the system, the sample was normally subjected to analysis by AAS and powder X-ray diffraction (XRD).

2.2.2. NiO-MgO Solid Solutions

Solid solutions of NiO-MgO were prepared in a similar fashion to those of CoO-MgO. Nickel nitrate (Analar) was used in appropriate amounts in the precursor mixture instead of cobalt nitrate.

2.2.3. CoO-Spinel Solid Solutions

Various methods[92,93] of producing Cobalt-Spinel solid solutions were attempted before a method which reproducibly gave material in a high surface area form was developed.

As with the MgO-based solid solutions described previously, the method used involved two stages which were as follows.

(1) impregnation of cobalt and magnesium salts on to high surface are alumina;

(2) firing of this precursor to produce the desired solid solution.

The precursor mixture was prepared by taking appropriate quantities of cobalt nitrate, magnesium nitrate (Analar) and alumina (Degussa, Alon C), stirring the alumina in a deoxygenated solution of the metal salts under nitrogen. The mixture was then gently heated (320-325 K) and evaporated to dryness in a large beaker over a period of several hours. In order to ensure good physical mixing of the components, the dry mixture was then re-slurried by the addition of more water a further two times. After the final evaporation to dryness, the mixture was ground with a pestle and mortar and then subjected to analysis by AAS in order to confirm that the correct quantities of cobalt, magnesium and aluminium were present.

A weighed quantity of the precursor mixture was transferred to the vacuum oven previously described and

a similar procedure was adopted to the one used with MgO-based preparations, differing only in the times and temperatures used. The final temperature of the furnace was normally 1275 K and was maintained at this level for at least 48 h and often considerably longer (in an attempt to minimize the quantity of unreacted MgO phase present).

After treatment in the high temperature system, samples were subjected to AAS and XRD to confirm the stoichiometry and the presence of the spinel structure.

In later stages of the work, freshly prepared samples were washed in dilute HNO_3 and dried in order to remove the contaminant MgO and CoO-MgO solid solution.

2.2.4. NiO-Spinel Solid Solutions

NiO-Spinel solid solutions were produced (for investigation by I.C.I. as a catalyst in various processes) and the general procedure adopted was the same as that employed in the case of the CoO-Spinel. No testing was carried on these samples.

2.2.5. Os/Al_2O_3, Os/SiO_2 and Os/MgO

Two methods were employed to produce Os/Al_2O_3, Os/SiO_2 and Os/MgO supported catalysts. These were:

(1) the "incipient wetness" method;

(2) the "dry pressing" method.

In both cases the source of osmium was OsO_4 which was converted to the carbonyl $Os_3(CO)_{12}$ by reaction with carbon monoxide at a pressure of 100 atm in an autoclave.

For the incipient wetness method, an amount of

osmium carbonyl $Os_3(CO)_{12}$ appropriate to give a nominal loading of 2% w/w osmium on the support was normally used.

Approximately 50 mg of $Os_3(CO)_{12}$ was weighed out accurately and ground to a fairly fine powder. This powder was then dissolved in freshly distilled CH_2Cl_2 in a round-bottomed flask under nitrogen.

Silica (Grace Davison 952), alumina (Degussa Alon C) or magnesia (prepared in a laboratory ex $Mg(OH)_2$) was pressed (20 tonnes, 0.5 h) and then sieved to give a particle size in the range 500-710 microns. An appropriate quantity of the oxide support was then weighed out (consistent with a 2% osmium loading, after allowance for ca 20% water content by weight) and placed in a flask connected to a vacuum system. This was heated to about 395 K for 3 h in order to remove physisorbed water (higher temperatures were also used at times to alter the condition of the surface of the support). After cooling, a solution of the osmium carbonyl in CH_2Cl_2 was introduced over the support in volumes just greater than the calculated pore volume of the support and solvent was then removed using a nitrogen stream.

Owing to the failure of this method to produce usable catalysts from $Os_3(CO)_{12}$, the dry pressing method was developed as an alternative in an attempt to improve the impregnation of the support by the osmium carbonyl. Silica or alumina was pretreated by heating in a vacuum frame at temperatures ranging from 395 to 775 K. This

material was then mixed with finely powdered $Os_3(CO)_{12}$ by shaking a mixture of the two components together in a large glass bottle. After mixing, the mixture was pressed at ca 20 tonnes for a period of 0.5 h. It was then broken up and sieved to give particles of 500-700 microns in size. These particles were placed in a vessel connected to a vacuum line and heated to 375 K for 3 h to remove any water physisorbed during preparation. At this time a small amount of the osmium was lost from the support and condensed on the glass walls in the vacuum system.

2.3. Catalyst Characterization

2.3.1. Atomic Absorption Spectroscopy (AAS)

A Varian AA275 atomic absorption spectrometer was used to measure the amount of Mg, Ni, Co and Al in solid solution precursor mixtures and in solid solutions themselves.

With MgO-based solid solutions a sample (100-200 mg) was accurately weighed out and dissolved in 20% v/v HNO_3 (50 ml). This solution was made up to 250 ml and then diluted further before being introduced into the spectrometer.

Normally three standards were used as references for each element being measured, and calibration procedures were carried out internally in the instrument.

The procedure in the case of spinel-based solid solutions was slightly different owing to the insolubility of the spinel. The sample (0.3-0.5 g) and

$KHSO_4$ (3-5 g) were heated in a platinum crucible over a bunsen until melting and evolution of H_2SO_4 was noted. The melt was maintained at red heat for approximately 2 h and was then cooled and dissolved in acid. Subsequent treatment was similar to that for MgO-based samples, except that the aluminium content was also calculated.

2.3.2 X-Ray Diffraction

The Debye-Scherrer method was used. In order to obtain a powder diffraction photograph, a sample of solid solution (ca 50 mg) was ground to a very fine powder and introduced into a Lindemann tube. The tube was then mounted in a Philips powder diffraction camera (Straumanis mounting) and exposed to Fe K_α radiation for between 4 and 5 h. Measurement was carried out by measuring line spacings directly off the developed negative by means of a special vernier measure.

2.3.3. Physical Adsorption and Chemisorption

The procedure adopted for physical adsorption and surface area determination is described in Section 2.4.1.3. and that for chemisorption in Section 2.4.1.5.

2.4. Apparatus and Procedures for Catalytic Studies

2.4.1. Vacuum System Studies

2.4.1.1. Description of Vacuum Systems

Two glass high vacuum systems were employed in the course of this work. The first system (Fig.2.2) was already in existence and this was later replaced by a

second system (Fig.2.3). Both systems were basically similar, and the main reason for replacing the original system was convenience of operation and the need to attain better vacuum conditions. The second system will be described in detail and the original system will be mentioned only where it differs significantly from the latter.

The apparatus comprised three basic parts which were the pumping system, the dosing bulbs and the reaction area.

The pumping system consisted of an Edwards "Speedivac" rotary pump and a mercury diffusion pump arranged conventionally with a liquid N_2 trap present upstream of the diffusion pump. This combination allowed the frame to be pumped down to pressures in the range 10^{-5} - 5 x 10^{-6} torr.

The pressure in the main system could be monitored by three electrical pressure devices or by a McLeod gauge. Two of the electrical devices were of the Pirani type (P_2,P_4), measuring the pressure from atmospheric to 10^{-3} torr; one of these was fitted close to the diffusion pump (P_2), whilst the other was installed as far from the pumps as possible in the gas dosing rail (P_4). The third electrical gauge in the main frame was of the Penning type (P_3), and was calibrated to read in the range 10^{-3} - 10^{-6} torr. Used in conjunction, these sensors, together with the McLeod gauge, made it relatively easy to locate and rectify leaks and maintain and monitor a good overall system vacuum.

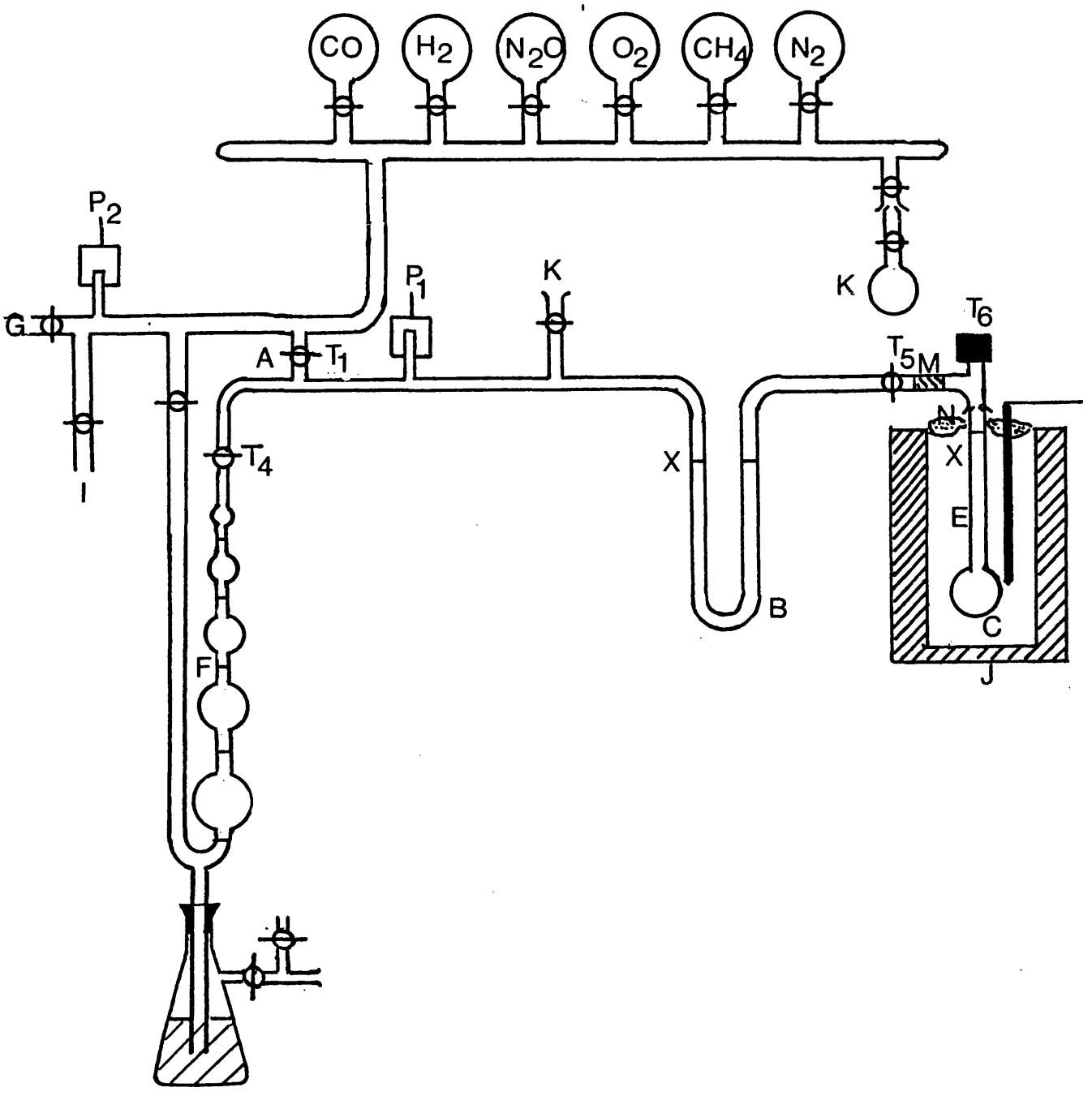

See page 45 for key

Fig 2.2 The First High Vacuum System

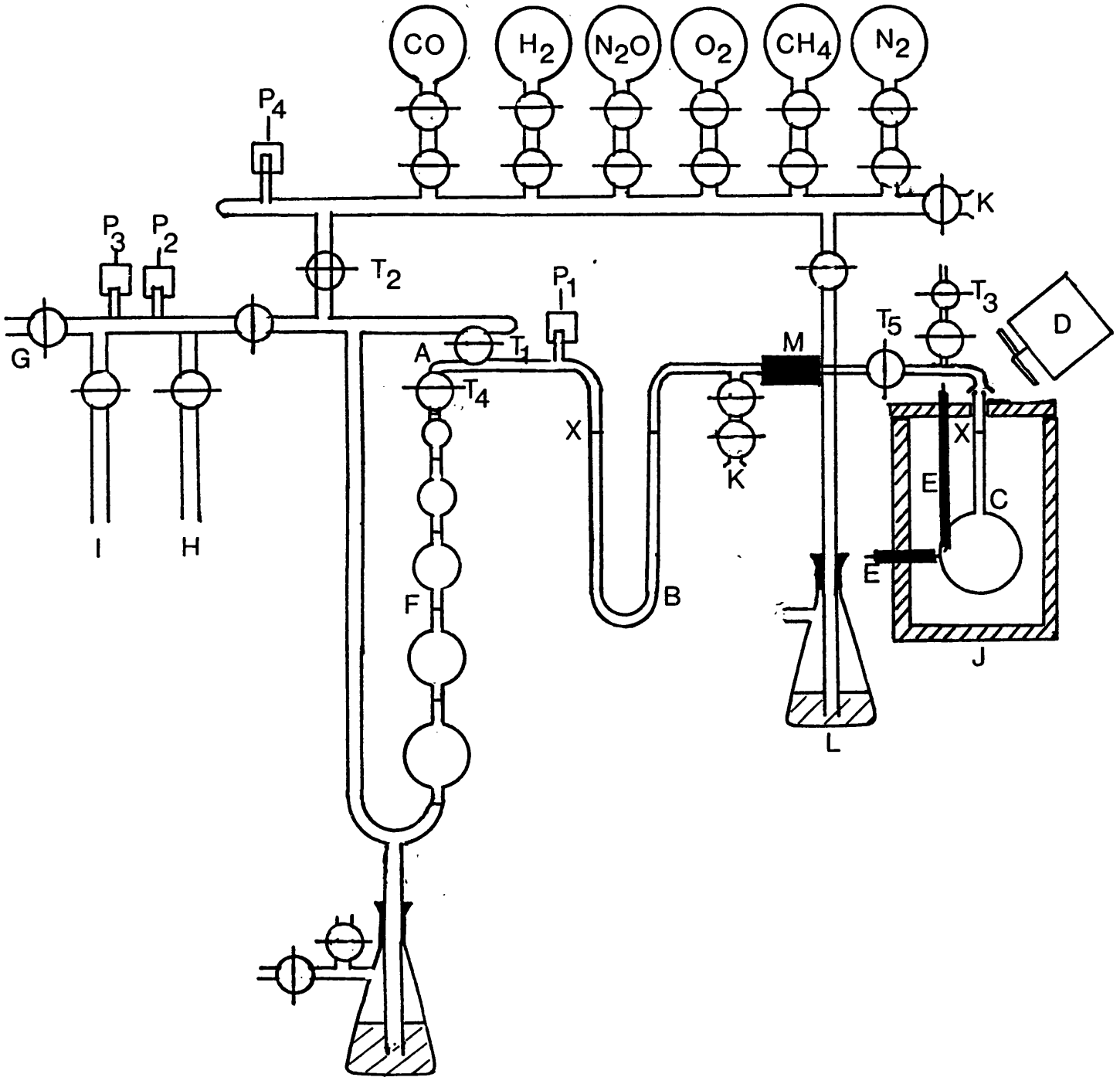

See page 45 for key

Fig 2.3 The Second High Vacuum System

Key to Figures 2.2. and 2.3

A-B-C	limits of reaction area
B	trap area
C	sample area
D	fan
E	thermocouple
F	doser bulbs with calibrated volumes
G	to diffusion pump
H	to McLeod gauge
I	bypass line
J	furnace
K	sample take-off point
L	mercury manometer
M	gold wire
N	insulation
P_1	0-50 torr pressure transducer
P_2,P_4	Pirani transducers
P_3	Penning transducer

The dosing bulbs were located on the back rail and provided sources of the following gases (Research Grade): carbon monoxide, hydrogen, nitrous oxide, oxygen, methane and nitrogen. This section could be isolated by the tap T_2.

The reaction system (the area bounded by ABC in Fig. 2.3) consisted of a known volume of narrow bore glassware which could be divided into two separate areas by closing the tap T_5. With tap T_5 closed, the volume on the left became the "trap area" and the volume on the right became the "sample area". The capacity of both areas was accurately known from calibration experiments (Section 2.4.1.2.).

The trap area was connected via tap T_1 to the main frame and pumps and via tap T_4 to a set of graduated glass bulbs used in surface area determination by the BET method (Section 2.4.1.3.). The pressure transducer in this part of the system (P_1) was a strain gauge which gave a linear response in the range 0-50 torr. This transducer was connected to a digital voltmeter arranged to give a display directly in torr, measuring with an accuracy of 0.1 $\pm$ torr.

The sample bulb was made of silica and could be heated by means of a small furnace. The maximum temperature used in practice was 1100 K. A thermocouple connected to a digital display was used to measure the temperature in the region of the sample. A ground glass joint connected the sample tube to the rest of the system and could be cooled by a fan to prevent leaking

during sample heating. The sample area could be raised to atmospheric pressure in isolation to the rest of the system by using tap T_3 (with tap T_5 closed).

Outputs from the digital thermometer recording sample temperature and from the pressure transducer located in the trap area were taken to a two-channel chart recorder (Philips RG 222) so that continuous monitoring of both temperature and pressure in the reaction area could be attained.

The principal reasons for constructing the second system were to avoid the following shortcomings of the first system.

(1) "Teflon" taps in the first system had become prone to leaking. Only glass taps were employed on the second vacuum system.

(2) Only one Pirani gauge was installed in the first system, rendering leak testing difficult.

(3) In the first system the strain-gauge pressure transducer within the reaction system was connected to an analogue display calibrated in arbitrary units. This display was difficult to read accurately, especially when low pressures ca 1-5 torr were being measured.

(4) Temperature measurement in the first system was carried out with a thermocouple connected to a potentiometer box. Although this method gave an accurate measure of temperature from voltage temperature tables, it was not a

continuous measurement and was inconvenient in operation;

2.4.1.2. Calibration of Vacuum Systems

Both the vacuum systems were calibrated by first accurately determining the volume of a removable portion (i.e. a bulb attached at K) by weighing filled with mercury. Expansion of known pressures of gas from this known volume was then performed in order to give the volumes of the other parts of the system.

In the case of the second system, the volume of each of the graduated glass bulbs was determined with mercury prior to installation and the system was calibrated using different "standard" volumes. In this way volumes were accurately measured as the mean of several readings. The variation between different measurements was small, being less than 0.3 ml.

2.4.1.3. Procedure for Surface Area Determination

A sample weighing 0.5-1.0 g was installed and outgassed in vacuo at 875-975 K. The outgassing temperature was chosen so as to be higher than any temperature to be used subsequently.

Nitrogen (white-spot) was introduced into the doser and the pressure measured with a cathetometer. The full quantity of gas from the doser was admitted to the remainder of the system including the sample bulb, and pressure was remeasured with the cathetometer. The system volume was then reduced systematically by raising the mercury level in the doser system one bulb at a

time, and the corresponding pressures measured at equilibrium. Liquid nitrogen was maintained around the sample bulb at a constant level.

Data of volume adsorbed versus pressure were plotted according to the BET equation

$$P/V_{ads}(P_o-P) = 1/V_mC + (C-1)P/V_mCP_o \qquad (8)$$

and V_m was determined from the slope and intercept. Using a standard value of 0.162 nm^2 for the cross-sectional area of N_2 at 77 K, the surface area was determined.

2.4.1.4. Reduction of Solid Solutions

Reduction of oxide solid solution samples was carried out after a BET determination in situ and after any necessary standardization of the oxidation state (Section 2.4.1.5.).

(a) Reduction of NiO-MgO solid solutions

The normal procedure was to cool Trap B in liquid nitrogen and then to admit a known volume of hydrogen to the trap area. Tap T_5 was then opened to the sample (0.5-1.0 g) at room temperature. By determining the difference between the observed and expected pressure (for no adsorption), the uptake was calculated. The temperature of the furnace surrounding the sample area was then raised to a chosen temperature for a prescribed period (typically 2-24 h), after which the sample was cooled to room temperature and the pressure was remeasured. The additional uptake was thereby determined. The process was repeated at successively

higher temperatures until a measurable amount of reduction had taken place (typically 875 K).

Assessment of temperatures and times to be chosen for precise measurement of uptake as described above was assisted by monitoring continuously the pressure during heating.

(b) Reduction of CoO-MgO solid solutions

The procedure for the reduction of cobalt-containing solid solutions was basically similar to that described for the nickel-containing samples. However, normally the Co-containing solid solutions were reduced by first treating them with carbon monoxide and then with hydrogen. Reduction with only hydrogen as the reductant was found to be very difficult unless the temperature was above 975 K.

(c) Reduction of nickel and cobalt spinel solid solutions

The reduction procedure was basically that described in (a) and (b) above. However, to effect reduction of the spinels harsher conditions were required, typically temperatures of up to 1025 K for 24 h or more.

2.4.1.5. Characterization by Chemisorption

Characterization by chemisorption was carried out using O_2, CO and H_2. The main significance was given to the irreversible uptake. This was obtained by deducting from the total amount the reversible amount (if significant) which could be desorbed and readsorbed at the temperature concerned.

Measurements of uptake were normally carried out at room temperature, but in the case of oxygen uptake was measured at ambient and higher temperatures.

Particularly in the case of cobalt-containing solid solution the M^{3+} species was sometimes formed during oxidation. Experiments to measure the extent of formation of this species were carried out so that estimates of M^{2+} and M^{o} were made as accurately as possible.

2.4.1.6. Procedure for Catalysis Studies

(1) Ethane hydrogenolysis

A known volume of ethane was introduced into the trap area by dosing and measuring the pressure with an electrical transducer. The trap was then cooled in liquid nitrogen to condense the ethane. Tap T_5 to the catalyst (0.5-1.0 g) was next opened and hydrogen was dosed into the reaction system to such a pressure that the molar quantities of both reactants were equal. The temperature of the sample was then raised to 575 K, this temperature being maintained by the proportional temperature controller to within $\pm$2 K.

When the temperature in the sample region was steady, the liquid nitrogen bath around the trap was removed. The ethane evaporated and the reaction proceeded. After 10, 20 and 30 minutes the ethane was quickly condensed so that the residual pressure of non-condensable gas (H_4 + CH_4) could be recorded. After the 30-minute reading had been taken, an accurate

determination of the amount of ethane decomposition was obtained as follows:

(i) the catalyst was cooled to room temperature and the pressure was measured with residual ethane first uncondensed and then condensed;

(ii) after re-evaporation of the ethane, a sample of the gas mixture was admitted to the evacuated flask and taken for mass-spectrometric analysis.

(2) Hydrogenation of carbon monoxide

Hydrogen was dosed on to the sample area and Tap T_5 (Fig. 2.3) was closed. After pumping out the trap area, carbon monoxide was introduced such that a prescribed molar ratio of carbon monoxide to hydrogen (normally 1:3) could be achieved after opening Tap T_5 and allowing the gases to mix. The total pressure was normally 35-45 torr, and this was monitored with the transducer and its associated chart recorder.

The furnace, already preheated to the reaction temperature (normally 525 or 575 K), was placed around the catalyst sample (0.5-1.0 g) and the reaction was allowed to proceed. The start of the reaction (zero time) was taken as the time at which the pressure in the system reached a maximum before falling off as the reaction proceeded. The pressure decrease from zero time was noted after 30 minutes in order to give a measure of the initial rate of reaction. The reaction was allowed to proceed for up to 24 h, after which the furnace was removed and the sample cooled to room

temperature. The pressure of the system was recorded and a sample of residual gas was analyzed by use of the mass spectrometer analysis system. The residual gas was evacuated, and the contents of the trap were allowed to evaporate into the trap area. The pressure was noted and a gas sample was taken for MS analysis.

2.4.1.7. The Mass Spectrometer Analysis System

A VG Micromass Model Q7 quadrupole mass spectrometer was used to analyze mixtures of gases derived from catalytic reactions and also to check the composition of the gas phase in some instances after reduction and chemisorption experiments.

The system comprised a separate glass high vacuum unit linked via stainless steel tubing and a leak valve to the mass spectrometer. The spectrometer was equipped with an ion pump and also an oil diffusion pump and two-stage rotary pump. The arrangement of the system is shown in Fig. 2.4.

In normal operation the system was used in the following way:

(1) the glass vacuum unit was pumped down to about 10^{-5} torr using its mercury diffusion pump and rotary backing pump;

(2) the spectrometer was continuously pumped by the ion pump.

(3) The purpose of the oil diffusion pump and its accompanying rotary pump was twofold. Firstly it enabled the spectrometer system to be evacuated to about

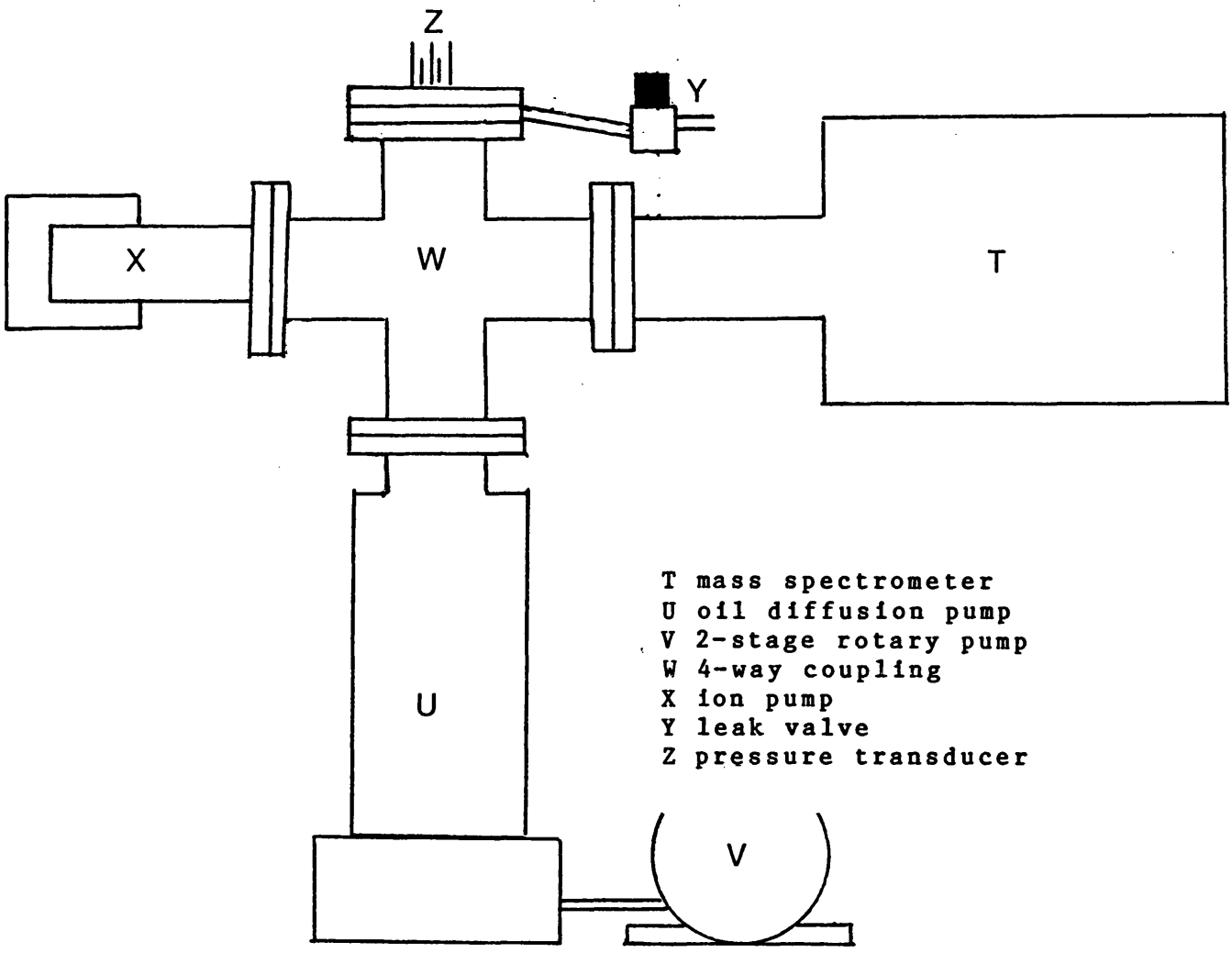

Fig 2.4 The Mass Spectrometer

10^{-7} torr before the ion pump was switched on. This situation occurred if the spectrometer had to be let up to atmospheric pressure (to change a filament). The second use of the secondary pumping system was that it allowed the ion pump to be baked at about 375 K overnight under conditions of dynamic vacuum in order to clean the pump and so increase its efficiency.
Gas samples taken from the reaction system described in the previous sections were introduced into the mass-spectrometer via the leak valve Y. The normal pressure level for analysis was approximately 5 x 10^{-8} torr. The mass spectrum of a mixture could be displayed on an oscilloscope or a permanent copy could be made using a Bryans chart recorder.

In order to quantify the results, calibration experiments were carried out using all the compounds commonly encountered. The method of calibration was as follows. Carbon monoxide was chosen as a reference and known mixtures of carbon monoxide and another gas were introduced and analyzed on the mass spectrometer. Using the mathematical relationship described in Section 3.2.2. it was possible to calculate the relative sensitivity coefficient for each gas used with respect to carbon monoxide. From these experiments unknown mixtures of gas could be analyzed to an accuracy of approximately 5%.

2.4.2. Flow System Studies at Normal Pressure

Two flow systems were used at Bath during this

work. The first was a relatively simple unit which was already in existence and the second was constructed to overcome certain shortcomings of the original system. A further two flow systems were used at I.C.I. Runcorn and these will be described later.

The first flow system (Fig. 2.5) was conventional in design but, in respect of the work to be undertaken, it suffered from a number of disadvantages which are summarized below.

(1) Coarse needle valves were used to control the flow of each gas. These were found to be difficult to adjust precisely to a particular flow rate and over a period of a few hours the set flow would vary quite considerably.

(2) Nylon tubing was used for connecting most of the elements of the flow reactor together. Joints between sections of tubing tended to leak and it was possible for significant amounts of air to enter the system such that a marked N_2 peak would appear on the gas chromatograph.

(3) The only accurate method of monitoring a particular gas flow was to switch off all the other gas flows and measure the flow rate of the gas in question with a bubble flow meter. Simple rotameters were fitted to the system but they were found to be unsatisfactory.

(4) Most of the taps in the system were of the toggle type. These did not provide an efficient shut-off when closed.

(5) The analytical system consisted of a Pye 104 gas chromatograph fitted with two thermal conductivity

detectors. Whilst this type of detector was adequate for analysis of carbon monoxide, hydrogen and methane it was not suitable for analysis of small quantities of non-methane hydrocarbons.

The second flow system was designed and constructed bearing all the above points in mind. The general arrangement of the system is shown in Fig. 2.6.

Normally CO, H_2 and He gas supplies were connected to the three input lines shown on the diagram. The gas passed first through a coarse pressure regulator, followed by a filter, a non-return valve, and then a Brooks flow controller before going through a high precision rotameter calibrated for the particular gas in question. This arrangement was such that in normal operation flows could be set very accurately and once set would not fluctuate. The rotameters, once calibrated, were found to be accurate to within a few per cent.

From the rotameters the gas streams were directed to a gas mixing chamber. The shape and construction of the chamber is shown inset in Fig. 2.6 and its final form was decided on as the best compromise between cost and complexity of manufacture and efficient mixing of the gases.

A total flow control device was installed in the system after the gas mixing chamber. This served two functions:

(1) it enabled the total flow rate of the gas mixture being used to be varied. This was more convenient than

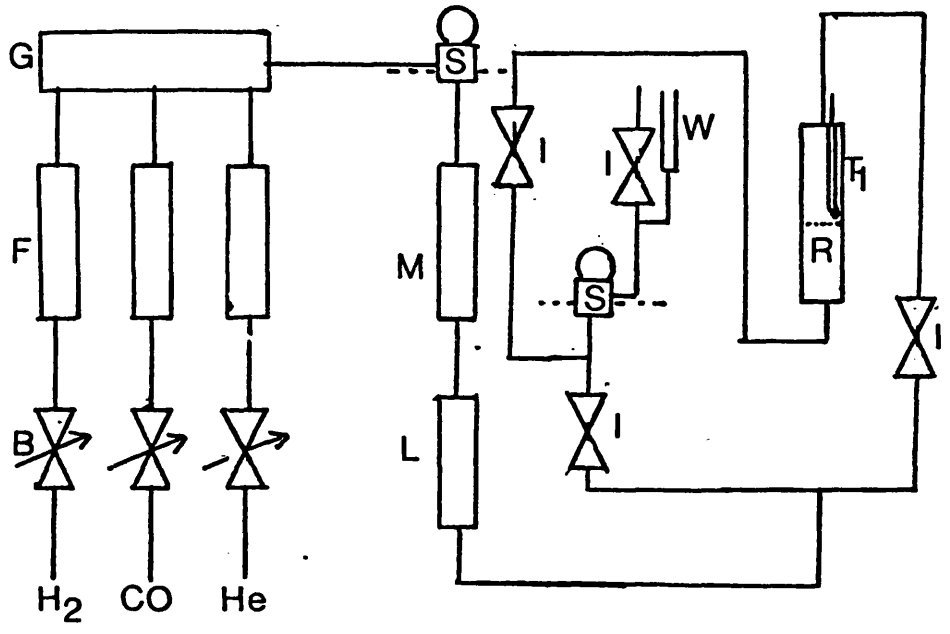

see page 60 for key

Fig. 2.5 The First Flow Reactor

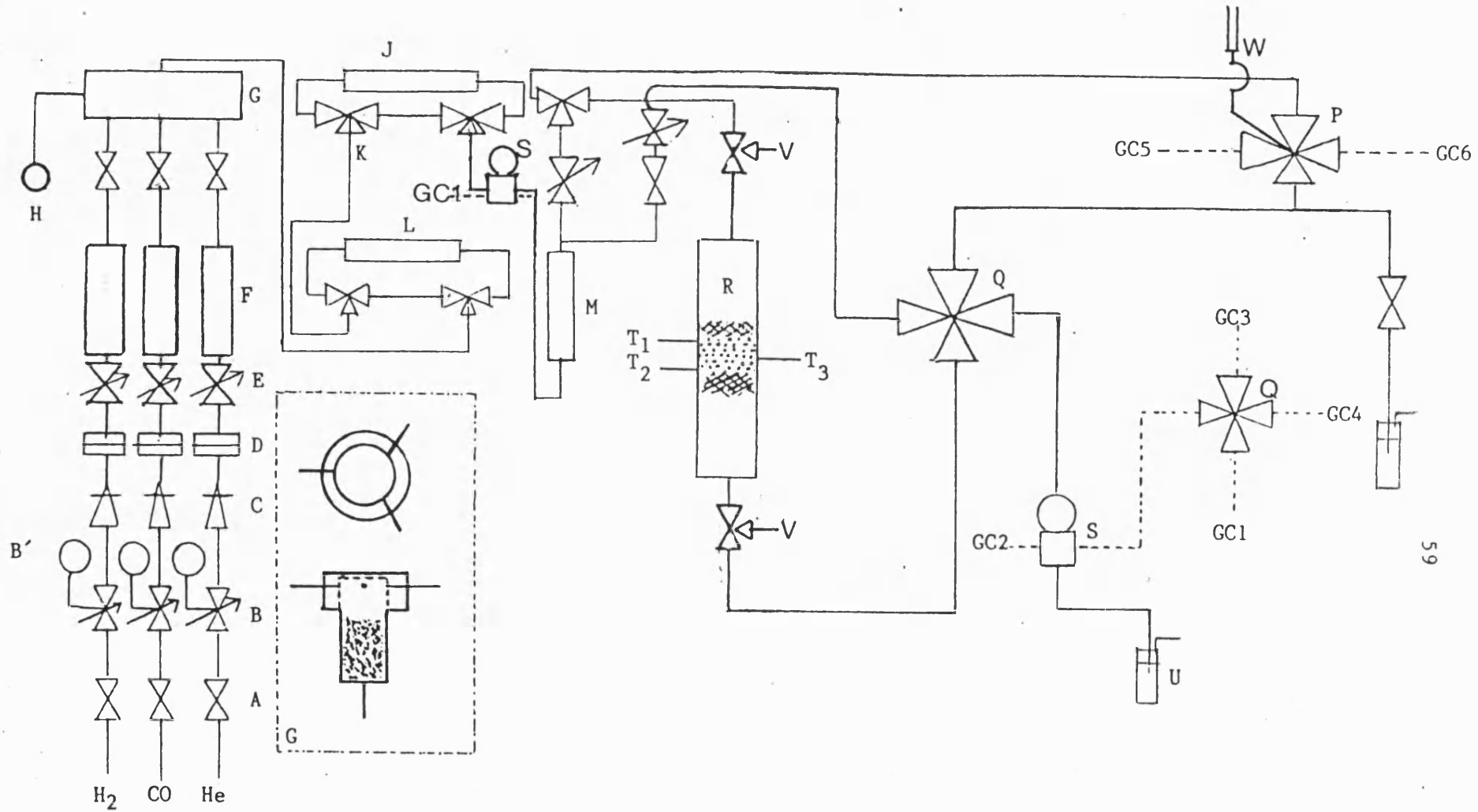

see page 60 for key

Fig. 2.6 The Second Flow Reactor

Key to Figs 2.5 to 2.9

A	on/off Whitey taps
B	needle valves
B′	pressure gauges
C	non-return valves
D	filters (normally 7 μ)
E	flow controllers
F	rotameters
G	mixing chamber (see inset Fig. 2.6)
H	back pressure indication
I	toggle-type on/off taps
J	molecular sieve unit
K	3-way Whitey tap
L	"De-oxo" unit
M	total flow rotameter
N	spare feed
P	4-into-1 Whitey valve
Q	crossover 4-way valve
R_1,R_2	reactors
S	sample valve
T_1,T_2,T_3	thermocouples
U	bubbler
V	flow chemisorption attachment points
W	bubble flow meter
X	restrictor
Y	pressure-limiting valve
Z	safety valve
1	mercury monometer
2	G.C. analytical system
3	to molecular sieve column and T.C. detectors
4	timer
5	pump
6	flow measurement system
7	reactor pressure control
8	G.C. analytical system splitter and columns
9	flow damper
10	electrical pressure transducer

adjusting each flow individually;
(2) it enabled the gases to be run into a constant back pressure (within certain limits). The advantage of this was that different catalyst packings generating different back pressures could be used with back pressure adjusted to that used to calibrate the system.

Catalyst was packed into the central part of the reactor tube adjacent to the thermocouples and held in position with glass wool. A two-part furnace was constructed to contain the reactor and enabled the temperature inside the tube to be raised to a maximum of 1100 K. The reactor tube to particle ratio was considerably greater than 10 to prevent excessive channelling of the tube wall.[94]

Analysis of the gas stream before and after contact with the catalyst was carried out using gas chromatography. The arrangement consisted of a Pye 204 Series isothermal GC equipped with one flame ionization detector (FID) and two thermal conductivity detectors (TCD). The flame ionization detector was used in conjunction with a Poropak Q column of length 5 ft and was used for analysis of hydrocarbons C_1 - C_4. The two thermal conductivity detectors were used with a molecular sieve MS80 column for analysis of carbon monoxide, hydrogen, methane and also any nitrogen and oxygen in the system. Both columns were run at 363 K with helium being used as the carrier gas at a flow rate of 30 ml min^{-1}.

The output from both detectors was fed to chart

recorders but was also connected to a Spectra Physics SP470 integrating microcomputer.

After the valves of the various variables in the system had been set (flow rate, temperature of columns, detector temperature, detector amplifier gain), calibration experiments were carried out by injecting into the analytical system from a loop of known volume pure samples of all the gases likely to be encountered during catalytic studies. The integrator was used to calculate the absolute response for each gas and from this the sensitivity of the system to each gas could be measured and hence relative sensitivities of each gas to a chosen standard could also be evaluated. By programming the machine with these relative sensitivity factors, automatic analysis of gas mixtures could be accurately carried out. The standards used were methane on the Poropak Q/FID column and carbon monoxide on the MS80/TCD system. Results based on the integration of peak areas modified by the application of a relative sensitivity factor were printed out directly in mol % terms for each gas analyzed. After the above calibration procedure, test mixtures of known composition were injected and analysis of the mixtures proved satisfactory.

As well as having the ability to carry out normal flow catalysis studies in the system, extra pipework and a further twin thermal conductivity detector unit were built into the system in order to enable flow chemisorption to be carried out. The arrangement of

this pipework and detectors is shown in Fig. 2.7 and is based on a design described by Gruber.[95,96] Gas was introduced into the helium carrier via a gas sampling valve and appropriately sized loop, and flowed past the first TC detector. It then passed over the catalyst where a fraction was adsorbed. The remainder flowed past the second TC detector and produced a peak corresponding to the gas not adsorbed. Hence the quantity of gas adsorbed could be estimated by comparing the initial and final peak heights. When the two peaks were of the same area the surface of the catalyst was saturated.

2.4.2.1. Pretreatment

Most catalysts used in the flow system were pre-reduced in the static system described previously before transfer to the flow-reactor. However, some samples were reduced directly in the flow system by first flowing CO over them for several hours at temperatures between 825 and 975 K and then flowing H_2 overnight at similar temperatures.

This treatment did not always result in satisfactory catalysts in that the activity tended to be lower than with similar samples which had been pre-reduced.

Re-reduction of pre-reduced catalysts was carried out by flowing H_2 at temperatures between 825 and 925 K for periods ranging from 4 to 12 h.

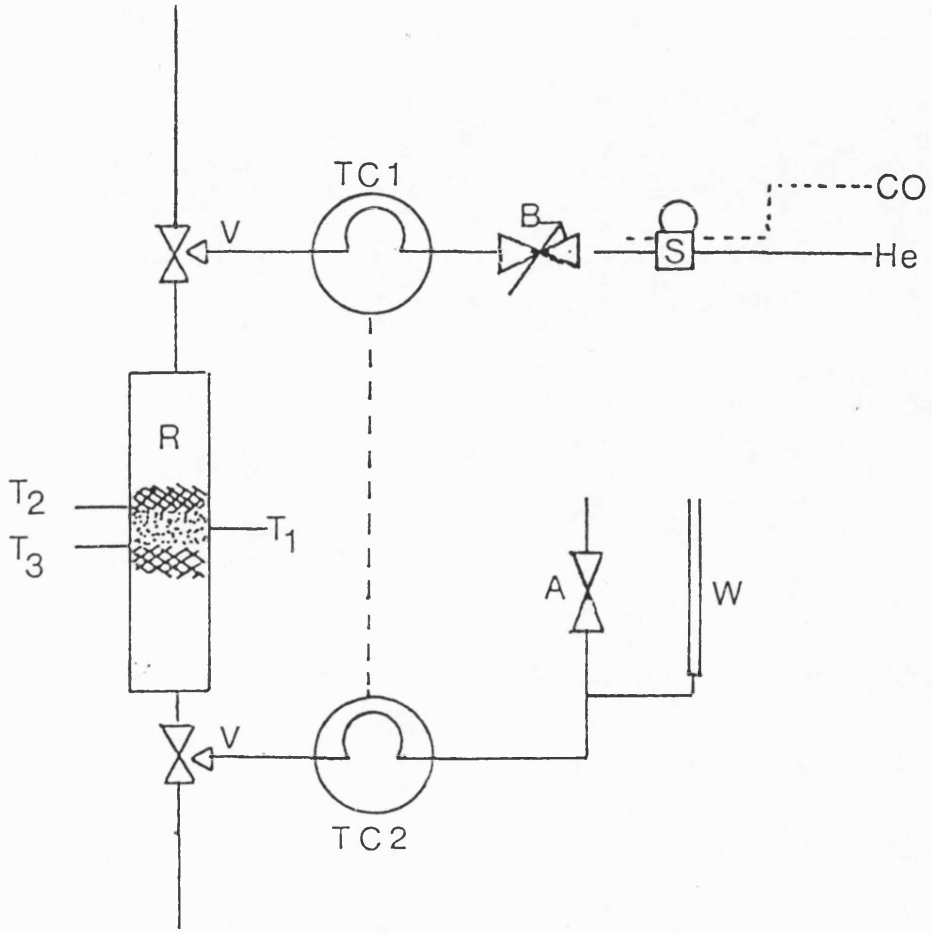

see page 60 for key

Fig. 2.7 The Flow Chemisorption Attachment

2.4.2.2. Procedure for Catalysis Studies

After carrying out activation, either by reduction or re-reduction of the catalyst in the flow reactor, a programme of catalyst testing was carried out which would normally include the following experiments, although not all the experiments described were carried out on all the catalysts studied.

(1) Reduction of the catalyst from freshly prepared solid solution or re-reduction of a catalyst previously reduced in the static system (see Section 2.4.2.1.).
(2) Initial exposure of catalyst to CO and H_2 mixture.
(3) Measurement of activation energy.
(4) Measurement of the order of reaction with respect to hydrogen.
(5) Measurement of the order of reaction with respect to carbon monoxide.
(6) Effects of changing feed gas ratio on products.
(7) Chemisorption and desorption experiments using the flow chemisorption system.
(8) Deactivation measurement over long time periods.

The order in which these experiments were carried out was normally that shown above. Between experiments, mild regeneration of the catalyst was carried out using hydrogen at about 775 K.

Initial exposure of catalyst to carbon monoxide and hydrogen

Before any other experiments were carried out the catalyst was used in a carbon monoxide and hydrogen

stream ($CO:H_2$ 1:3, temp. normally 575 K, flow rate 40 ml min^{-1}) and the products, in particular methane, were monitored on the GC system until the decrease in the methane peak area with time was relatively small. The reason for carrying out this procedure was to condition the catalyst and to ensure that all catalysts studied were in approximately the same condition so that comparisons between catalysts were as valid as possible.

Measurement of activation energy

A carbon monoxide/hydrogen stream (normally 1:3 at 40 ml min^{-1}) was set flowing over the catalyst and the temperature was stablized (normally between 500 and 525 K). The system was allowed to reach the steady state (typically 1 h) and the products were analyzed at this temperature two or three times using the GC system so that a mean result could be calculated. The temperature was then raised by about 25 K and the system was allowed to reach the steady state, after which analysis was again carried out. This procedure was repeated at successively higher temperatures until four or five readings had been obtained. The temperature of the reactor was then reduced to the initial value and after stabilization the products were again analyzed. In this way the quantities of methane and other hydrocarbon products were measured at various temperatures and the amount of deactivation could be estimated from a comparison of the methane peak area at the beginning and the end of a run. Corrected values of the methane peak area (in counts) were used to plot ln

CH_4 peak area vs. I/T and so calculate the activation energy for methane formation. Activation energies for other products were calculated in the same manner.

Measurement of order of reaction with respect to hydrogen

A gas flow rich in hydrogen was set up at a fixed temperature as the initial conditions for this experiment (typically $CO:H_2$ 1:4, flow rate 50 ml min^{-1}, T = 575 K) and after stablization the products were analyzed. The concentration of hydrogen in the gas stream was then reduced, the total flow rate being kept constant by increasing the proportion of helium. After sufficient time for the system to reach the steady state (typically 1 h) two or three analyses of the gas stream past the reactor were carried out. The hydrogen content of the gas stream was again reduced and the process repeated. In this way the products of four or five different feed gas ratios were analyzed whilst keeping the total flow rate over the catalyst constant. The hydrogen content of the feed gas would typically be reduced from 80% to 20% of the total during the course of a run. By plotting ln (methane peak area) versus ln (hydrogen partial pressure) the order of reaction in hydrogen for methanation could be determined. As in the case of activation energy measurements, at the end of a run (i.e. after the last point had been measured) the system was returned to the initial conditions used so that the deactivation over the period of the run could be estimated and the measured values obtained for each

point could, if necessary, be corrected.

Measurement of order of reaction with respect to carbon monoxide

The procedure for this experiment was similar to that carried out for hydrogen. The only difference was in the range of carbon monoxide partial pressures used. In order to prevent excessive deactivation of the catalyst by using a very CO-rich feed gas, the maximum proportion of carbon monoxide in the feed was normally 50% (i.e. $CO:H_2$ 1:1) and during a run this would be decreased to 10% of the total flow.

Effect on products of changing feed gas ratio

When the experiments to measure order of reaction were carried out changes were noted in the relative proportions of the hydrocarbon products produced. However, in these experiments the gas stream was not normally composed solely of carbon monoxide and hydrogen (helium was present to keep the total flow constant).

In order to see the effect of varying the feed gas ratio ($CO:H_2$) mixtures ranging from 1:1 to 1:8 were used. The flow rate was normally between 30 and 40 ml min^{-1}.

Chemisorption experiments

Prior to attempting a chemisorption experiment, the surface of the catalyst was cleaned using hydrogen and/or helium at approximately 775 to 825 K. Carbon monoxide was then injected in accurately known amounts into a helium stream flowing over the catalyst, and by

measuring the peak area before and after contact with the catalyst the gas taken up by the catalyst could be estimated. When the peak area before and after contact was identical it was assumed that the catalyst surface was saturated.

Deactivation measurements over long time periods

Deactivation experiments were carried out by setting up a CO/H_2 feed under normal conditions ($CO:H_2$ 1:3, flow rate 40 ml min^{-1}, T = 575 K) and monitoring the reduction in the various product peak areas over a long period of time (typically 40-60 h).

Most of the experiments carried out as detailed in this section made use of measurement relative to methane (and higher hydrocarbons). Normally at one or two points during a run the conversion would be measured by analyzing the carbon monoxide peak area before and after contact with the catalyst. Also periodically the $CO:H_2$ ratio set on the rotameters would be checked by analyzing the gas mixture for carbon monoxide and hydrogen prior to contact with the catalyst.

2.4.3. Studies at Elevated Pressure

Some flow reactor work was carried out on osmium catalysts at I.C.I. New Science Group, Runcorn.

Two reactors were used at Runcorn:

(1) a 10 atm laboratory flow reactor similar to that used in Bath;

(2) a high pressure (100 atm) reactor of the Berty type.

2.4.3.1. The 10 atm Laboratory Flow Reactor

A diagram of the 10 atm reactor is shown in Fig. 2.8. The reactor was of conventional design and only those parts which vary significantly from the 1 atm reactor at Bath will be described.

It can be seen from the diagram that the 10 atm reactor was not equipped with needle valve type flow controllers for adjustment of individual gas flows. Instead, calibrated restrictors were used and the relative proportions of carbon monoxide and hydrogen were varied by adjustments to the upstream pressure on each restrictor using the regulator attached to the supply cylinder. Typical pressures upstream of the restrictors would be approximately 300 psi and the composition of the gas mixture was measured not by using rotameters but by injection into the G.C. analysis system and subsequent adjustment (if appropriate) on one or the other of the gas supply regulators. Pressure in the system was maintained by use of pressure-limiting valves which allowed gas to bleed past them once the pressure in the system reached a pre-determined level. The G.C. analytical system consisted of two FID detectors used to analyze hydrocarbons and oxygenates respectively, and a separate thermal conductivity detector for the analysis of CO and H_2. The columns used for hydrocarbon and oxygenate analysis were operated non-isothermally. The column used for CO, H_2 analysis was operated isothermally. The output from the GC detectors was fed via A to D converters to a Texas

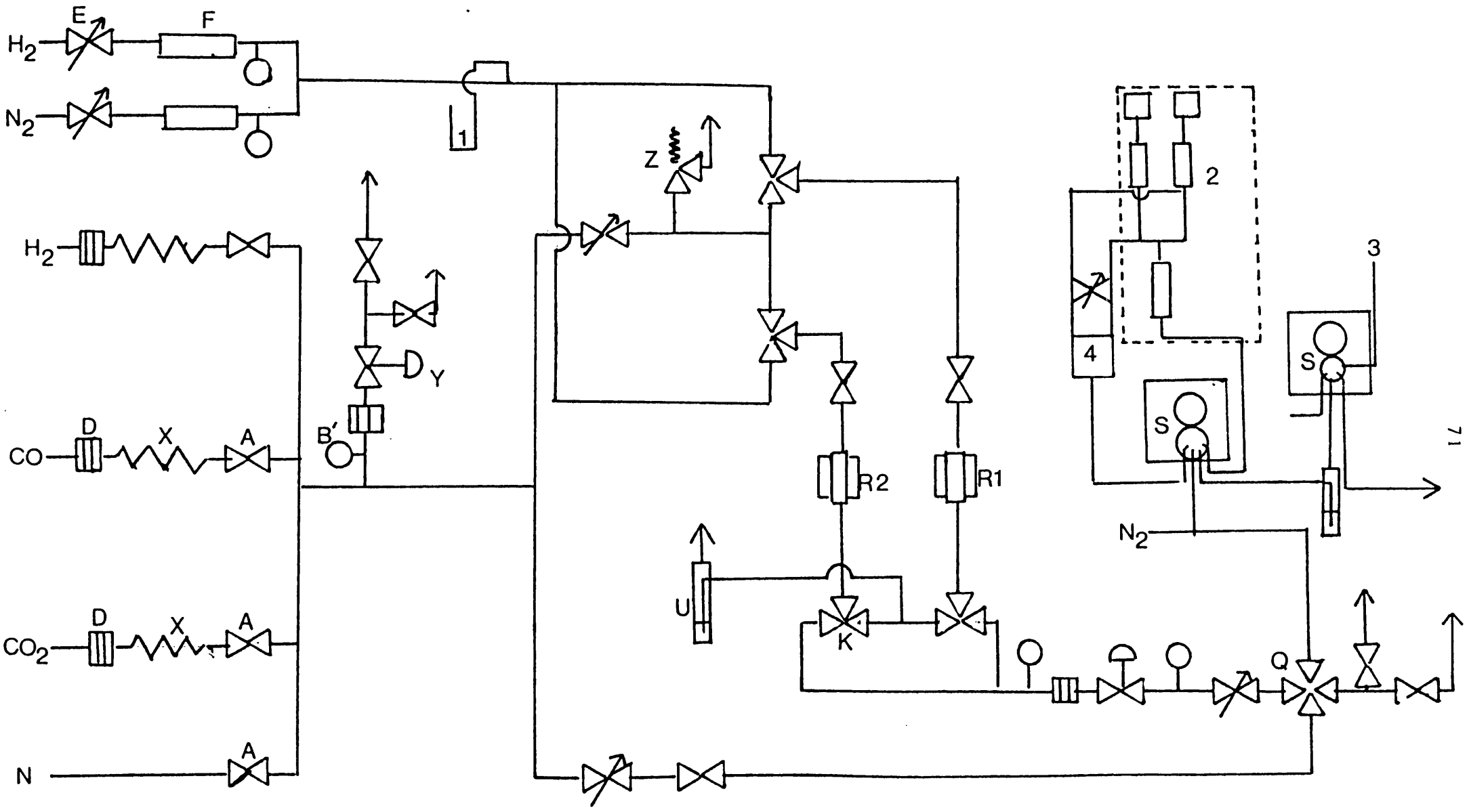

see page 60 for key

Fig. 2.8 The 10 atm Flow Reactor

mini mainframe "Labnet" computer and, after integration of peak areas, quantities of products, conversion, turnover frequencies etc. were calculated automatically by a sophisticated analysis program retained in the computer.

Samples were introduced into the reactor and nitrogen was flowed over the catalyst at room temperature for about 1 h. The temperature was then raised to about 475 K and a nitrogen hydrogen mixture (4:1) was used to activate the catalyst at temperatures up to approximately 575 K. Catalytic testing normally took place using a 1:1 $CO:H_2$ mixture at various temperatures between 500 and 575 K. Spectroscopic techniques were applied to some catalysts before and after testing (SIMS, XPS, TEM). A rough estimate of the metal surface area was obtained by carbon monoxide adsorption on to the catalyst in a separate apparatus.

2.4.3.2. The 100 atm reactor

A 100 atm reactor of the Berty type[97-99] was briefly used at Runcorn. The general arrangement of the equipment is shown in Fig. 2.9. The system was remotely operated by means of a PET microcomputer and totally manual operation was not possible. The catalyst was loaded into the reactor which was then bolted up and leak-tested by observing the pressure drop with the reactor isolated, filled with nitrogen at 100 atm, over a period of time.

Carbon monoxide and hydrogen were then fed via a

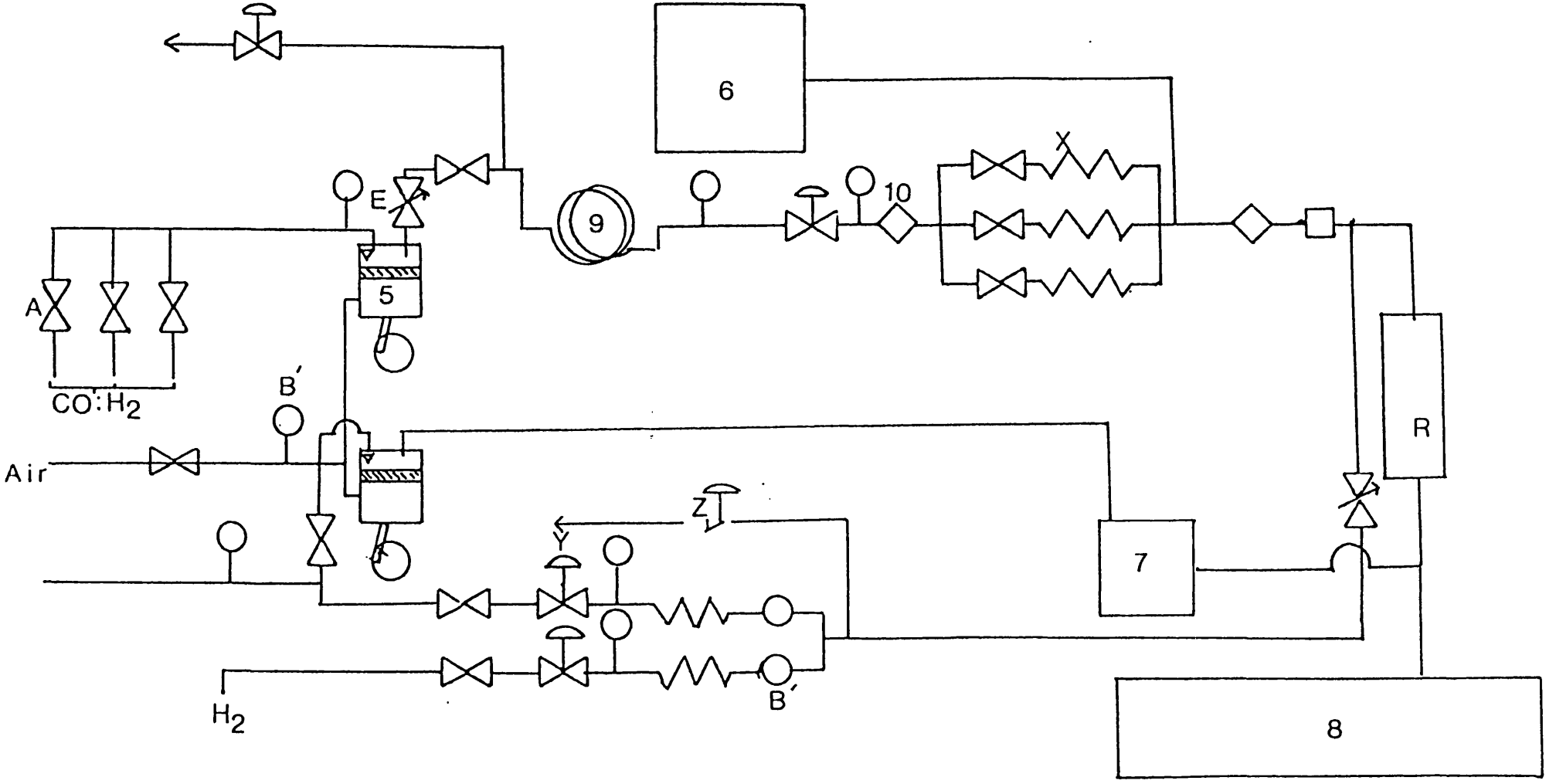

see page 60 for key

Fig. 2.9 The 100 atm Berty Reactor

reservoir into the reactor until the pressure reached 100 atm. Flow rates of the gas mixture through the reactor were of the order of 30 ml min^{-1}. Products of the reaction were analyzed in the same way as with the 10 atm reactor using a similar GC analytical system, the only difference being that the analysis was entirely automatic, sampling taking place via sample valves controlled directly by the PET micro-computer.

3. RESULTS

3.1. Adsorption, Reduction and Catalysis Studies using the First Static System

3.1.1. 3% NiO-MgO

Two samples of NiO-MgO containing 3 mol% Ni, namely 3NiO-MgO 1 (0.727 g, SA = 110 m^2g^{-1}) and 3NiO-MgO 2 (0.662 g, SA = 101 m^2g^{-1}), were studied.

Prior to severe treatment in hydrogen to reduce Ni^{2+} ions, the surface was characterised with respect to superficial Ni^{3+} formation by the following procedure. The samples were heated in oxygen, cooled to room temperature, evacuated, then heated in hydrogen. Uptakes of oxygen and hydrogen were measured at each stage. Results are shown in Table 3.1, where the temperature in brackets indicates the highest temperature used. The inference to be drawn from Table 3.1 is that the hydrogen uptake is due to the reduction of superficial Ni^{3+} to Ni^{2+} .

After these treatments the samples were heated in hydrogen to 803-903 K in order to effect the reduction of Ni^{2+} ions. The additional uptakes of hydrogen are shown in Table 3.2, where the brackets indicate the treatment given.

Oxygen chemisorption was studied on the reduced samples first at room temperature and then at temperatures up to 523-573 K to give a measure of the

Table 3.1

Oxygen and Hydrogen Uptakes on 3NiO-MgO

Treatment	Uptake/micromol m^{-2}	
	3NiO-MgO 1	3NiO-MgO 2
Oxygen	0.137 (853 K)	0.015 (623 K)
Hydrogen*	0.287 (679 K)	0.052 (633 K)

* Samples became pale green after this treatment

Table 3.2

High Temperature Reduction of 3NiO-MgO

Hydrogen uptake/micromol m^{-2}	
3NiO-MgO 1	3NiO-MgO 2
0.730 (803 K, 2 h)	0.430 (903 K, 2 h)

Table 3.3

Oxygen Chemisorption at Room Temperature (RT) and Above on Reduced 3NiO-MgO

Treatment	Uptake/micromol m^{-2}	
	3NiO-MgO 1	3NiO-MgO 2
Exposure to oxygen at room temp.	0.018	0.039
Further exposure up to ca 525 K and cooling to room temp.	0.031	0.064

amount of reduced nickel (Table 3.3).

The cycles were then repeated. The samples were re-reduced in H_2, oxygen chemisorption was remeasured as before, and finally there was again reduction in H_2. Respective values are shown in Table 3.4.

Following the above reaction, the catalytic reactions of ethane hydrogenolysis and carbon monoxide hydrogenation were carried out on both samples using the procedure described in Section 2.4.1.6. Results are given in Table 3.5.

Ethane hydrogenolysis was conducted at 573 K using a 1:1 mixture and the fraction of ethane reacted in 30 minutes (denoted by x) was taken as the measure of activity. The initial pressure of hydrogen (with

Table 3.4

Uptakes of Hydrogen and Oxygen During Further Reduction-Oxidation Cycles on 3NiO-MgO

Treatment	Uptake/micromol m^{-2}	
	3NiO-MgO 1	3NiO-MgO 2
Hydrogen	0.162 (853 K)	0.211 (529 K)
Oxygen at room temp.	0.016	0.034
Oxygen to 525 K	0.053	0.088
Hydrogen	0.094 (597 K)	0.201 (585 K)

ethane condensed) was measured (p_o) and also the pressure of $CH_4 + H_2$ after 30 minutes with residual ethane condensed (p_{30}). Consider the reaction of a moles of ethane with a moles of hydrogen according to the stoichiometry $C_2H_6 + H_2 = 2CH_4$. After 30 minutes the initial number of moles of H_2 (proportional to p_o) will be reduced from a to a(1-x), and 2ax moles of CH_4 will have formed, giving a total amount of $CH_4 + H_2$ equal to a(1+x) moles (proportional to p_{30}).

Thus $p_{30}/p_o = a(1+x)/a = 1 + x$.

Hence $$x = (p_{30}/p_o) - 1 \qquad (9)$$

CO hydrogenation was conducted at 523 K using a 1:3 $CO:H_2$ mixture and an initial total pressure of 20-25 torr. The activity given in Table 3.5 is the initial activity averaged over the first thirty minutes

Table 3.5

Ethane Hydrogenolysis and Carbon Monoxide Hydrogenation Over Reduced NiO-MgO

	Catalyst	
	3NiO-MgO 1	3NiO-MgO 2
Activity for ethane hydrogenolysis at 573 K	0.32	0.84
Initial activity for CO hydrogenation at 523 K	0.33	0.55
Conversion in CO hydrogenation w.r.t.H_2/%	55*	91**
Products of reaction	only CH_4 detected	CH_4 and traces (<1%) of C_2H_4 and C_2H_6

* After 1.33 h reaction ** After 0.5 h reaction

of reaction, and is expressed as $(p_o-p_{30})/p_o$ where p_o is the total initial pressure (measured with the sample at 523 K) and p_{30} is the total pressure after 30 minutes reaction at 523 K.

3.1.2. CoO-MgO

3.1.2.1. 3% CoO-MgO

Three samples of CoO-MgO containing 3 mol % cobalt were studied. As in the case of the nickel samples, these will be referred to as 3CoO-MgO 1, 3CoO-MgO 2 and 3CoO-MgO 3, respectively. General data on the three catalysts are shown in Table 3.6. After measurement of

the surface areas, oxygen and hydrogen uptakes were measured as in the case of NiO-MgO (Section 3.1.1.). The results of these experiments are shown in Table 3.7.

Reduction of 3CoO-MgO solid solutions

The same general procedure was followed as for the nickel systems (Section 3.1.1), but CO was dosed to the samples prior to any attempt to reduce Co^{2+} ions in hydrogen. After CO chemisorption at room temperature, the temperature was raised to 875-900 K for a period of a few hours. This CO pretreatment had been found to

Table 3.6

Data for 3CoO-MgO Catalysts

	3CoO-MgO 1	3CoO-MgO 2	3CoO-MgO 3
Wt. loaded /g	0.654	0.596	0.680
Initial outgas max. temp. /K	933	894	922
BET surface area /m^2g^{-1}	105	175	89

be essential in the case of low cobalt concentrations if any measurable reduction by hydrogen below 1000 K was to take place.[50,89] The actual uptakes of CO are shown in Table 3.8 (no data are shown for 3 CoO-MgO 2 since the results were unreliable). Table 3.8 also shows the hydrogen uptakes.

Table 3.7

Oxygen and Hydrogen Uptakes (micromol m^{-2}) on 3CoO-MgO Samples Prior to Sustained Reduction of Co^{2+} Species

	3CoO-MgO 1	3CoO-MgO 2	3CoO-MgO 3
Oxygen uptake	0.067* (RT)	0.135* (RT)	0.096* (RT)
	0.166 (837 K,5 h)	0.484 (823 K,3 h)	0.144 (520 K,4 h)
Subsequent hydrogen uptake	0.000* (RT)	0.000* (RT)	0.000* (RT)
	0.387** (543 K,2 h)	0.198** (568 K,3h)	0.356** (588 K,3 h)

* exposure at room temperature (RT) for typically 2 h

** reduction of superficial Co^{3+} to Co^{2+}

Table 3.8

High Temperature Reduction of 3CoO-MgO

Treatment	Uptake /micromol m^{-2}		
	3CoO-MgO 1	3CoO-MgO 2	3CoO-MgO 3
CO	0.143 (870 K,2 h)	unreliable data	0.366 (895 K,5 h)
H_2	0.045 (900 K,3 h)	0.025 (1000 K,5 h)	0.000 (950 K,4 h)

As can be seen from Table 3.8, the uptake figures for hydrogen are very much smaller than in the

equivalent nickel case (Section 3.1.1.). The small uptakes made subsequent oxygen chemisorption measurements on the reduced cobalt very inaccurate; for example, the value obtained for oxygen chemisorption at room temperature on 3CoO-MgO 1 was 0.072 micromol m^{-2} but prior to high temperature reduction the figure was 0.067 micromol m^{-2}. As reduction was so very slight, the latter figure must be subtracted from the former to obtain a net value, i.e. 0.005 micromol m^{-2}. Because of the errors inherent in this treatment the oxygen chemisorption values obtained were not meaningful and therefore have not been quoted.

In the case of 3CoO-MgO 3, where no uptake of hydrogen was found, CO was redosed at 900 K for 12 h. An uptake of 0.480 micromol m^{-2} was observed, but this was probably due to the Boudouard reaction ($2CO \rightarrow C+CO_2$), with CO_2 being condensed in the cold trap, rather than to reduction of $Co^{2+}O^{2-}$ ion pairs by CO.

Catalytic behaviour of 3CoO-MgO samples

Ethane hydrogenolysis and carbon monoxide hydrogenation were carried out as test reactions after the treatments described above. Table 3.9 shows the activity in ethane hydrogenolysis, the activity being calculated in the same way as for the nickel system (Section 3.1.1.).

After the ethane hydrogenolysis, 3CoO-MgO 1 and 3CoO-MgO 3 were tested for carbon monoxide hydrogenation and the results are shown in Table 3.10.

Table 3.9

Ethane Hydrogenolysis Over Reduced 3CoO-MgO

	3CoO-MgO 1	3CoO-MgO 2	3CoO-MgO-3
Activity at 573 K	0.39	0.31	0.06

Table 3.10

Carbon Monoxide Hydrogenation at 525 K Over Reduced 3CoO-MgO

Catalyst	$CO:H_2$ ratio	Init. rate	Conversion %	Products/%			
				CH_4	C_2H_6	C_2H_4	$>C_2$
3CoO-MgO 1	1:2.7	0.25	1.8(0.5h)	96.0	⟵3.2⟶		0.9
3CoO-MgO 3	1:3.8	0.21	v.small	-	-	-	-
3CoO-MgO 3*	1:3.6	0.28	68(8h)	96.0	1.5	1.1	0.6

* After high temperature outgas to 975 K

After the catalytic testing it was found that the surface area of 3CoO-MgO 1 was 61.2 m^2g^{-1}, i.e. a decrease of about 50%.

As more non-methane products were produced by these catalysts than with the nickel-containing catalysts, further testing was carried out on 3CoO-MgO 3 to investigate the effect of changing the feed gas ratio. Table 3.11 shows the results of these experiments. Prior to these experiments the catalyst was again exposed to

Table 3.11

Carbon Monoxide Hydrogenation at 525 K Over 3CoO-MgO 3 Using Different Feed Gas Ratios

$CO:H_2$ ratio	Initial rate	Conversion % w.r.t.CO	Products				
			CH_4	C_2H_6	C_2H_4	$>C_2$	CO_2
1:1.1	0.28	51 (24 h)	40	3.8	11	9.2	36
1:3.6*	0.28	68 (8 h)	96	1.5	1.1	0.6	0.0
1:8.1	0.11	100 (4 h)	100	0.0	0.0	0.0	0.0

* From Table 3.10

hydrogen at temperatures up to 990 K but no uptake of hydrogen was measured.

3.1.2.2. 10% CoO-MgO

Studies with CoO-MgO containing 10 mol% Co were limited to one sample. 0.617 g (SA = 37 m^2g^{-1}) were loaded into the reaction vessel and outgassed at 893 K. After treatment in H_2 to reduce any Co^{3+} present to Co^{2+} (cf. Table 3.7), oxygen was admitted, giving uptakes of 0.047 micromol m^{-2} and 0.618 micromol m^{-2} at room temperature and 673 K respectively. Hydrogen uptake following evacuation of the unadsorbed oxygen was 1.238 micromol m^{-2}.

The solid solution was then given a sustained reduction treatment in H_2 over several days at 823 K, resulting in a further uptake of 1.182 micromol m^{-2}.

After the high temperature reduction treatment,

oxygen chemisorption/oxidation was performed to measure the extent of reduction. The total uptake was 0.250 micromol m^{-2} at room temperature increasing to 0.761 micromol m^{-2} at about 575 K.

The system was re-reduced using hydrogen at temperatures up to 675 K and the ethane hydrogenolysis test reaction was carried out at 575 K. The activity measured under the same conditions as described above (Section 3.1.1.) was found to be 0.45.

The carbon monoxide hydrogenation reaction was then carried out at 525 K using different $CO:H_2$ ratios. Between each catalytic run the catalyst was exposed to hydrogen at 675 K. The results of these experiments are summarized in Table 3.12.

Oxygen chemisorption was performed after the catalytic testing. Table 3.13 shows the changes in the total uptake before and after the catalysis. Finally the sample was exposed to hydrogen at about 550 K to see how closely the uptake corresponded with the total oxygen uptake after catalysis. The value obtained was 1.280 micromol m^{-2} which is in fairly good agreement with that expected from the final figure in Table 3.13, ($2 \times 0.732 = 1.464$ micromol m^{-2}).

Before removal of the sample from the system, another BET surface area determination was carried out. The value obtained was 31 m^2g^{-1}, a reduction of 17% on the value measured initially. The weight of the

Table 3.12

CO Hydrogenation at 525 K Over Reduced 10CoO-MgO

$CO:H_2$ ratio	Initial rate	Conv.% wrt CO	Products/mol%						
			CH_4	C_2H_6	C_2H_4	C_3H_8	C_3H_6	$>C_3$	CO_2
1:1.1	0.16	74/12h	44	2.5	6.9	1.6	16	3.3	25.6
1:3.2	0.42	86/27h	96	2.3	←———	0.5	——→		1.2
1:8.0	0.23	72/32h	93	←———		7	——→		-

Table 3.13

Comparison of Oxygen Uptake on Reduced 10CoO-MgO Before and After Catalytic Testing

	Uptake /micromol m^{-2}	
	Before	After
Uptake at RT	0.250	0.258
Total to 575 K	0.761	0.732

sample was found to have increased by about 1%, possibly due to carbon deposition during testing.

3.1.3. Cobalt-containing Spinel Solid Solutions

3.1.3.1. $MgAl_2O_4$

In order to be able to assess "blank" uptakes of hydrogen, oxygen and CO by the solvent ($MgAl_2O_4$) surface prior to testing spinel solid solutions containing

cobalt, a high surface area sample of $MgAl_2O_4$ prepared in the same manner as the catalysts was studied. The weight of the sample was 0.550 g, and the surface area (BET) was 36.0 m^2g^{-1}. Adsorptions were studied at room temperature (RT) and at elevated temperature (Table 3.14), the sample being outgassed to about 875 K between the adsorption measurements for each gas.

3.1.3.2. 10% Cobalt-Spinel

Two samples were studied, denoted as 10CoSpinel 1 and 10CoSpinel 2, respectively.

10CoSpinel 1

The weight of the sample loaded into the system was 0.468 g. After a high temperature outgas, the surface area of the sample was measured (BET) as 71.4 m^2g^{-1}.

Table 3.14

Adsorption on $MgAl_2O_4$

Gas	Uptake/micromol m^{-2}
O_2 at RT	0.036
O_2 at 725 K	0.036
CO at RT	0.035
CO at 725 K	0.267
H_2 at RT	none
H_2 at 575 K	none

The sample was then dosed with hydrogen (15 torr). No uptake was recorded at room temperature, nor after increasing the temperature in stages to 1000 K. In spite of this apparent lack of reduction, catalytic testing was carried out using carbon monoxide and hydrogen in various ratios, with results as shown in Table 3.15.

10CoSpinel 2

A sample (0.467 g, SA = 67.1 m^2g^{-1}) was tested for activity in CO hydrogenation without any attempt at pre-reduction. In this way it was hoped that the activity of the unreduced solid solution for this reaction could be tested. It was found that the initial relative rate (as previously defined) was 0.020 when the $CO:H_2$ ratio was 1:3. This is about one-third the value obtained for 10CoSpinel 1 under similar conditions (Table 3.15).

Table 3.15

Carbon Monoxide Hydrogenation over 10CoSpinel 1

$CO:H_2$ ratio	Temp K	Init rate	Conv. %/t	Products/mol%						
				CH_4	C_2H_4	C_2H_6	C_3H_6	C_3H_8	C_4	CO_2
1:1.0	575	0.194	-	-	-	-	-	-	-	-
1:2.5	525	0.066	84/26h	56.3	15.7	7.1	2.0	11.6	1.0	6.3
1:3.0	575	0.065	83/8h	67.0	11.1	2.9	1.2	1.7	0.0	16.1

Further studies with the cobalt-containing spinel solid solutions were carried out in the second static system and these are described in Section 3.2.

3.2. Adsorption, Reduction and Catalysis Studies Using the Second Static System

Reduction, chemisorption and catalysis were investigated on Co-containing spinels with cobalt concentrations ranging from 5 to 20 mol % cobalt. The system calibrations and the mass spectrometer calibrations will first be described.

3.2.1. Volume and Pressure Calibrations

The volume of each of the graduated bulbs fitted to the system was measured by weighing empty and then filled with mercury. The values obtained were (in cm^3) 6.82, 15.37, 27.98, 55.21 and 95.44 respectively. The total volume of the McLeod gauge and the volume per cm of capillary were similarly found by weighing with mercury. The resulting calibration gave

$$p/\text{torr} = 5.8 \times 10^{-6} \times (h_2 - h_1)^2 \qquad (10)$$

where $(h_2 - h_1)$ is the height difference of the mercury levels in the capillaries. The electrical pressure transducer was calibrated by comparing pressure readings with those obtained using the mercury manometer. The mean of several sets of readings was used and the data are presented in graphical form in Fig. 3.1.

Having calibrated the transducer the known volumes of the graduated bulbs were used to calibrate the remainder of the system volumes using gas expansion (Table 3.16). When this process was complete the

Table 3.16

System Volumes (in cm^3) by Gas Expansion

Trap area	25.6
Trap area (liq N_2)*	36.7
Sample area	12.8
Sample area (liq N_2)*	33.5

* Liquid nitrogen level to fixed mark.

calculated volumes were used to recalculate the volume of the graduated bulbs. Comparison with the values obtained by mercury weighing showed the difference to be less than 1%.

3.2.2. Calibration measurements for mass spectrometric analysis

Attempts were made to improve the analysis obtained with the mass spectrometer already in use with the first static system. The procedure adopted was based on the analysis procedure previously employed.

Fragmentation patterns for CO, CO_2, CH_4, C_2H_6, C_2H_4, N_2,O_2 were measured under the conditions employed in the reaction studies. The procedure previously employed for mixtures was to measure the length of a line specific to a particular gas and from it to deduce the contribution of that gas to all other lines in the spectrum. These contributions were then subtracted from the total spectrum. By repeating this process for successive gases, the total contribution to

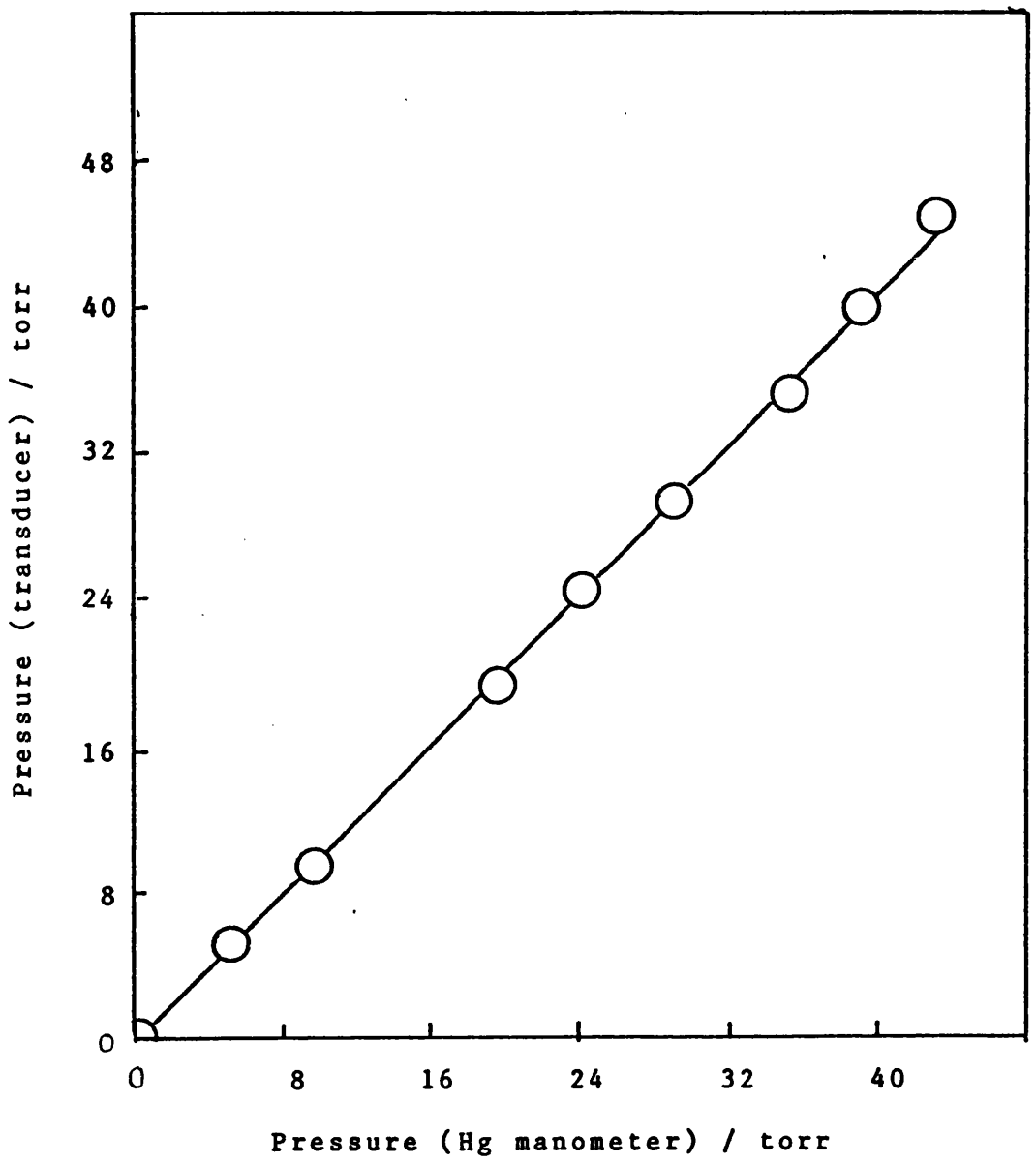

Fig. 3.1 The Calibration for the Electrical Transducer

the spectrum of each gas could be found. The sum of all the line lengths for each individual gas should then be equal to the total length of all the lines in the spectra (assuming no unknown gas present). The partial pressure of a particular contributor was originally taken as its total line length divided by the total line length of the spectra.

The above treatment implies that the spectrometer responds similarly to each gas, which is unlikely to be the case. Ideally, calibrations for each individual gas are needed. However, calibration experiments involving known quantities of gas were impracticable, since gas samples were admitted to the spectrometer via a leak valve. The solution devised for the present work was to introduce sensitivity factors for each gas as follows. CO was chosen as standard (sensitivity factor = 1.00), and factors for each other gas (X) were determined by making known mixtures of gas X with CO (mol fraction n_x) and measuring the mass spectrum. The relation used was then:

$$n_x = (L_x S_x)/(L_{CO} S_{CO} + L_x S_x) \qquad (11)$$

where

n_x = mol fraction of X in the mixture with CO,

L_x = total line length due to x,

L_{co} = total line length due to CO,

S_x = sensitivity factor for x,

S_{CO} = sensitivity factor for CO, defined as 1.00.

The above equation can be rearranged to:

$$n_x L_{CO} = S_x(L_x - n_x L_x) \qquad (12)$$

Hence a plot of $n_x L_{CO}$ versus $L_x - n_x L_x$ will give the value of S_x from the gradient of the straight line. Details of the procedure for hydrogen are given in Table 3.17 and Fig. 3.2. The other gases for which values are quoted were treated in a similar way and the values of the sensitivity factors obtained are shown in Table 3.18. The value for CO_2 varied between 0.95 and 1.05, so a mean value of 1.0 has been used in calculations. When the factors had been established, mixtures of uncondensed gas (CO, H_2 and CH_4) could be analyzed with maximum errors of about 3% for each gas.

It was intended that a similar procedure should be adopted for the condensed products of the hydrogenation reaction, but calibration experiments proved unsatisfactory due to problems involved in obtaining sample gas which was sufficiently pure. Fortunately, the relative quantities of condensed products were normally small compared to the uncondensed gas. For this reason the errors introduced by taking the sensitivity factors of condensed gases to be equal to unity were thought to be small, and therefore this procedure was adopted for these products. However, in order to improve and standardize the analysis of condensed gas, a computer program was developed to calculate the mole percentage of each gas on the basis of its total line length (Appendix 1.)

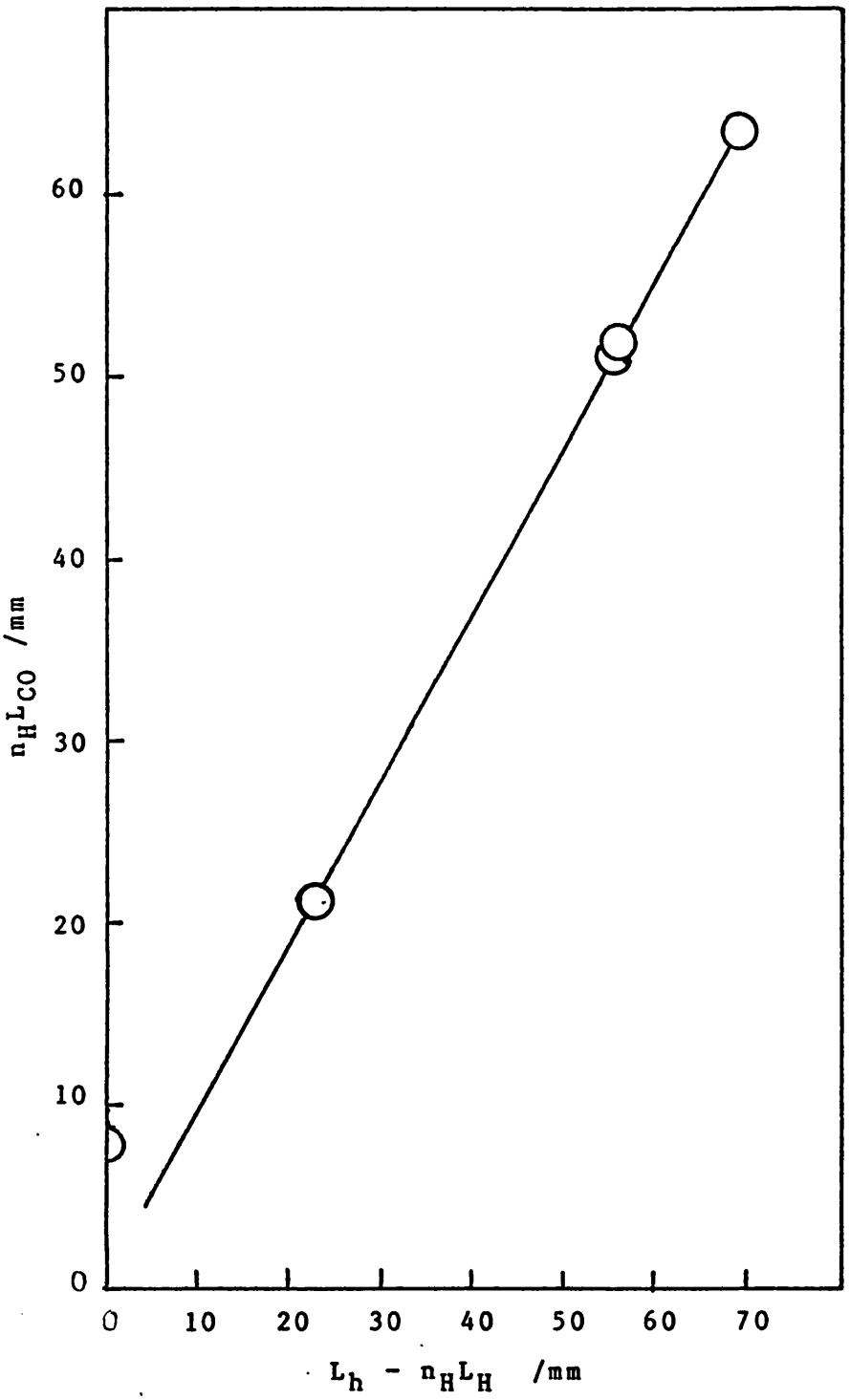

Fig. 3.2 The Mass Spectrometric Calibration for H_2

Table 3.17

Determination of Sensitivity Factor for Hydrogen in the Mass Spectrometer

Mixture /mol % CO	Mixture /mol % H_2	Mol fraction of H_2 (n_H)	Total line length/mm CO	Total line length/mm H_2	$L_H - n_H L_H$	$n_H L_{CO}$
20.1	79.9	0.799	27	110	22.11	21.57
39.8	60.2	0.602	85	137	54.53	51.17
60.0	40.0	0.400	159	114	68.40	63.60
80.0	20.0	0.200	259	70	56.00	51.80
00.0	100.0	1.000	8	155	0	8

Table 3.18

Calculated Sensitivity Factors (S_x) for Mass Spectrometric Analysis

Gas	S_x
CO	1.00 (assigned)
H_2	0.94
CH_4	0.76
C_2H_6	0.43
CO_2	0.95 - 1.05

3.2.3. 5% Cobalt-Spinel

One sample of 5% Cobalt-Spinel (5CoSpinel 2,

0.146 g, SA = 72 m^2g^{-1}) was studied. The sample was one which had been washed with nitric acid to remove CoO-MgO phase.

Initial treatment was with CO up to 920 K for 1 h and an uptake of 0.530 micromol m^{-2} was recorded. Subsequent treatment in H_2 gave a hydrogen uptake of 0.051 micromol m^{-2} (7 h, 930 K), after which a CO hydrogenation experiment was attempted. The activity was negligible. Further treatment in hydrogen at increasing temperatures with catalytic testing (CO + H_2) between reduction treatments is shown in Table 3.19. After each catalytic run the sample was subjected to outgassing at high temperature, typically 875 K. An oxygen chemisorption experiment was also carried out. Unless otherwise stated, uptake values are in micromol m^{-2}. The ratio of CO to H_2 in the catalytic tests was 1:3. and initial activity (rate) is as defined in Section 3.1.

For catalytic runs where measurable activity was noted, product distributions are shown later in a summary table (Table 3.24). After the final hydrogenation experiment, the catalyst was transferred to the flow reactor for further study (Section 3.4.1).

3.2.4. 10% Cobalt-Spinel

A 10% Cobalt-Spinel sample (10CoSpinel 3, 0.403 g, SA = 61 m^2g^{-1}) which had been acid washed was used in these experiments. A procedure similar to that used with the previous sample was then employed, i.e.

reduction treatment of increasing severity followed by testing for catalytic activity.

The results are shown in Table 3.20 where the conditions are as in Table 3.19 unless otherwise stated. Product distributions for runs where activity was seen is shown in Table 3.24.

3.2.5. 15% Cobalt-Spinel

0.420 g of 15CoSpinel (acid-washed, SA = 55 m^2g^{-1}) was used. The results of the reduction treatments and the catalytic testing are shown in Table 3.21. Further details of the second and third catalytic tests are shown in Table 3.24. At the end of the experimental sequence the B.E.T. surface area of the spinel was again measured, and no reduction was seen.

A series of experiments on oxygen chemisorption/ oxidation was carried out to study the effect of gas pressure on uptake. Results are shown in Table 3.22, where each entry indicates admission of a new dose of gas after evacuation at 295 K.

3.2.6. 20% Cobalt-Spinel

An acid-washed sample (20CoSpinel 2, 0.715 g, SA = 53 m^2g^{-1}) was used. Results of the experiments carried out are shown in Table 3.23. More detailed results of the catalytic experiments are shown in Table 3.24.

As with the previous sample a B.E.T. surface area determination was carried out at the end of the experimental sequence. The value obtained was slightly higher than the original measurement and it was

concluded that no reduction in surface area had occurred.

Table 3.19

Reduction and Catalytic Behaviour of 5CoSpinel 2

Treatment	Temp./K (max.)	Result (Uptake values in micromol m^{-2})
CO/1 h	920	Uptake 0.530
H_2/7 h	930	Uptake 0.051
CO + H_2	575	No reaction after 4 h
H_2/3 h	940	Uptake 0.143
CO + H_2	575	No reaction after 2 h
CO + H_2	633	No reaction after 2 h
H_2/3 h	975	Uptake 0.445
CO + H_2	575	No reaction after 3 h
CO + H_2 $CO:H_2$ = 1:2.9	613	Init. rate 0.001; Conv. 26% over 1.5 h; Mostly methane, some CO_2. See Table 3.24,a
H_2/6 h	1005	Uptake 1.000
CO + H_2	575	No reaction after 1 h
CO + H_2	643	Init. rate 0.023; Conv. 14% over 4 h; Large formation CO_2. See Table 3.24,b
H_2/13 h	1030	Uptake 0.552
O_2/ 0.2 h	293	Uptake 0.266
O_2/ 1.2 h	600	Uptake 1.714
H_2/ 4 h	625	Uptake 3.150
CO + H_2 $CO:H_2$ = 1:2.8	575	Init. rate 0.066; Conv. 18% over 6 h. Traces of C_2. See Table 3.24,c.

In this and the following tables conversion is based on carbon-containing products.

Table 3.20

Reduction and Catalytic Behaviour of 10CoSpinel 3

Treatment	Temp./K (max.)	Result (Uptake values in micromol m^{-2})
CO/1 h	890	Value of uptake not reliable
H_2/1.5 h	870	Uptake 1.103
CO + H_2	573	No reaction after 1 h
H_2/1.5 h	940	Uptake 0.932
CO + H_2	575	No reaction after 1 h
CO/2 h	980	Sample holder accidentally leaked to atm pressure at 980 K. for approximately 1 min. SA check follows
Outgas	980	
B.E.T.	77	SA = 62 m^2g^{-1}(no change)
CO/4 h	990	Uptake 1.212
H_2/9 h	1000	Uptake 1.266
CO + H_2	580	No measurable reaction after 10 h
H_2/8 h	1070	Uptake 0.724
CO + H_2 $CO:H_2$ = 1:2.7	574	Init. rate 0.049; Conv. 15% after 60 h. The C_2 and C_3 account for 15% of products; Small (ca.2%)CO_2. See Table 3.24,d.
O_2/2 h	292	Uptake 0.703
O_2/1.5 h	660	Uptake 1.108
H_2/1 h	693	Uptake 3.422
CO + H_2 $CO:H_2$ = 1:2.3	ca 575	Init. rate 0.143; Conv. 30% /20 h; Significant C_2 and C_3. See Table 3.24,e.
O_2/1 h	291	Uptake 0.732
O_2/1.5 h	685	Uptake 1.271
H_2/6 h	687	Uptake 3.161

Table 3.21

Reduction and Catalytic Behaviour of 15CoSpinel

Treatment	Temp./K (max.)	Result (Uptake values in micromol m^{-2})
$CO + H_2$	575	Init. rate very slow; Conv. not measured; No analysis of products
CO/0.5 h	291	Uptake 0.144
CO/17 h	933	Uptake 0.874
H_2/20 h	971	Uptake 2.180
$CO + H_2$ $CO:H_2 = 1:3:4$	575	Init. rate 0.669; Conv. 61% over 6 h. Condensed products mostly CO_2. See Table 3.24,f
O_2/1 h	290	Uptake 0.732
O_2/1 h	623	Uptake 1.468
H_2/5 h	585	Uptake 2.628
O_2	295	See Table 3.8
H_2/12 h	620	
O_2/0.5 h	293	Uptake 0.588
O_2/2 h	671	Uptake 1.354
H_2/3 h	664	Uptake 3.490
$CO + H_2$	575	Init. rate 0.622; Conv 32%; Cond. products mostly CO_2. See Table 3.24,g

Table 3.22

O_2 Uptake on 15CoSpinel

Run no.	T/K	Pressure /torr	Uptake /micromol m^{-2} Each run	Total
1	295	nil	0.531	0.531
2	295	3.38	0.103	0.634
3	295	4.65	0.073	0.707
4	295	11.22	0.016	0.723
5	295	17.60	nil	0.723

Note: Pressure refers to final value

Table 3.23

Reduction and Catalytic Behaviour of 20CoSpinel 2

Treatment	Temp./K (max.)	Result (Uptake values in micromol m^{-2})
CO/1 h	293	Uptake 0.313
CO/20 h	952	Uptake 1.059
H_2/12 h	980	Uptake 0.826
O_2/0.5 h	293	Uptake 0.297
O_2/2 h	675	Uptake 0.749
H_2/3 h	703	Uptake 1.925
CO/0.5 h	293	Uptake 0.110
CO + H_2 CO:H_2 = 1:3.2	573	Init. rate 0.194; Conv. 41% over 12 h. See Table 3.24,h
O_2/0.5 h	292	Uptake 0.288
O_2/1.5 h	975	Uptake 0.893
H_2/7 h	613	Uptake 1.675
CO + H_2 CO:H_2 = 1:4.1	575	Init. rate 0.426; Conv. 41% over 4 h. See Table 3.24,i

Table 3.24

Products of CO Hydrogenation

Over Cobalt-Spinel Catalysts

Ref.	$CO:H_2$ ratio	Catalyst	Conv.* /%	Products/mol%				
				CH_4	C_2H_4	C_2H_6	C_3	CO_2
a	1:2.9	5CoSpinel 2	26	95.6	0.3	1.1	0.7	2.3
b	1:3.0	5CoSpinel 2	14	85.4	4.4		0.4	9.8
c	1:2.8	5CoSpinel 2	18	92.3	0.7		0	8.2
d	1:2.7	10CoSpinel 3	15	82.7	2.7	10.1	1.9	2.6
e	1:2.3	10CoSpinel 3	30	29.4	23.3	24.7	8.6	14.0
f	1:3.4	15CoSpinel	61	68.2	0.8	0.1	0.3	30.6
g	1:3.0	15CoSpinel	32	90.7	2.0		0	7.3
h	1:3.2	20CoSpinel 2	41	86.0	8.7		0	5.3
i	1:4.1	20CoSpinel 2	57	98.6	0.9		0	0.5

* Conversion with respect to CO

3.3 Catalytic Studies in the First Flow System

Studies in the first flow system were aimed more at assessment of the apparatus design rather than detailed study of any one catalyst. However, in addition to various isolated experiments, the 10NiO-MgO system was studied. All quantitative work was based on the supposition that (for a symmetrical peak) the peak area was proportional to the height of the peak times the width of the peak at half height. This assumption was needed as no integrator was available at this time.

10NiO-MgO

10NiO-MgO (0.40 g) was loaded into the reactor and re-reduced in H_2 overnight (the sample had already been reduced in the static system). The activation energy for methanation was measured using the method described in Section 2 (see also Section 3.4 below) by making runs at various temperatures and monitoring the size of the methane peak. By plotting ln (peak size) versus 1/T, the activation energy was calculated as 153 kJ mol^{-1} (Fig. 3.3 $CO:H_2$ = 1:3, 575 K).

Orders of reaction for methanation were established by varying the partial pressure of each gas. The values obtained were -0.9 for CO and 0.9 for hydrogen (see Fig. 3.4).

The deactivation of the catalyst was studied at 575 K ($CO:H_2$ = 1:2) and the information is shown in Fig. 3.5. Fig. 3.6 shows the increase in the size of the methane peak in another experiment after the CO stream was turned off.

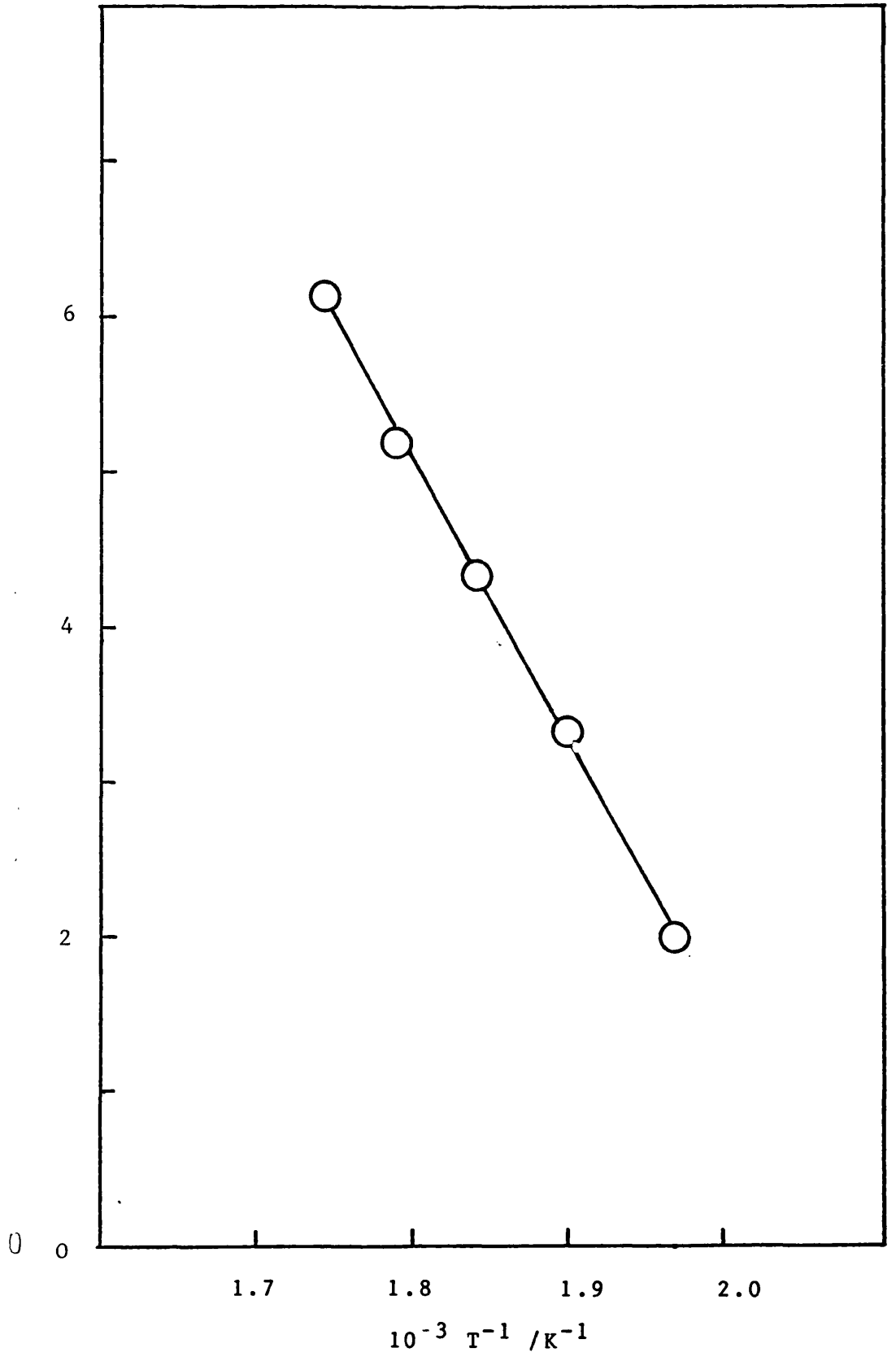

Fig. 3.3 Arrhenius Plot for 10NiO-MgO

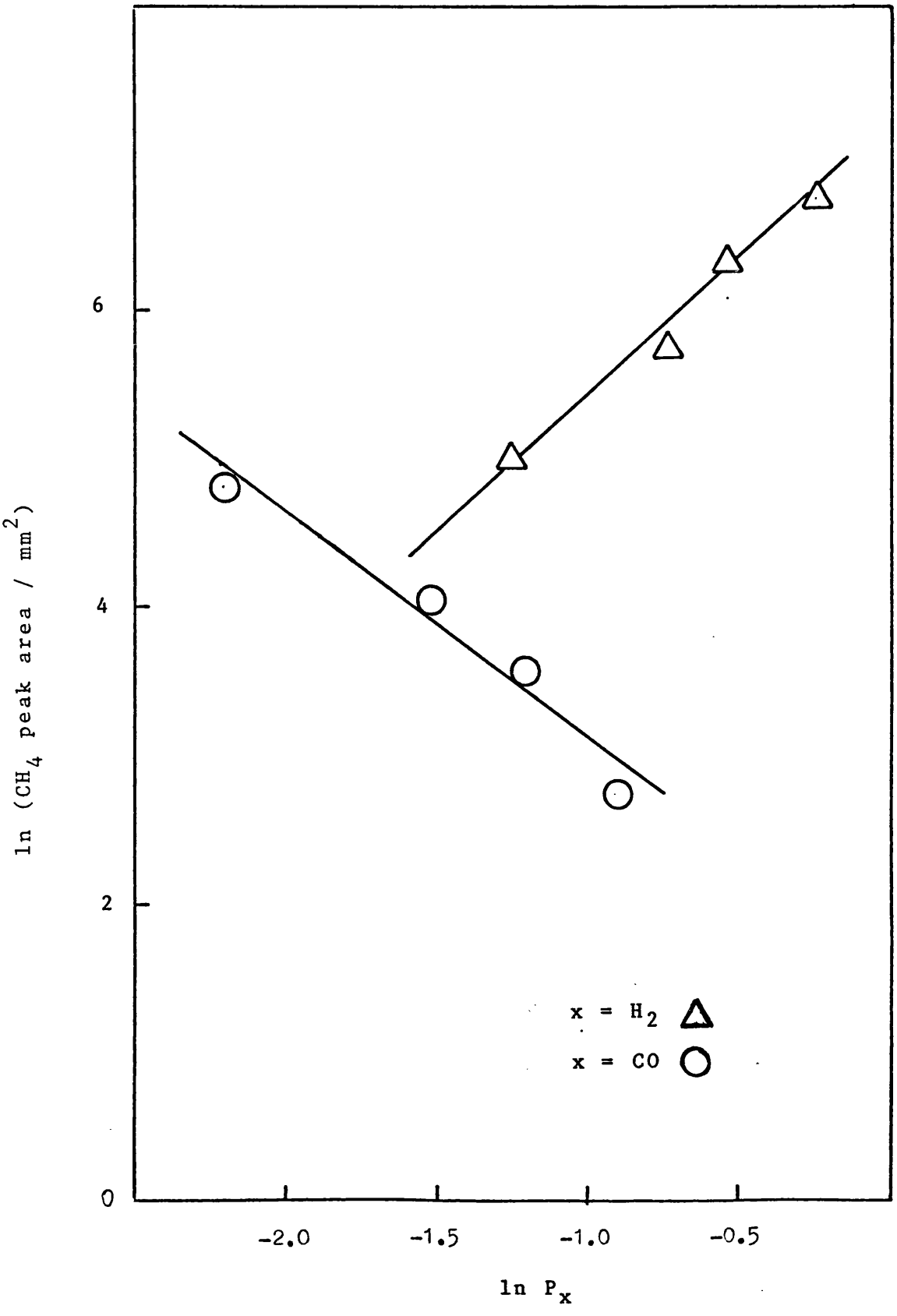

Fig. 3.4 Orders of Reaction for Methanation Over 10NiO-MgO

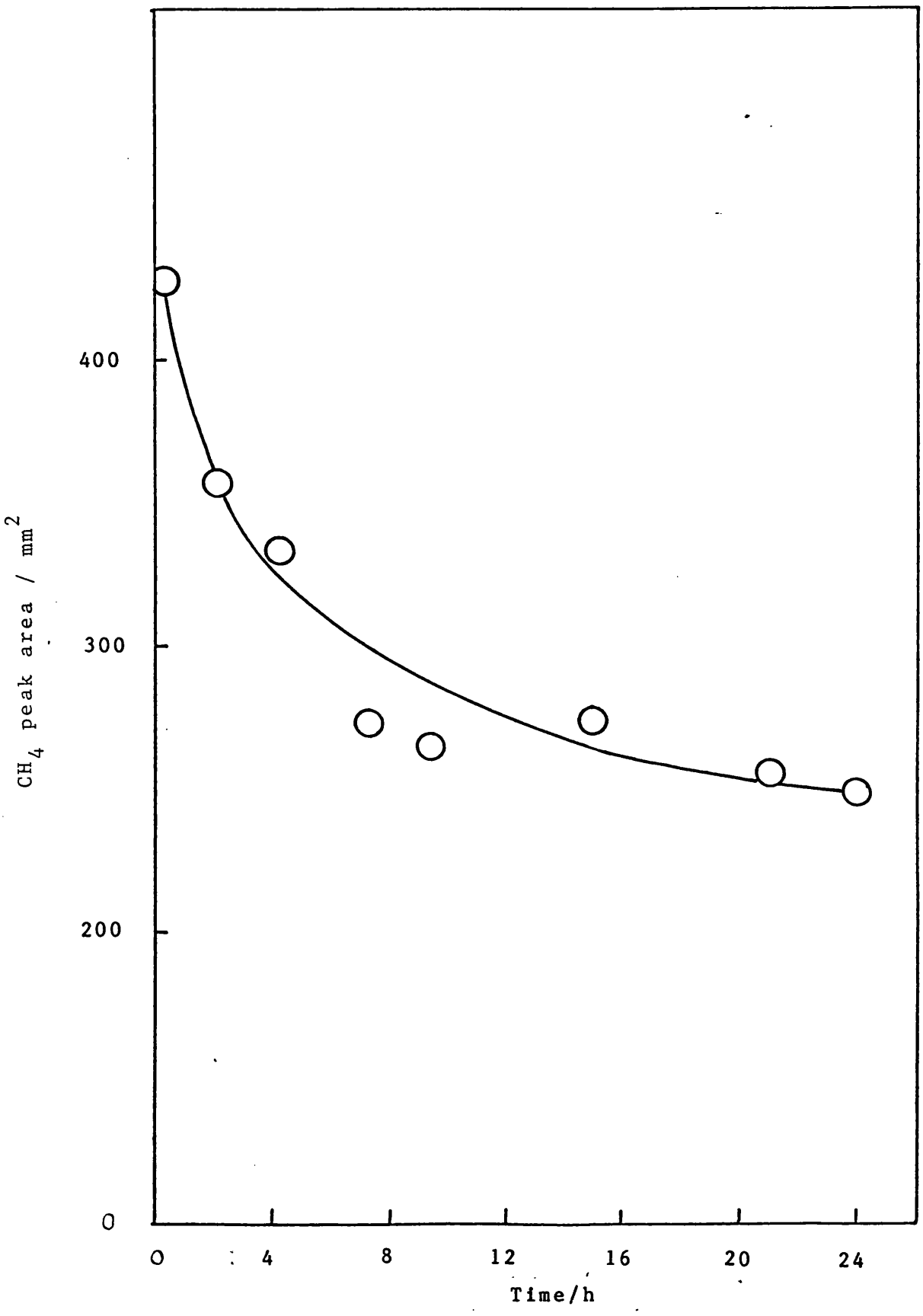

Fig. 3.5 Deactivation with Time of 10NiO-MgO

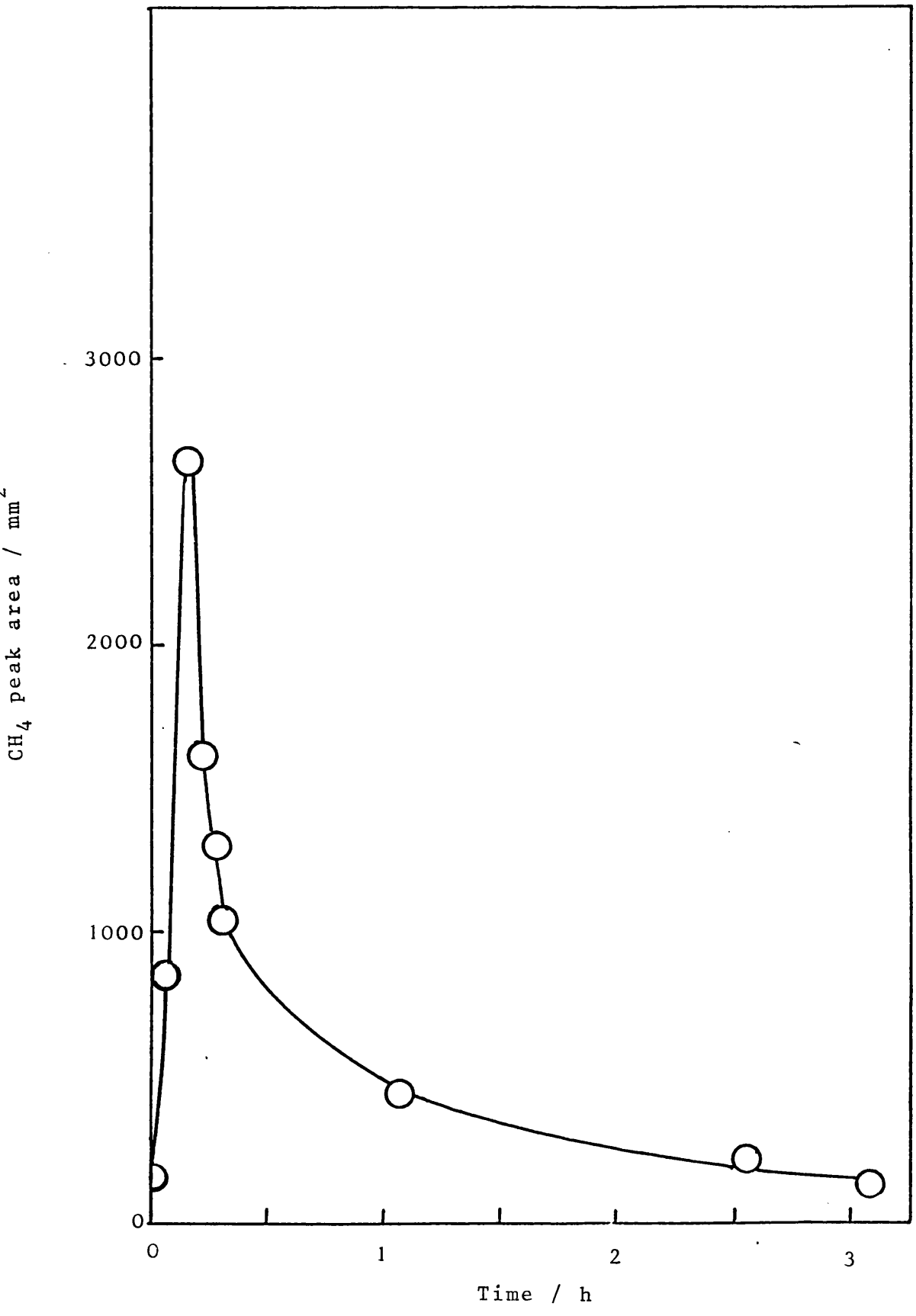

Fig. 3.6 Methane Peak Area with Time after CO Turned off Over 10 NiO-MgO

3.4. Catalytic Studies in the Second Flow System

CO hydrogenation was investigated on reduced Co-containing spinels with cobalt concentrations ranging from 5 to 20 mol % cobalt. The gas flow and GC analysis system will first be described.

The flow system (Section 2.4.2.) contained rotameters for the helium, hydrogen and CO streams. These were supplied with a notional set calibration by the manufacturers but the calibrations were checked after installation. The calibrations were found to be nearly linear, but flow rates departed considerably from the set values. Results are shown in Table 3.25.

The normal operating conditions for the GC analysis were those given in Table 3.26. The sensitivity of both detector systems was determined for all expected feed and product gases. The method used was to inject pure samples of each gas into the system using the same sample loop and integrate the response of the detector into a "count number " by means of a computing integrator. By setting the count for one gas equal to unity, the difference in response of the detector to different gases could be taken into account by introducing a "sensitivity factor" into analysis calculations. For each gas the retention time was also measured. Using the thermal conductivity detector the factor was set at 1.00 for carbon monoxide, and Table 3.27 shows the results of this procedure. The flame ionization detector was calibrated in the same

Table 3.25

Comparison of Indicated Flow to True Flow for Gases Used in the Flow System

Gas	Set flow rate $cm^3\ min^{-1}$	Measured flow rate $cm^3\ min^{-1}$			
		1	2	3	Mean
Helium	6	6.1	6.1	6.1	6.1
	10	10.4	10.4	10.4	10.4
	20	23.0	23.2	22.9	23.0
	30	35.5	35.7	35.7	35.6
	40	47.2	48.0	48.6	47.9
	50	62.5	62.5	62.5	62.5
	60	77.9	77.9	78.3	78.0
Hydrogen	10	10.8	10.8	10.9	10.8
	20	21.6	21.4	21.4	21.5
	30	31.9	32.2	32.2	32.1
	40	42.8	42.8	43.1	42.9
	60	66.7	66.7	66.7	66.7
	80	86.5	87.4	86.5	86.8
	100	107.1	105.8	107.1	106.7
Carbon monoxide	10	10.5	10.5	10.4	10.5
	20	21.3	21.1	21.1	21.2
	30	32.9	32.8	32.9	32.9
	40	44.8	44.8	44.9	44.8
	50	56.6	56.5	56.6	56.6
	60	68.8	69.0	68.7	68.8

Table 3.26

Normal Operating Conditions for GC Analysis

Parameter	Normal setting
Column carrier flow rate	30 cm^3 min^{-1}
Column temperature	363 K
Injector temperature	353 K
Detector temperature	423 K
Flame ionization detector attenuation	80
Thermal conductivity detector attenuation	4
Rear column packing	Poropak Q (F.I.D.)
Front column packing	Molecular sieve 5A
Injection loop size (pre-reactor)	0.20 cm^3
Injection loop size (post reactor)	0.23 cm^3

Table 3.27

Retention Time, Peak Area and Calculated Sensitivity Factors Using the T.C.D. System

Gas	Mean retention time /min	Mean Integrated peak area /counts	Sensitivity coefficient
Oxygen	1.87	10522090	1.12
Carbon monoxide	7.77	11797955	1.00
Hydrogen	1.10	174865	67.46
Methane	4.63	9615481	1.23

way. In this case methane was used as the internal standard and was assigned a sensitivity coefficient of 1.00. The results for the F.I.D. are shown in Table 3.28.

In order to provide a check on the accuracy of the calibration system, a known mixture of gas was analyzed using the T.C. detector. The results of this are shown in Table 3.29. No suitable gas mixture was available for the FID system at this time and hence the corresponding experiment was not performed. Much later a suitable sample mixture was made available by I.C.I. Plc which, when analyzed, indicated that the procedure was accurate to better than 10% for all gas mixtures encountered, and considerably more accurate in most instances.

Table 3.28

Retention Time, Peak Area and Calculated Sensitivity Factors Using the F.I.D. System

Gas	Mean retention time /min	Mean integrated peak area /counts	Sensitivity coefficient
Methane	0.77	67274804	1.00
Ethene	1.38	104432426	0.64
Ethane	1.50	113599076	0.59
Propene	3.79	270682440	0.25
Propane	3.95	260116460	0.26
Butene	13.62	790465516	0.08
Butane	10.38	700625860	0.10

Table 3.29

Analysis of Known Mixture Using the TC Detector

Gas	Actual/mol %	T.C.D. Analysis/mol %
Methane	22.5	23.5
Hydrogen	56.8	57.1
Carbon monoxide	20.7	18.4

The following sections describe the catalytic results for 5, 10, 15 and 20 mol % cobalt-containing magnesium aluminate spinels, respectively.

3.4.1. 5% Cobalt-Spinel

3.4.1.1. 5CoSpinel 1

A weight of 0.600 g of the solid solution was loaded into the reactor. In order to assess the activity of the sample prior to reduction of divalent cobalt, the solid solution was tested with a mixture of carbon monoxide and hydrogen immediately after loading into the flow reactor. The sample was then treated with CO ($20cm^3\ min^{-1}$) for 4 h at 775 K before testing again for catalytic activity.

After this the catalyst was exposed to CO (875 K, 20 h), before again testing for CO hydrogenation activity. The results of the catalysis experiments are shown in Table 3.30, where the activity for methane formation is shown.

Table 3.30

Initial Activity of 5CoSpinel 1

Ref.	Temp/K	Set flow/cm^3 min^{-1}		Activity/ counts
		CO	H_2	Methane
a	623	10	30	7046
b	621	8	30	10933
c	587	10	30	1112
d	584	10	30	4525

a: After 0.5 h at set flow
b: After 1.5 h at set flow
c: After CO 20 cm^3/min 775 K,4 h
d: After CO 20 cm^3/min 875 K,20 h

Reduction using hydrogen was then attempted. The sample was left in hydrogen at 875 K overnight and was then tested for activity in the catalytic reaction. As can be seen from the results, this treatment resulted in a large increase in activity (Table 31).

In all the following results, the data obtained for propene (or propene plus propane if the two were not resolved) have been corrected for the known small amount in the CO feed gas. The correction was applied by analysis of the feed gas ahead of the reactor and subtraction of the appropriate count from the propene integration prior to calculation of percentage product distribution. A typical correction was 20000 counts. Errors due to differences in gas density before and after the reactor were estimated to be small, and were

neglected.

The catalytic data in Table 3.31 allowed the activation energy with respect to methane to be evaluated. The activation energy calculated from the plot of ln(CH_4 count) vs 1/T (Fig. 3.7), was 152 kJ mol^{-1}.

The effect of varying the CO:H_2 ratio at 575 K is shown in Table 3.32. The orders of reaction with respect to CO and hydrogen for methane formation were calculated from the plots of ln(CH_4 count) vs. ln[(CO flow)/(total flow)] or ln[(H_2 flow)/(total flow)], respectively. These are shown in Fig. 3.8 and lead to values of -0.6 for CO and 1.1 for H_2.

Between the sets of runs for activation energy determination, order with respect to CO and order with respect to H_2, the catalyst was treated with hydrogen at 775 K to clean the surface of carbonaceous deposits. Each set of runs typically occupied 4-5 h.

Finally, the long-term deactivation of the catalyst was tested by flowing a 1:3 CO:H_2 mixture over the sample for about 60 h. The results of this experiment are shown in Table 3.33 and Fig. 3.9.

3.4.1.2. 5CoSpinel 2

This sample of 5% CoSpinel was treated differently to the first one in that after preparation in the high temperature oven it was washed with nitric acid to remove any CoO-MgO phase (Section 2.2.3). The sample was then studied in the static system (Section 3.2.2)

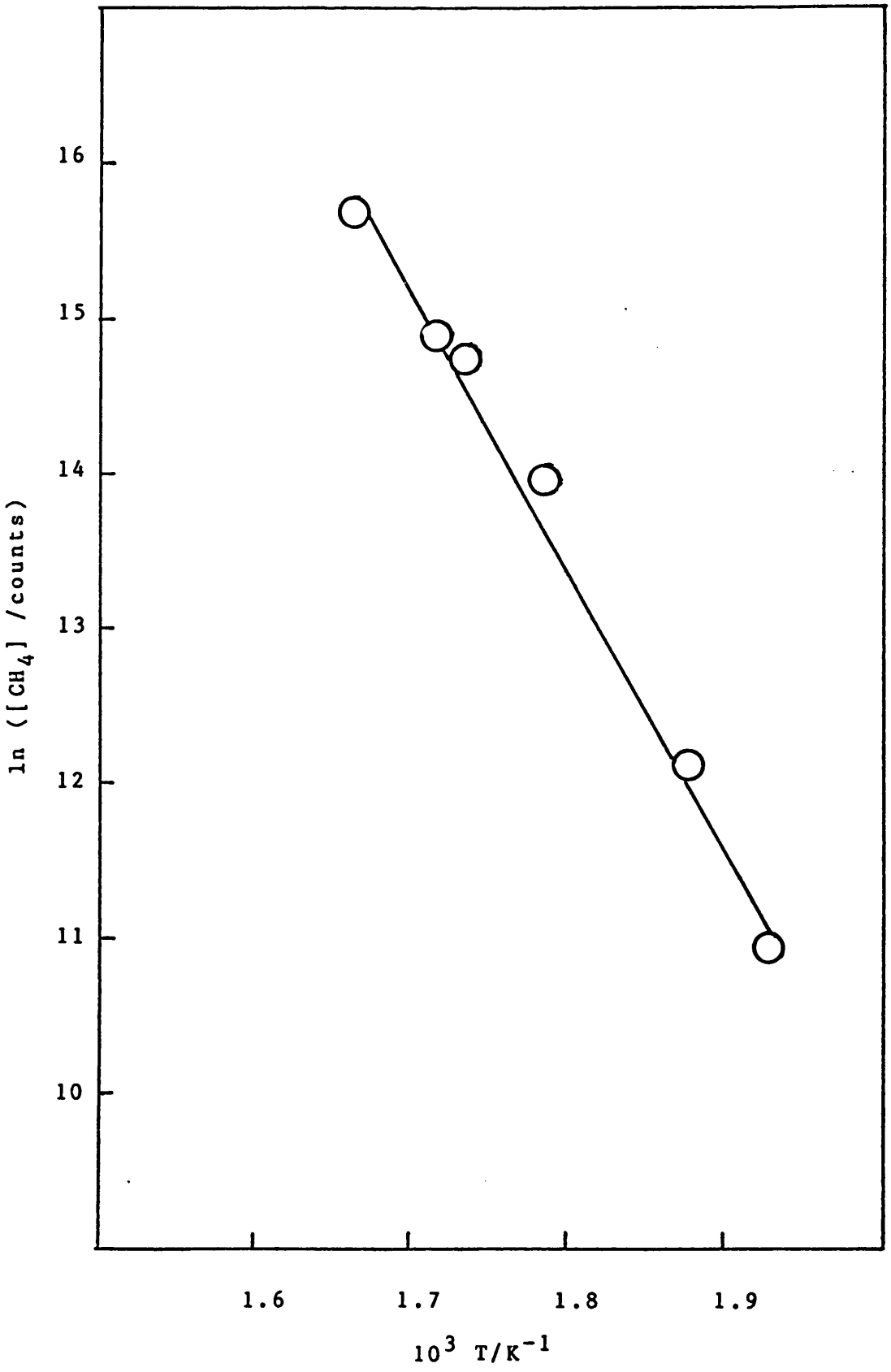

Fig. 3.7 Arrhenius Plot for 5CoSpinel 1

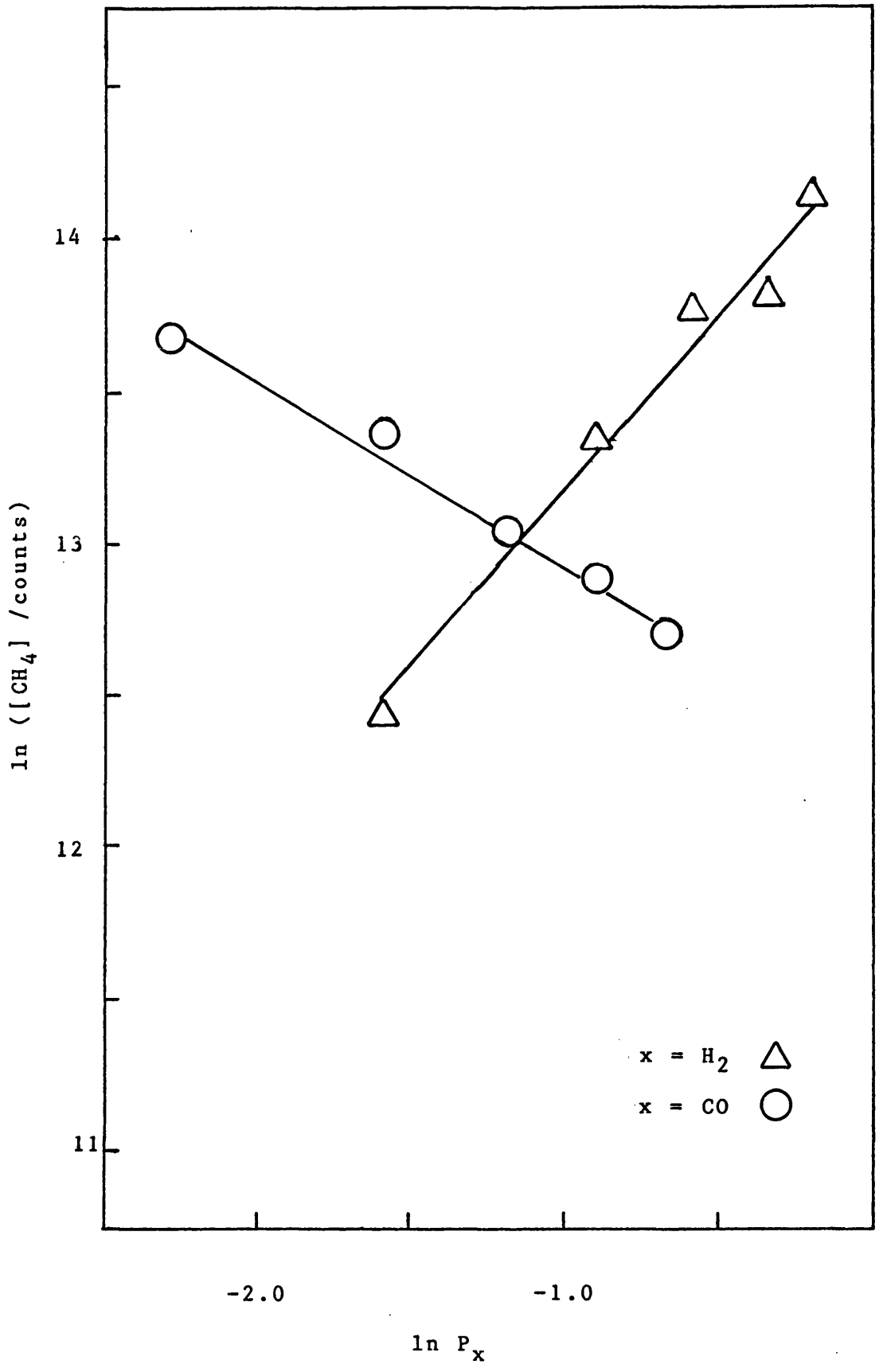

Fig. 3.8 Orders of Reaction for Methanation Over 5CoSpinel 1

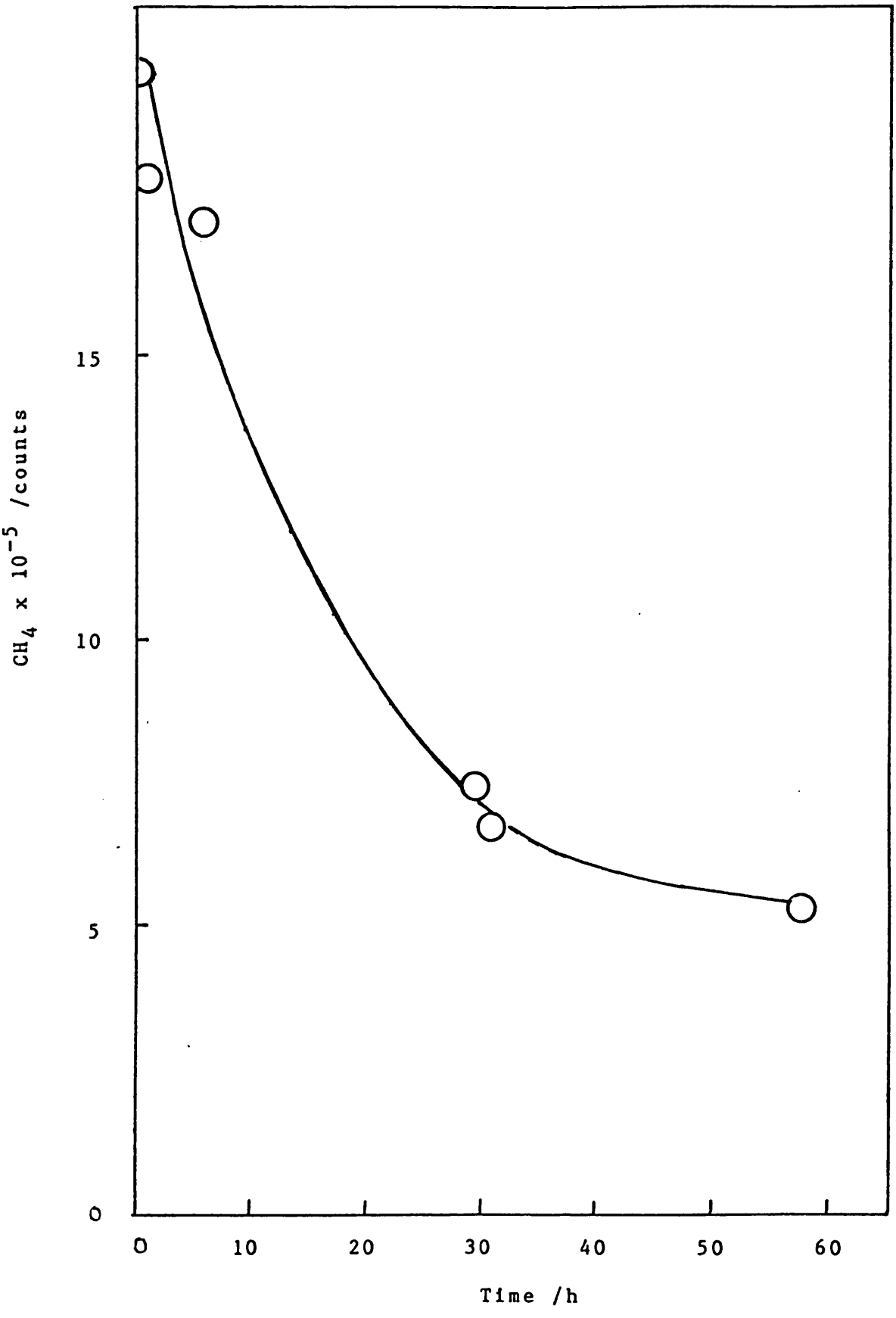

Fig. 3.9 Deactivation with Time of 5CoSpinel 1

and was subjected to high temperature reduction in hydrogen. 0.14 g was then loaded into the flow

Table 3.31

Activity of 5CoSpinel 1 in Carbon Monoxide Hydrogenation after High Temperature Reduction in Hydrogen ($CO:H_2=1:3.5$)

T/K	Products /counts (mol %)*				
	CH_4	C_2H_4	C_2H_6	C_3	Total count
519	54821	7977	6986	13067	82851
	81.44	7.58	6.12	4.86	
533	198515	11454	33514	37943	281426
	84.44	3.12	8.41	4.03	
559	1132753	187728		132197	1452678
	88.73	8.68		2.59	
575	2565720	355882		198499	3120101
	90.81	7.43		1.76	
580	2949602	395129		202169	3544900
	91.24	7.21		1.55	
599	6590176	665213		247454	7502843
	93.55	5.57		0.88	
518**	44913	7773	7648	15689	76023
	77.01	8.53	7.74	6.72	

* N.B. In this and all succeeding similar Tables "Products /counts (mol %)" signifies entries in which the first row of any pair gives the number of counts and the second row the respective molar percentage.

** This run performed as a check on deactivation

Table 3.32

Effect of Varying $CO:H_2$ Partial Pressures for CO Hydrogenation Over 5CoSpinel 1 at 575 K

Flow rate $cm^3 min^{-1}$			Products /counts (mol %)			
CO	H_2	He	CH_4	C_2H_4	C_2H_6	C_3
25	25	0	335390 68.69	86134 11.29	83357 10.07	194357 9.95
20	25	5	400271 73.17	70003 8.19	100725 10.86	170035 9.95
15	25	10	459122 78.29	48056 5.24	108227 10.89	130910 5.58
10	25	15	645546 84.34	158439 12.21		105480 3.46
5	25	20	880299 89.24	150653 9.01		69220 1.75
10	40	0	1413882 89.83	217755 8.16		126697 2.01
10	35	5	1014155 88.64	173072 8.92		111589 2.44
10	30	10	970545 86.79	193483 10.21		134459 3.00
10	20	20	631454 82.40	171812 13.23		134094 4.37
10	10	30	252702 70.68	129066 21.30		114759 8.02

Table 3.33

Deactivation of 5CoSpinel 1 at 575 K ($CO:H_2$ = 1:3)

Over 60 Hours

Run time /hours	Products /counts (mol %)			
	CH_4	C_2H_4	C_2H_6	C_3
0.0	2002910 86.32	420022 10.68		277974 3.00
1.0	1818311 86.36	378062 10.59		256633 3.05
5.5	1735109 86.45	358251 10.53		242146 3.02
29.5	745489 82.61	63693 4.52	131877 8.62	153623 4.25
30.5	676131 82.64	65132 5.09	111654 8.05	138045 4.22
57.7	529459 81.87	68668 6.80	78043 7.12	109056 4.21

reactor and left overnight at 625 K in flowing hydrogen. A higher temperature was not used as this sample had already been pre-reduced. Catalytic testing subsequent to this is described in Table 3.34.

It was noted that the activity of this sample was much less than that of 5CoSpinel 1 (compare counts in Tables 3.31 and 3.34). Activation energy measurements were made and were found to be unexpectedly low (75 kJ

Table 3.34

Initial Activity of 5CoSpinel 2

T/K	Products /counts (mol %)				
	CH_4	C_2H_4	C_2H_6	C_3	Total count
565	51617 65.84	27330 22.31		37177 11.85	116124
564	49887 68.30	23410 20.51		32706 11.19	106003

N.B. $CO:H_2$ ratio = 1:3
The second run was 0.5 h after the first

mol^{-1}). Repetition after repacking the reactor and using lower flow rates failed to give larger values. It was suspected that diffusion effects in the reactor were responsible, and no further work with this sample was undertaken.

3.4.2. 10% Cobalt-Spinel

This sample (10CoSpinel 3) was one which had been previously studied in the static system and had therefore been exposed to high temperature reduction treatment. The weight of catalyst loaded was 0.345 g. The sample was one which had been washed to remove any CoO-MgO phase. After treatment in hydrogen at 725 K overnight, the catalytic behaviour of the sample was measured at various temperatures as before and the activation energy was found to be 87 kJ mol^{-1} (Table 3.35 and Fig. 3.10).

The order of reaction with respect to CO and hydrogen was then found by varying the partial pressure of the gases at constant temperature and the data from these experiments are shown in Table 3.36, the corresponding ln plots being Fig. 3.11. The values obtained were -0.6 for CO and 1.5 for H_2

The deactivation of this catalyst was measured (Table 3.37 and Fig. 3.12) and following this, the activation energy was again measured in the normal manner and the value calculated was then 90 kJ mol^{-1}.

An attempt was made to measure CO chemisorption using a flow chemisorption technique but no measurable uptake was recorded.

3.4.3. 15% Cobalt-Spinel

One 15CoSpinel sample was studied as a 0.40 g washed sample (nitric acid treatment as before to remove CoO-MgO phase) and had been previously subjected to high temperature treatment in hydrogen in the static system.

Before any other treatment, an attempt was made to measure CO uptake on the sample using a flow chemisorption technique. After an overnight treatment in hydrogen at 615 K, a plug of CO of accurately known volume was flowed over the catalyst, and the peak due to the gas was measured before and after exposure to the catalyst using the extra T.C.D. detector attached to the system. The results of the experiments did not compare well with similar (but more accurate) experiments carried out on the same catalyst in the static system.

Table 3.35

Activity of 10CoSpinel 3 in Carbon Monoxide Hydrogenation After Reduction in Hydrogen at 775 K ($CO:H_2$ = 1:3)

T/K	Products /counts (mol %)				
	CH_4	C_2H_4	C_2H_6	C_3	Total count
570	49286	17771	5116	34339	106512
	68.20	15.73	4.18	11.89	
530	11806	5132		12857	29795
	64.50	17.94		17.56	
544	18709	5975	2097	15994	42775
	69.30	14.17	4.58	11.91	
550	23023	7389	2992	17293	50697
	68.03	13.97	5.23	12.77	
557	30045	13724		21150	64919
	68.11	19.91		11.98	
570	46974	18686	5412	32374	103446
	66.89	17.03	4.55	11.52	

The uptakes recorded were only a few per cent of those expected on the basis of the static system experiments.

The material was then tested in CO hydrogenation (Table 3.38) and a very large activity, as seen from the total count, was found. The sample was left in flowing hydrogen for 12 h and then an attempt was made to measure the activity at various temperatures in order to determine the activation energy. It was found difficult to make the measurements as the material was deactivating more quickly than other catalysts studied,

Table 3.36

Effect of Varying CO:H_2 Partial Pressures for CO Hydrogenation Over 10CoSpinel 3 at 575 K

Flow rate $cm^3 min^{-1}$			Products /counts (mol %)			
CO	H_2	He	CH_4	C_2H_4	C_2H_6	C_3
25	25	0	50670 54.26	33627 23.05		84746 22.69
20	25	5	60801 60.13	35373 22.39		70737 17.48
15	25	10	77396 66.85	36707 20.29		59542 12.86
10	25	15	105645 76.42	35912 16.63		38413 6.95
5	25	20	149721 87.25	28605 10.67		14260 2.08
10	40	0	176280 81.81	20169 5.99	25096 6.87	45950 5.33
10	30	10	105493 75.64	23552 10.81	14408 6.10	41587 7.45
10	20	20	52867 66.85	27591 22.33		34229 10.82
10	15	25	33690 61.91	22274 26.20		25877 11.89
10	10	30	19814 55.74	16226 29.21		21402 15.05

Table 3.37

Deactivation of 10CoSpinel 3 at 575 K ($CO:H_2$ = 1:3)

Over 65 Hours

Run time / hours	Products /counts (mol %)			
	CH_4	C_2H_4	C_2H_6	C_3
0.00	89430 65.15	30259 14.11	20252 8.71	66076 12.03
0.75	74414 66.07	24818 14.10	15943 8.35	51732 11.48
1.50	73016 66.06	24449 14.16	15103 8.06	51837 11.72
3.00	68392 65.87	24015 14.80	13717 7.79	47921 11.54
5.00	67812 66.71	23570 14.84	12711 7.38	45016 11.07
29.00	53186 64.69	30702 23.90		37517 11.41
49.00	43943 62.19	26840 24.31		38162 13.50
65.00	42066 61.21	26021 24.24		40000 14.55

but after about 8 h the rate of deactivation reduced and the nessessary runs were made. Table 3.39 shows how the activity and selectivity vary with temperature and the methanation activation energy was found to be 110 kJ mol^{-1} (Fig.13). Orders of reaction were calculated from appropriate experimental runs as before. The values obtained were -0.5 for CO and 1.5 for H_2

(Table 3.40 and Fig. 3.14). The effect of altering the feed gas ratio (but without making up the flow with He) was

Table 3.38

Initial Activity of 15CoSpinel 1

T/K	Products /counts (mol %)				
	CH_4	C_2H_4	C_2H_6	C_3	Total count
565	9817972 96.86	461912 2.92		89864 0.22	10369748
573	11885846 97.45	457871 2.40		74504 0.15	12418221

Table 3.39

Activity of 15CoSpinel in CO Hydrogenation ($CO:H_2$ = 1:3)

T/K	Products /mol % (counts)				
	CH_4	C_2H_4	C_2H_6	C_3	Total count
517	328729 82.09	25932 4.14	51290 7.56	99456 6.21	505407
528	607931 84.15	30442 2.70	95626 7.80	154563 5.35	888562
548	1713368 87.62	279863 9.16		251573 3.22	2244804
561	2747774 89.78	381384 7.98		273820 2.24	3402978
582	5725178 92.75	592168 6.14		274231 1.11	6591577

Table 3.40

Effect of Varying CO:H_2 Partial Pressures for CO Hydrogenation Over 15 CoSpinel at 575 K

Flow rate $cm^3 min^{-1}$			Products /counts (mol %)			
CO	H_2	He	CH_4	C_2H_4	C_2H_6	C_3
25	25	0	83997 60.21	49365 22.65		95646 17.14
20	25	5	111541 62.57	64558 23.19		101487 14.24
15	25	10	123888 67.41	60082 20.92		85814 11.67
10	25	15	157179 72.44	66526 19.62		68943 7.94
5	25	20	212441 79.13	44308 10.56	24691 5.43	52440 4.88
10	40	0	1228174 88.44	192361 8.86		149756 2.70
10	35	5	863726 87.30	145226 9.39		130880 3.31
10	30	10	548033 86.28	34327 3.38	76530 6.95	137604 5.30
10	20	20	392139 82.94	39455 5.34	49958 6.23	103762 5.49
10	15	25	263892 77.49	50136 9.43	28517 4.94	110948 8.14
10	10	30	116839 68.33	50999 19.08		86105 12.59

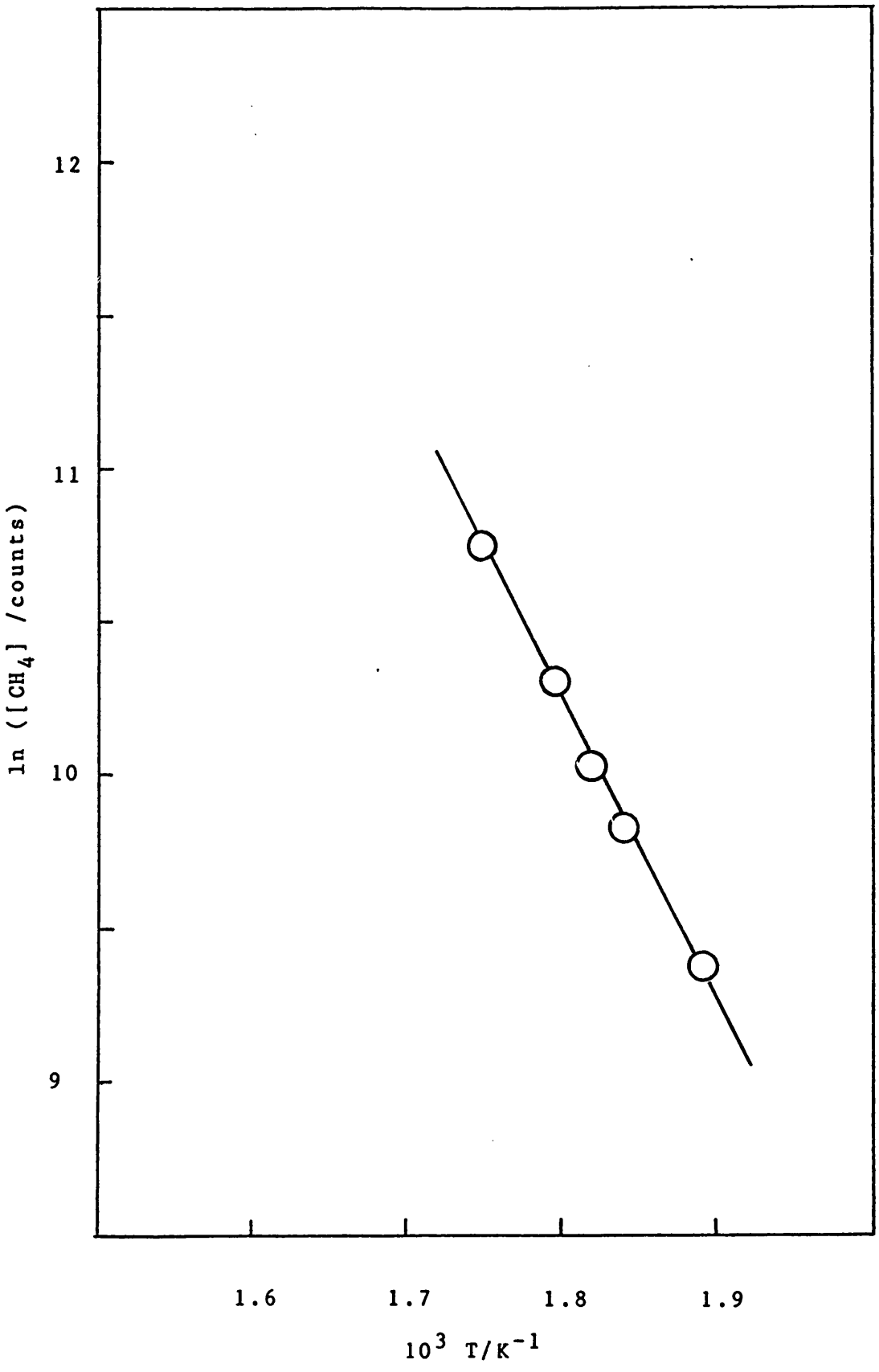

Fig. 3.10 Arrhenius Plot for 10CoSpinel 3

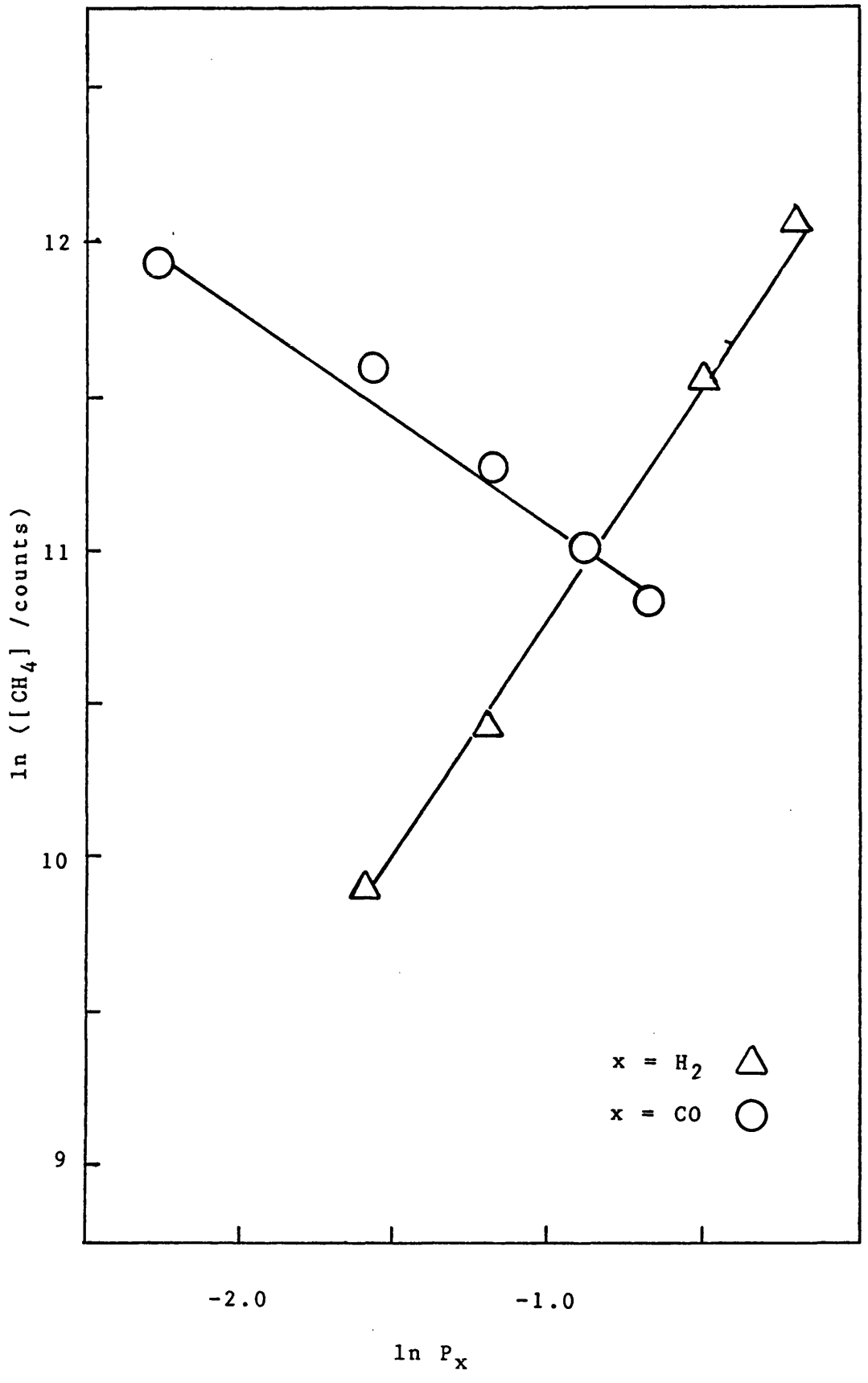

Fig. 3.11 Orders of Reaction for Methanation Over 10CoSpinel 3

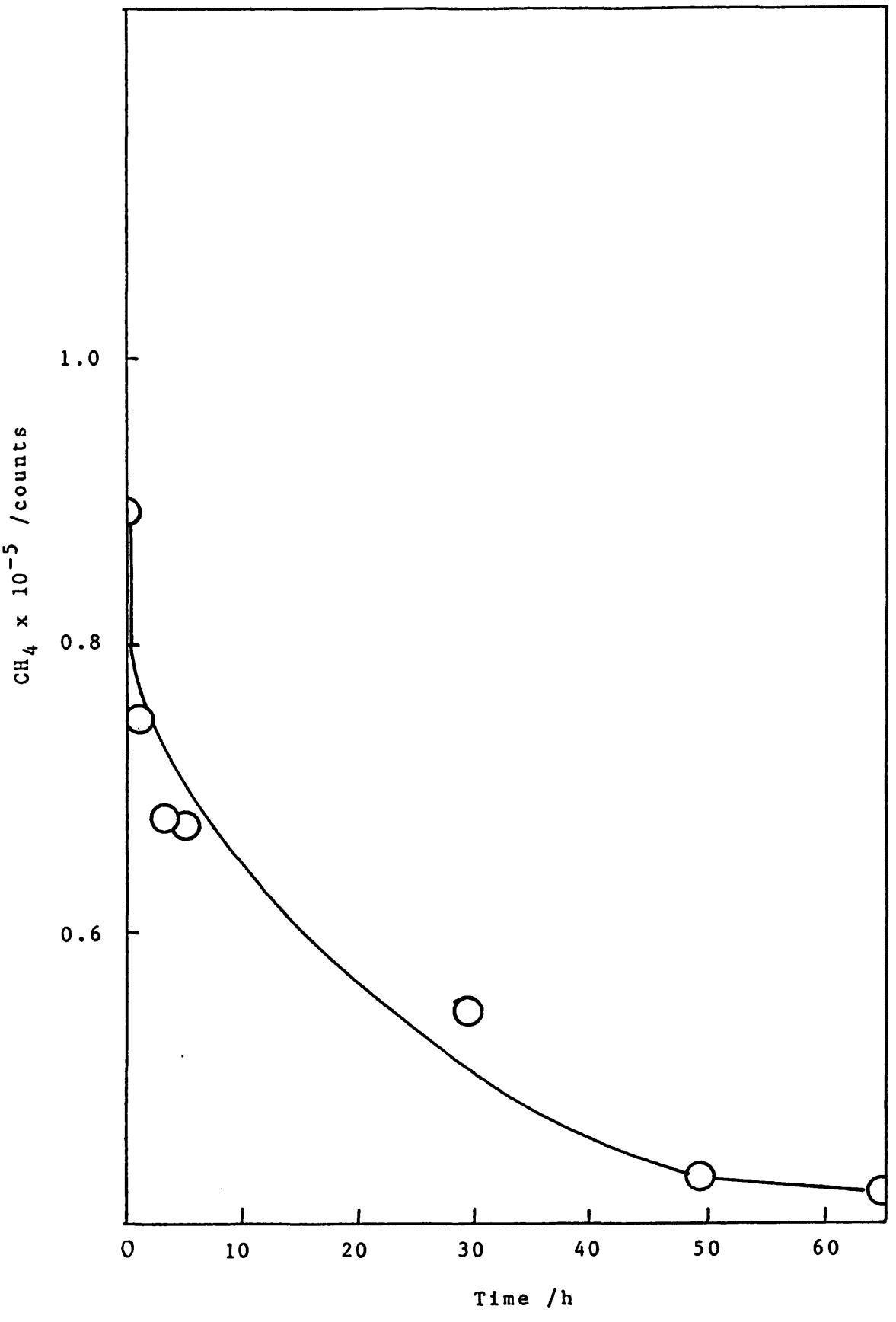

Fig. 3.12 Deactivation with Time of 10CoSpinel 3

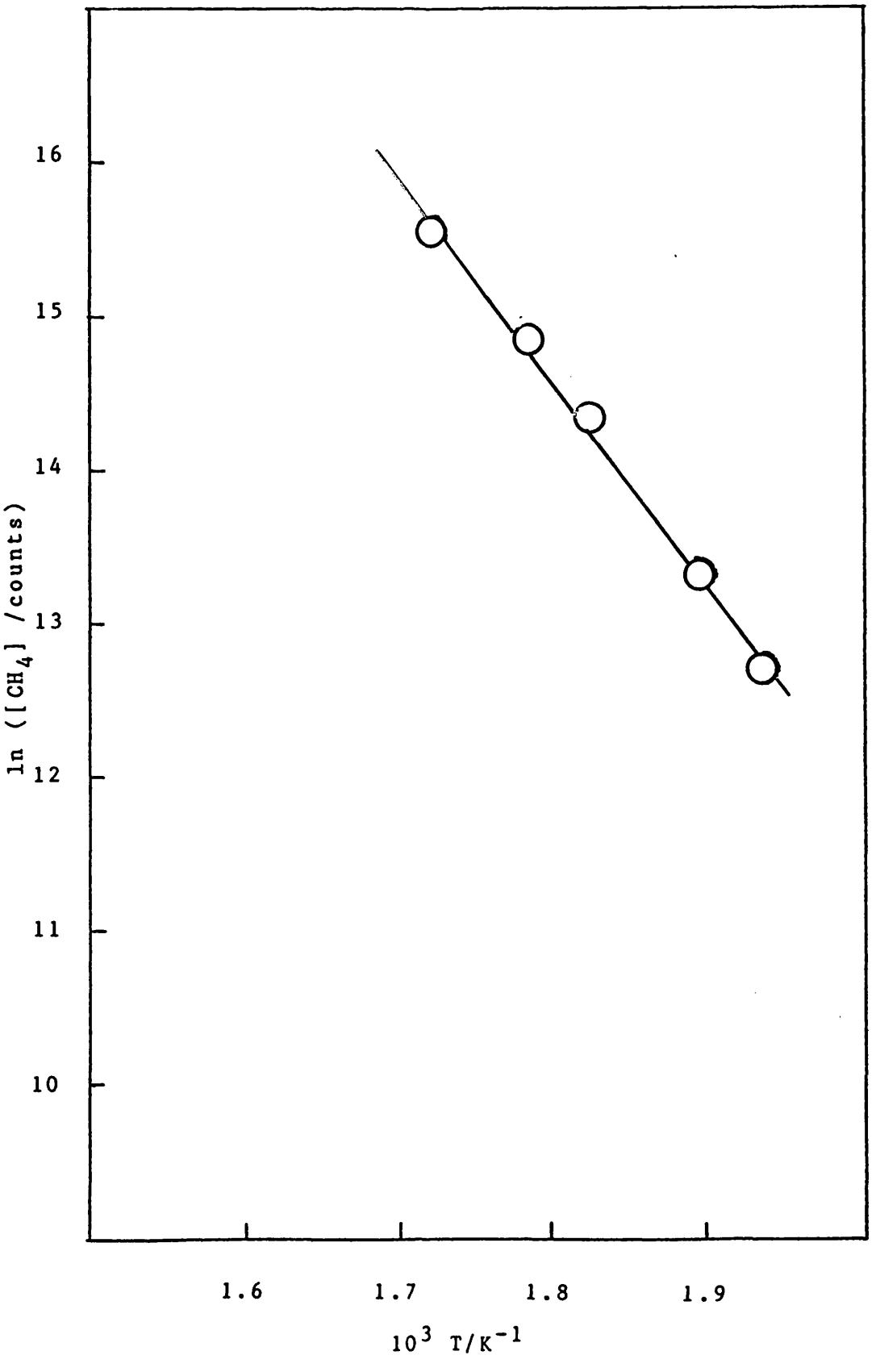

Fig. 3.13 Arrhenius Plot for 15CoSpinel 1

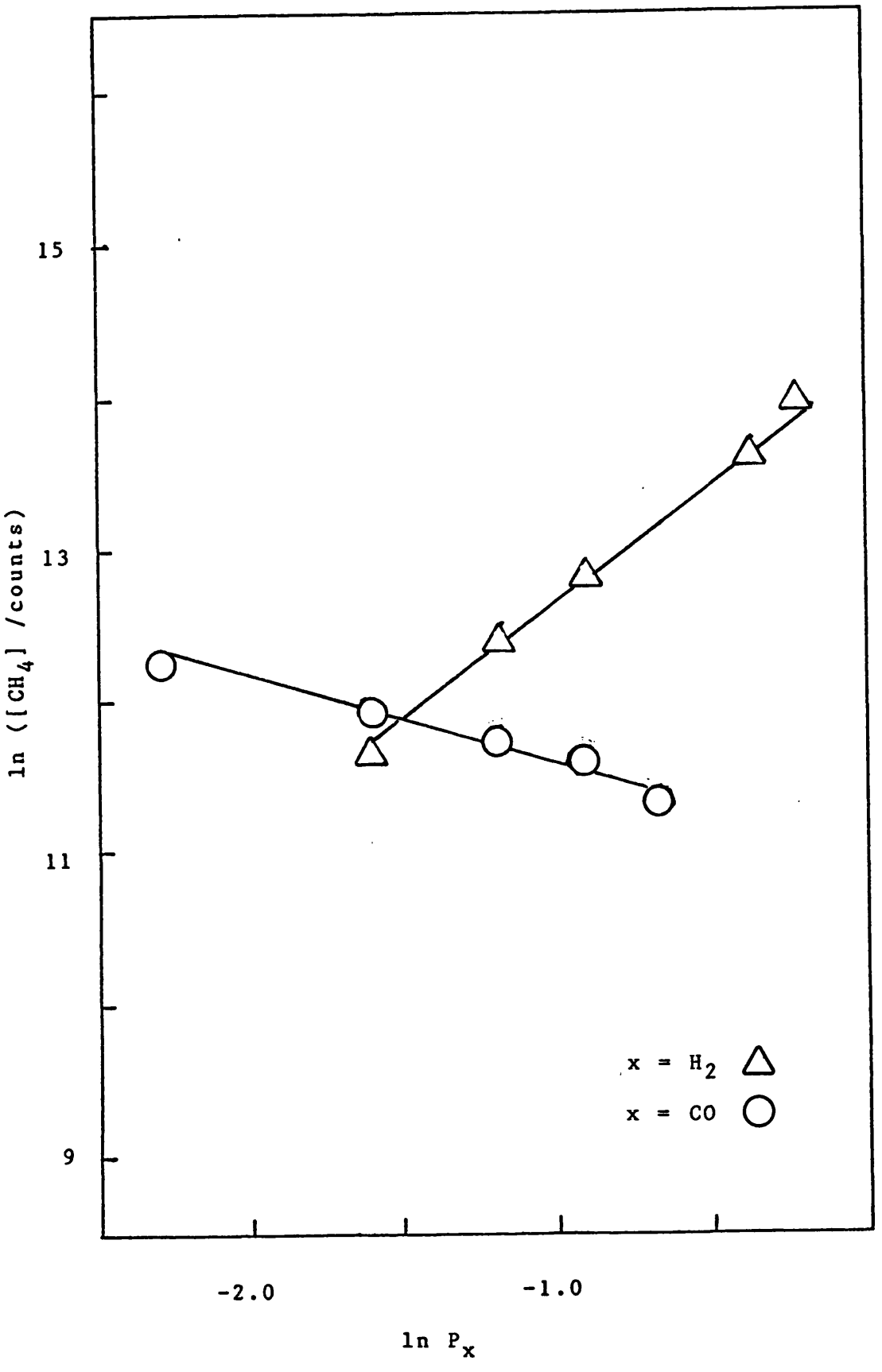

Fig. 3.14 Orders of Reaction for Methanation Over 15CoSpinel 11

investigated (Table 3.41). After this the deactivation behaviour of the catalyst was checked using a 1:3 $CO:H_2$ mixture at 575 K (Table 3.42 and Fig. 3.15).

Table 3.41

Effect of Varying $CO:H_2$ Feed Gas Ratio for CO Hydrogenation Over 15CoSpinel

Gas ratio	T/K	Products/counts (mol %)			
$CO:H_2$		CH_4	C_2H_4	C_2H_6	C_3
1:2	489	32446 75.17	8639 12.41		22556 12.42
1:1	489	22629 63.06	6071 10.49		37960 26.45
2:1	489	16283 51.72	3061 6.03		53199 42.25
1:2	569	292419 69.36	143814 31.15		160066 9.49
1:1	571	203741 59.70	141902 25.78		198139 14.52

Table 3.42

Deactivation of 15CoSpinel at 568 K ($CO:H_2$ = 1:3)

Run time /hours	Products / counts (mol %)			
	CH_4	C_2H_4	C_2H_6	C_3
0.0	193620	90482		75779
	72.07	20.88		7.05
4.5	156179	70379		65132
	72.27	20.19		7.54
18.0	115011	44216		43743
	74.99	17.88		7.13
20.5	113875	42937		38825
	75.81	17.72		6.46
22.7	111787	40367		36115
	76.65	17.16		6.19
32.5	98588	36221		30320
	76.65	17.46		5.89
39.7	96806	32472		29586
	77.86	16.19		5.95

3.4.4. 20% Cobalt-Spinel

3.4.4.1 20CoSpinel 1

20CoSpinel 1 (0.367 g), unwashed and unreduced, was tested for CO hydrogenation (Table 3.43), then treated with flowing CO (875 K, 12 h) and re-tested (Table 3.44). Next the catalyst was exposed to flowing hydrogen at 895 K, following which $CO-H_2$ runs were conducted to determine activation energy (Table 3.45 and Fig. 3.16) and the effect of CO and H_2 partial pressures on activity and selectivity (Table 3.46 and Fig. 3.17).

Table 3.43

Initial Activity of 20CoSpinel 1

at 623 K ($CO:H_2$ = 1:3)

Ref.	Products/counts (mol %)				
	CH_4	C_2H_4	C_2H_6	C_3	Total count
a	27724	11974	4447		43965
	76.70	20.23	3.08		
b	35864	24578	19343		79785
	64.11	27.24	8.64		
c	34828	25278	15856		75962
	63.95	28.78	7.28		

a: After 20 min
b: After 1 h
c: After 1.25 h

Table 3.44

Activity of 20CoSpinel 1 in CO Hydrogenation ($CO:H_2$=1:3)

After Exposure to CO at 875 K

T/K	Products/ counts (mol %)				
	CH_4	C_2H_4	C_2H_6	C_3	Total count
611	4082	1767	5140		10989
	63.16	16.95	19.88		
613	3546	1842	3663		9051
	63.28	20.38	16.34		

Table 3.45

Activity of 20CoSpinel 1 in Carbon Monoxide Hydrogenation after High Temperature Reduction in Hydrogen ($CO:H_2=1:3$)

T/K	Products/counts (mol %)				
	CH_4	C_2H_4	C_2H_6	C_3	Total count
506	19965	7369		11234	38568
	73.02	16.71		10.27	
531	108729	36667		47886	193282
	75.80	15.85		8.35	
535	135435	45893		55504	236832
	76.19	16.01		7.80	
555	433666	73510	62509	142817	712502
	78.38	8.50	6.67	6.45	
571	822417	100041	130510	215035	1268003
	80.85	6.29	7.57	5.29	
608	2849222	193010	488454	516782	4047468
	84.04	3.64	8.50	3.82	
618	7649023	1208684		690670	9548377
	89.24	8.74		2.02	

Table 3.46

Effect of Varying CO:H_2 Partial Pressures for CO Hydrogenation Over 20CoSpinel 1

Flow rate cm^3 min^{-1}			Products /counts (mol %)			
CO	H_2	He	CH_4	C_2H_4	C_2H_6	C_3
5	25	20	382459 89.15	45816 6.83	17547 2.41	27530 1.60
10	25	15	235209 82.16	64539 13.98		44250 3.86
15	25	10	128953 76.31	44574 16.35		49596 7.34
20	25	10	125034 73.21	48491 17.60		62729 9.18
10	40	0	1114859 84.20	1567974 7.59	118425 5.28	155466 2.94
10	30	10	724539 82.32	205012 14.44		113878 3.23
10	20	20	488577 80.51	158459 16.19		80133 3.30
10	10	30	223649 78.97	82277 18.01		34149 3.01

The activation energy for methanation derived from Fig. 3.16 was 152 kJ mol^{-1} and the order of reaction from Fig. 3.17 was 1.2 for H_2 and -0.8 for CO.

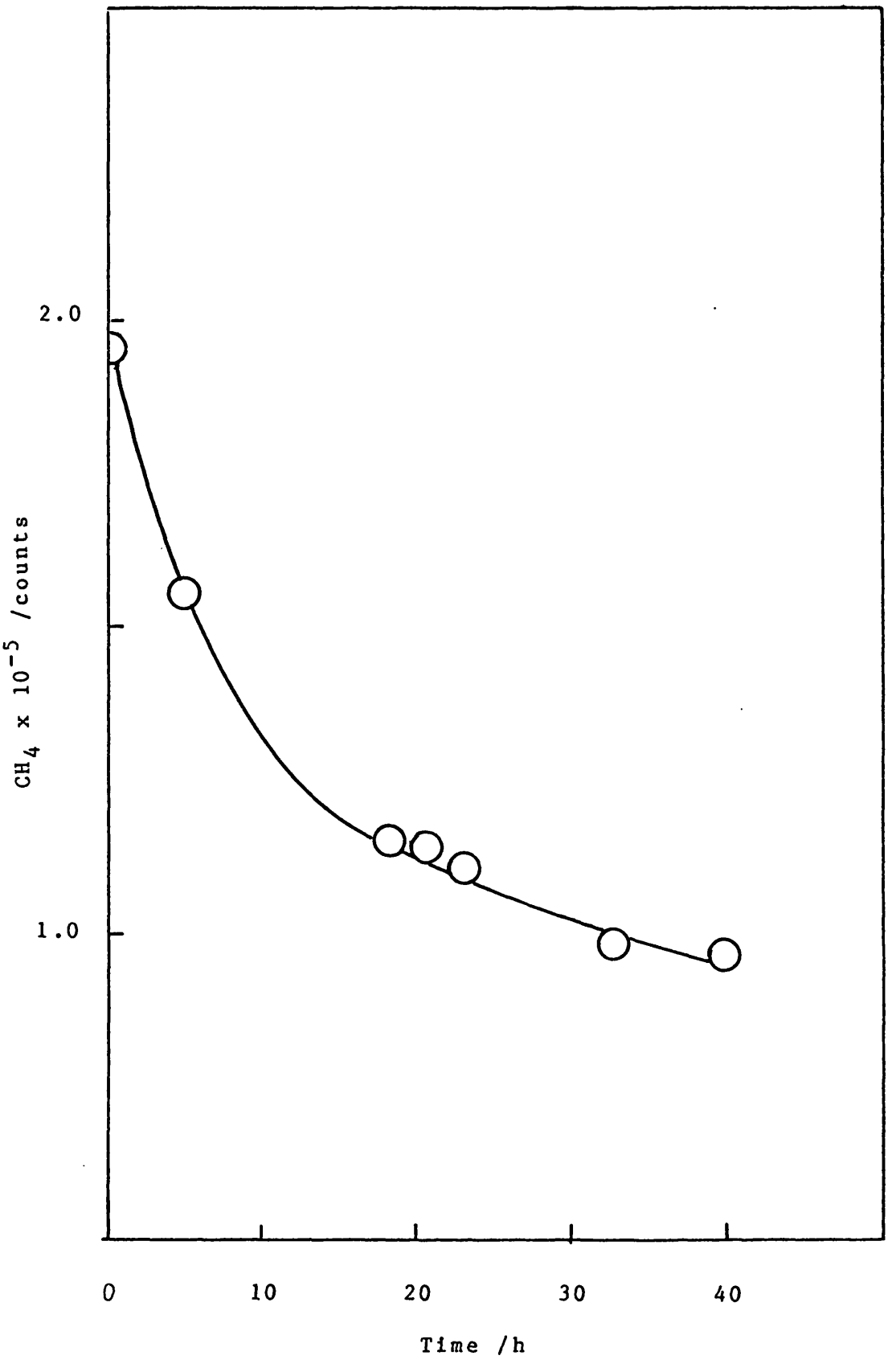

Fig. 3.15 Deactivation with Time of 15CoSpinel 1

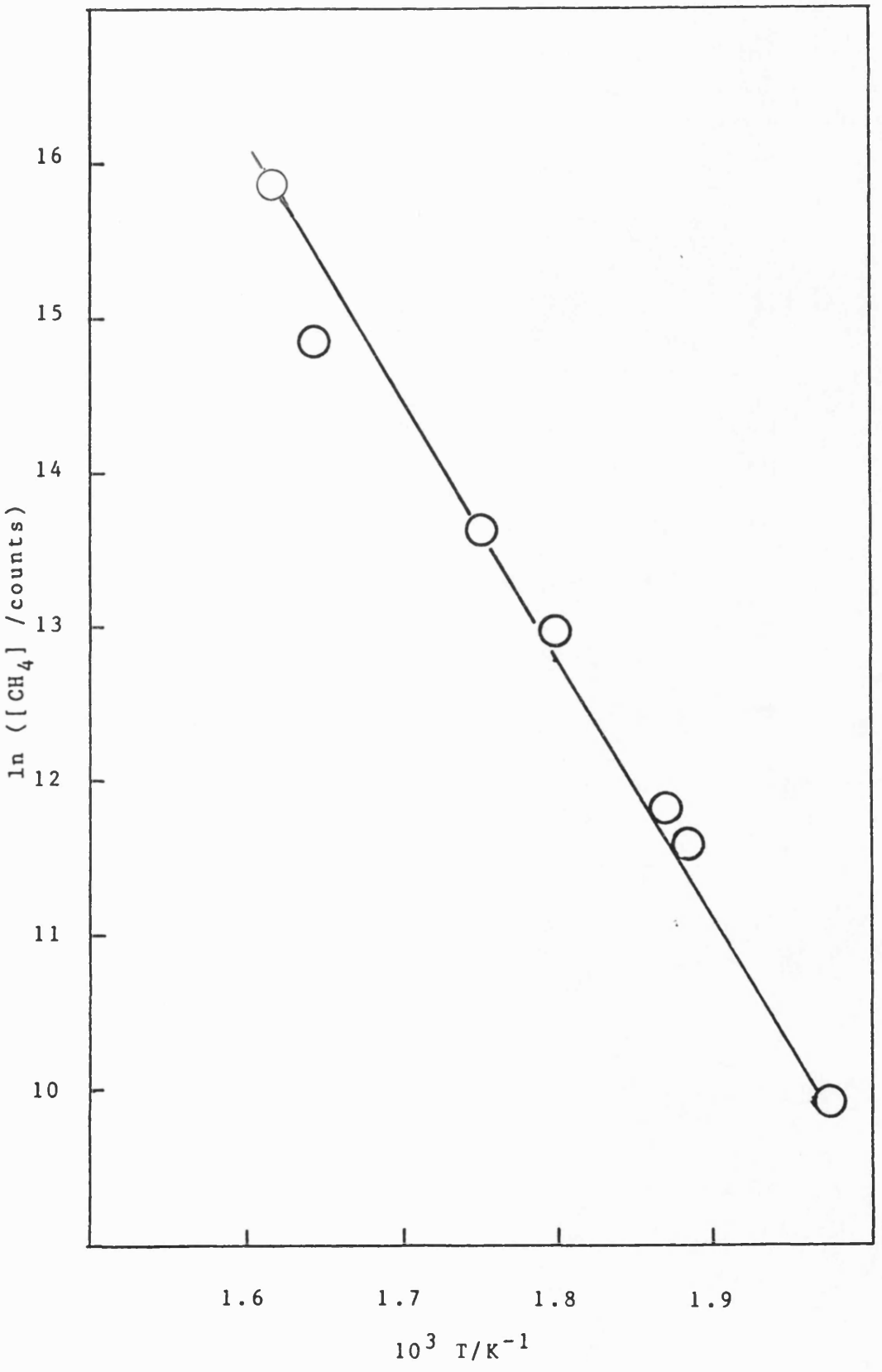

Fig. 3.16 Arrhenius Plot for 20CoSpinel 1

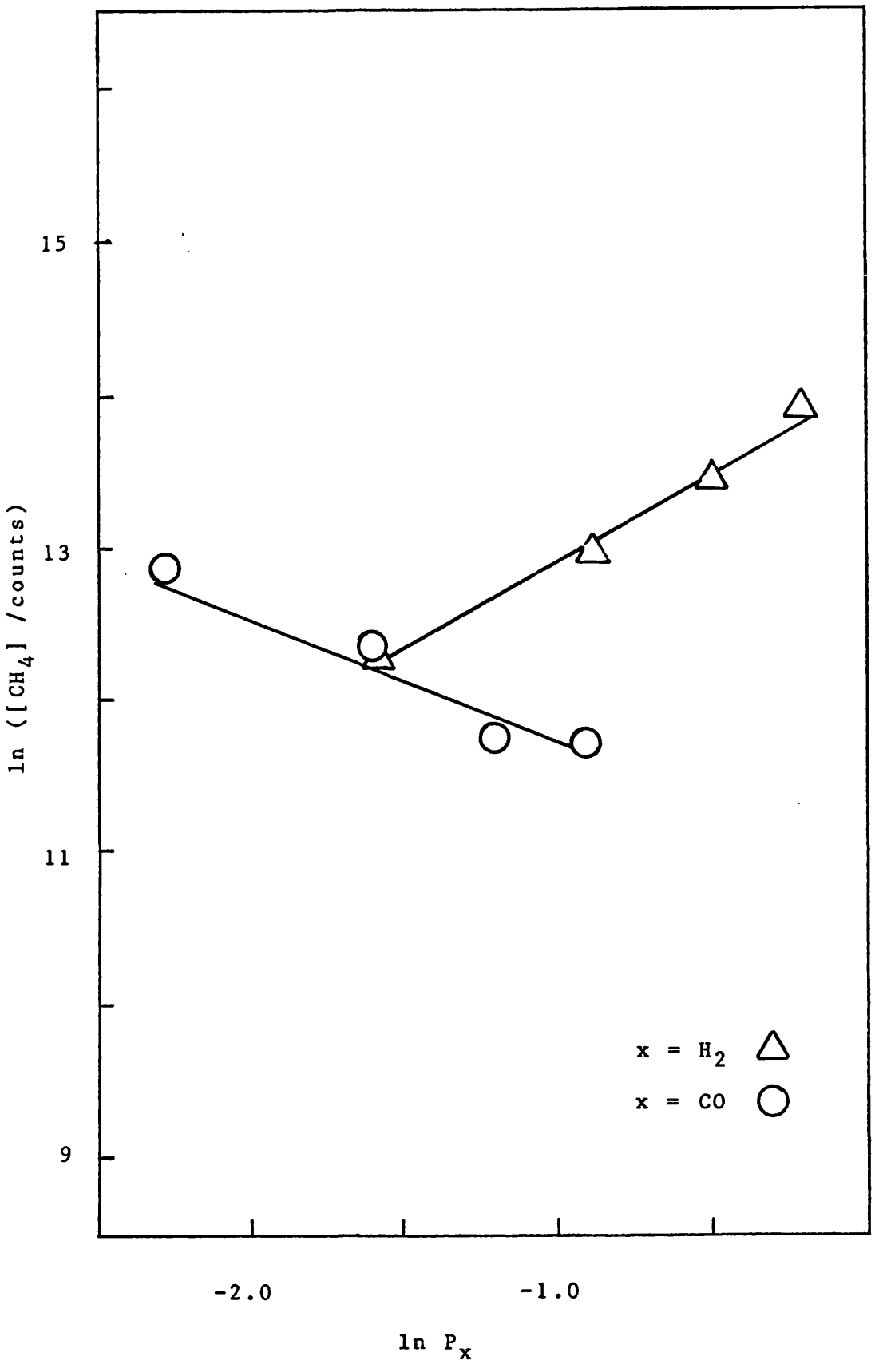

Fig. 3.17 Orders of Reaction for Methanation Over 20CoSpinel 1

After the order of reaction experiments were completed, the CO feed was turned off and the size of the methane peak was monitored with time with only hydrogen flowing over the catalyst. The results are shown in Table 3.47 and Fig. 3.18. The aim of this experiment was to give some information on the extent of carbon laydown during the the previous hydrogenation runs. Finally the effect of changing the feed gas ratio (without helium balancing) was studied and the results are shown in Table 3.48.

3.4.4.2. 20CoSpinel 2

A weight of 0.670 g of the sample was used. The sample was one which had been subjected to washing in nitric acid to remove any CoO-MgO phase. The solid had been exposed to high temperature reduction and catalytic testing in the high vacuum system prior to the treatments described in this section.

After treatment in flowing hydrogen overnight at 675 K to re-reduce the system after atmospheric contamination, the catalyst was immediately tested for activity in CO hydrogenation (Tables 3.49 and 3.50, and Figs. 3.19 and 3.20). The methanation activation energy was 83 kJ mol^{-1}, and the orders of reaction for hydrogen and CO were 1.6 and -0.2, respectively.

During the above runs a larger than usual, but very broad, peak corresponding to C_4 products was observed (but not counted). After taking sensitivity factors

Table 3.47

Effect of Switching the CO Stream off on Methane Count After CO Hydrogenation Over 20CoSpinel 1

Time/h	Methane peak area/counts
0.00	651688
0.15	141027
0.22	91798
0.27	79711
0.52	55167
1.43	31193
3.45	19489
20.00	2072

Table 3.48

Effect of Varying $CO:H_2$ Feed Gas Ratio for CO Hydrogenation Over 20CoSpinel 1

Gas ratio	T/K	Products /counts (mol %)			
$CO:H_2$		CH_4	C_2H_4	C_2H_6	C_3
1:9	574	837662 92.96	34411 2.44	54526 3.58	36837 1.02
1:4	574	410332 88.39	69691 9.31		42733 2.30
1:3	573	295597 84.37	67800 12.00		50881 3.63
1:2	573	232867 80.63	65963 14.16		60112 5.21

into account, it was estimated that the maximum contribution was about 5 mol %. With the other systems studied, C_4 was sometimes seen (but not integrated) in amounts estimated at about 0.5 to 1.0% of total products. On removal from the flow system, the catalyst was found to be bright blue.

Table 3.49

Activity of 20CoSpinel 2 in CO Hydrogenation ($CO:H_2=1:3$)

T/K	Products /counts (mol %)				
	CH_4	C_2H_4	C_2H_6	C_3	Total count
530	16616 58.02		10223 22.15	22722 19.83	49571
543	26596 56.53		18952 24.97	34810 18.50	80358
557	41845 55.19		33916 27.74	51751 17.07	127512
574	70212 53.80		63732 30.28	83074 15.92	217009
594	142649 53.23		140471 32.49	153103 14.28	436223

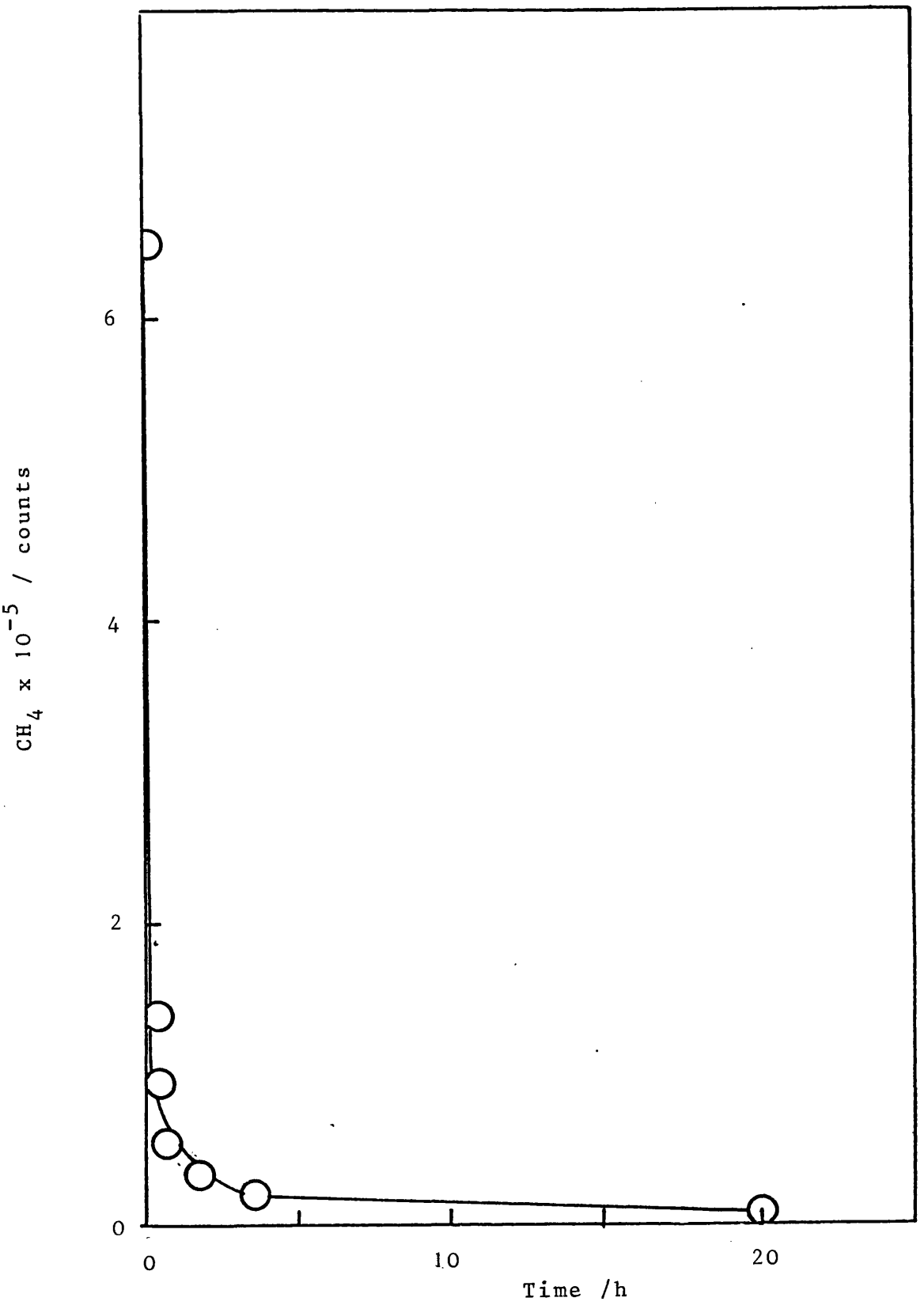

Fig. 3.18 Methane Peak Area with Time after CO turned off Over 20CoSpinel 1

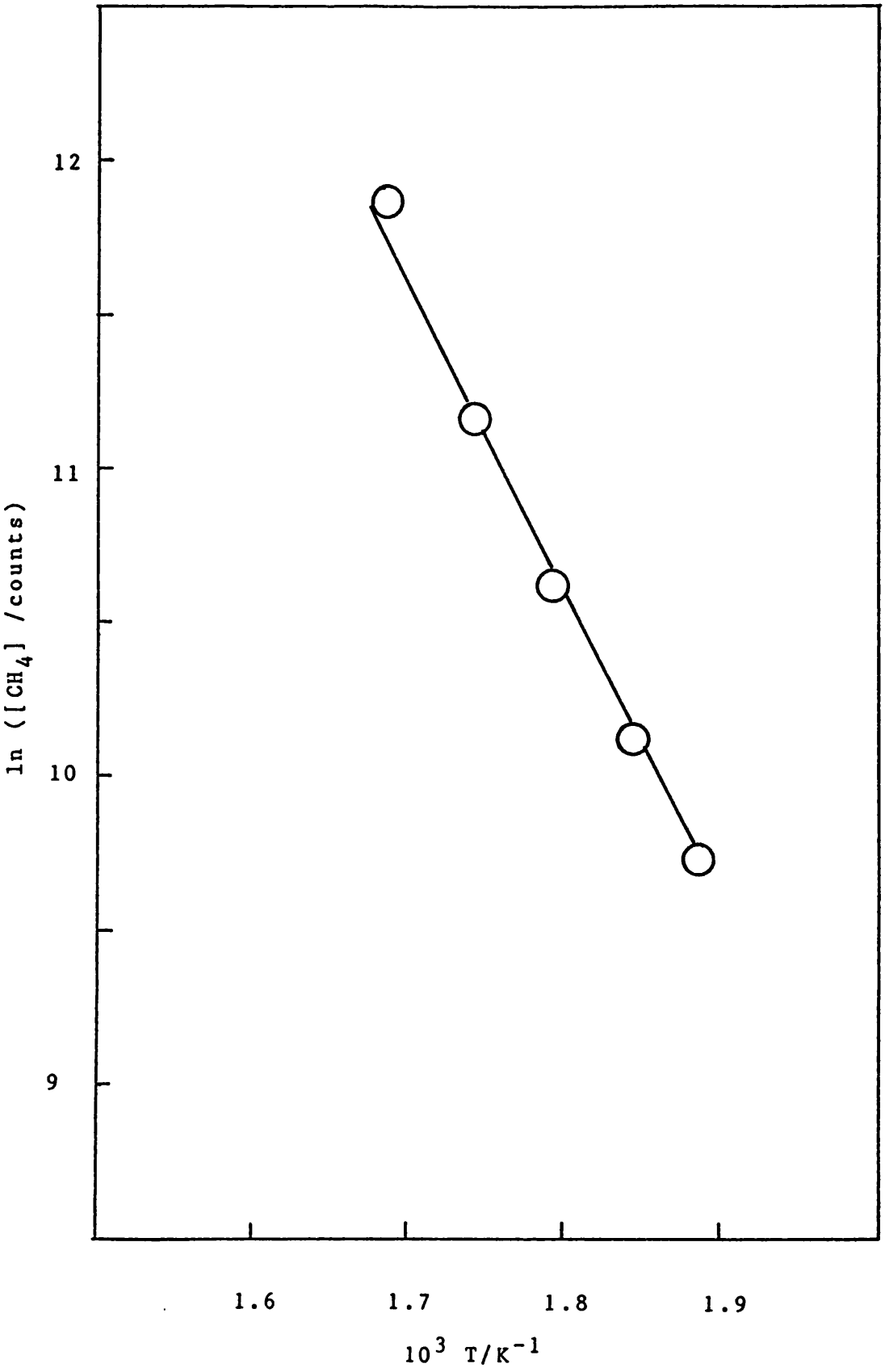

Fig. 3.19 Arrhenius Plot for 20CoSpinel 2

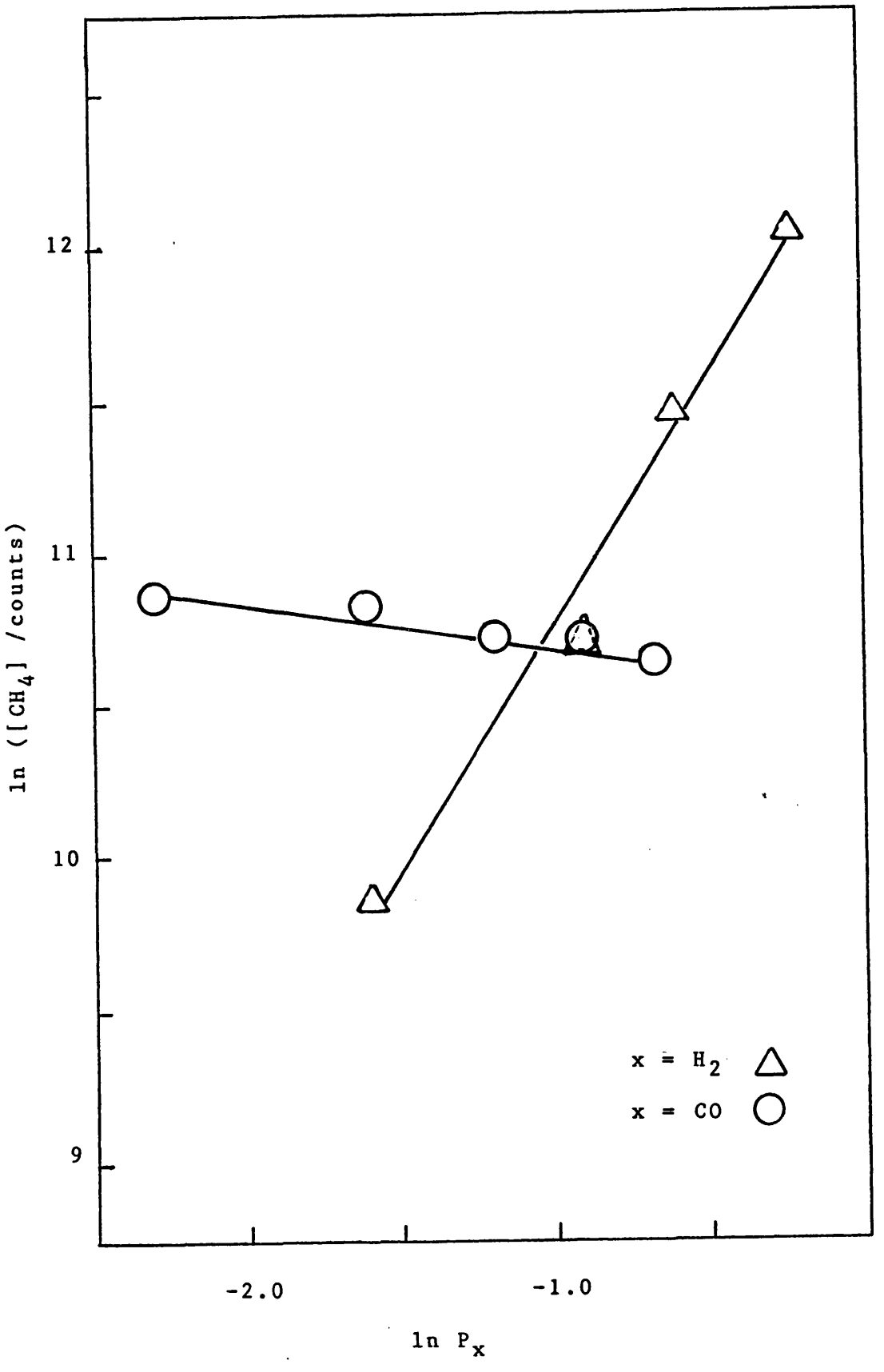

Fig. 3.20 Orders of Reaction for Methanation Over 20CoSpinel 2

3.4.5. Osmium Systems

Two conventional supported catalysts consisting of osmium (derived from $Os_3(CO)_{12}$) impregnated on to high surface area alumina and magnesia, respectively were studied in order to obtain results for CO hydrogenation activity at 1 atm for comparison with results obtained using 10 and 100 atm reactors at I.C.I., Runcorn.

3.4.5.1. Os/alumina

0.744 g of Os/alunina catalyst (3.2% w/w) was loaded into the reactor. Owing to the high surface area of the support, the volume of the sample was large compared with other systems studied. The bed length of the catalyst in the reactor was about 5 cm.

The activation/reduction of the catalyst followed the method employed at I.C.I. on similar systems. A 4:1 $He:H_2$ mixture was flowed over the catalyst at room temperature for several hours, after which the temperature was increased to 575 K for 4 h with the same gas mixture flowing. The mixture was then changed to give the desired ratio of H_2 and CO.

The results of initial catalytic testing on the sample are shown in Table 3.51. The activation energy was not calculated from these runs as the catalyst was deactivating rapidly. When the rate of deactivation had fallen to a relatively low level, runs were carried out to determine the product distribution and the methanation activation energy and reaction orders

(Tables 3.52 and 3.53, and Figs. 3.21 and 3.22). The

Table 3.50

Effect of Varying CO:H_2 Partial Pressures for

CO Hydrogenation Over 20CoSpinel 2 at 573 K

Flow rate $cm^3 min^{-1}$			Products /counts (mol %)			
CO	H_2	He	CH_4	C_2H_4	C_2H_6	C_3
25	25	0	42633 38.80		61615 34.77	116172 26.43
20	25	5	45698 41.20		63648 35.48	103499 23.32
15	25	10	46366 43.90		59457 34.90	195356 21.20
10	25	15	51110 48.87		57713 34.21	70757 16.92
5	25	20	52936 59.71		43988 30.76	33800 9.53
10	40	0	176392 69.33		92276 22.49	83264 8.18
10	30	10	97660 60.29		71893 27.52	78987 12.19
10	20	20	45667 52.56		44672 31.88	54064 15.56
10	10	30	19715 45.16		25809 36.66	31750 18.18

Table 3.51

Initial Activity of Os/Alumina

T/K	Products/ counts (mol %)				
	CH_4	C_2H_4	C_2H_6	C_3	Total count
502	625418	34391	81173	122122	863104
	86.16	3.03	6.60	4.21	
517	1779797	253030		233304	2266131
	89.21	7.86		2.93	
535	7658441	580844		324267	8563552
	94.55	4.45		1.00	

N.B. $CO:H_2$ ratio = 1:3

Table 3.52

Activity of Os/Alumina in Carbon Monoxide Hydrogenation

After Activation in Hydrogen/Helium ($CO:H_2$ = 1:3)

T/K	Products/ counts (mol %)				
	CH_4	C_2H_4	C_2H_6	C_3	Total count
510	232509	37830	14430	56561	341330
	83.22	8.67	3.05	5.06	
524	554858	48037	48920	84315	736130
	87.30	4.84	4.54	3.32	
548	2221029	186830		89114	2496973
	94.15	4.91		0.94	
566	7198770	261010		53892	3120101
	97.62	2.19		0.19	
578	16006073	337237		37826	3544900
	98.65	1.29		0.06	

Table 3.53

Effect of Varying $CO:H_2$ Partial Pressures for CO Hydrogenation Over Os/Alumina at 578 K

Flow rate $cm^3 min^{-1}$			Products/ counts (mol %)			
CO	H_2	He	CH_4	C_2H_4	C_2H_6	C_3
25	25	0	2951986 93.39	91991 1.86	1901314 3.57	149422 1.18
20	25	5	4237658 95.53	282181 3.94		93119 0.53
15	25	10	5605408 96.77	276493 2.96		63493 0.27
10	25	15	8224820 98.39	202891 1.50		35473 0.11
5	25	20	13131837 99.17	169966 0.80		16781 0.03
10	25	15	8272116 98.49	191045 1.41		32703 0.10
10	20	10	5988877 98.52	134935 1.38		23613 0.10
10	15	25	4258634 98.50	97523 1.40		18021 0.10
10	10	30	2569389 98.48	63601 1.52		456 0.00
10	5	35	1225925 98.15	10502 0.54	27442 1.30	681 0.01

was the same as described for the spinel systems except that, between sets of runs and at the end of experiments, the catalyst was exposed to a hydrogen/helium mixture rather than pure hydrogen, in order to avoid the risk of sintering in hydrogen to which these catalysts may be susceptible. The activation energy derived was 153 kJ mol^{-1} and the orders were 1.1 for H_2 and -0.85 for CO.

3.4.5.2. Os/Magnesia

A 0.330 g sample of Os/MgO (5.9% w/w) was studied. As with the Os/Al_2O_3 sample, the bed length was considerable owing to the high surface area (ca 300 m^2 g^{-1}) of the support. The sample was left overnight in a 4:1 helium-hydrogen mixture and was then heated in the gas mixture to 550 K for about 8 h. The temperature was then raised to 575 K for 4 h, after which initial catalytic testing was carried out (Table 3.54). As before, cooling, heating and cleaning between experimental runs was always carried out in helium/hydrogen mixtures to avoid the risk of hydrogen sintering.

Runs were carried out at various temperatures (after the initial rapid deactivation) in order to obtain the activation energy for methanation and the selectivity at different temperatures (Table 3.55 and Fig. 3.23). The calculated value for the activation energy for methanation was 134 kJ mol^{-1}. During these experimental runs a small extra peak appeared on the chromatogram but was not recognised by the integrator.

The retention time was such that it seemed likely that this product was methanol. The size of the peak varied between 1000 and 10000 counts. The effect of changing the CO:H_2 ratio was investigated (Table 3.56), and then orders of reaction were calculated (Table 3.57 and Fig. 3.24). The order for H_2 and CO were 1.1 and -0.6, respectively. Finally the deactivation of the catalyst over many hours was measured (Table 3.58 and Fig. 3.25). The rate of deactivation was very much less than that indicated by comparing Tables 3.54 and 3.55, as the catalyst had been much more extensively used by this time.

After the catalytic studies, some flow-chemisorption experiments were attempted with this deactivated catalyst, using the apparatus described in Section 2.4.2., in order to determine the characteristics for CO adsorption. Results are shown in Table 3.59 (first series) for the deactivated sample which had only been treated with He/H_2 at room temperature. In a second experiment (Table 3.59 second series) the pretreatment prior to studying CO chemisorption at room temperature was at 575 K. The results appear to be as expected but cannot be very accurate, as a repeat of the second experiment (pretreatment-cooling to RT-chemisorption) gave a result which was half as large. The results have only been shown to give an idea of what is possible using this method.

Table 3.54

Initial Activity of Os/MgO

T/K	Products /counts (mol %)				
	CH_4	C_2H_4	C_2H_6	C_3	Total count
576	194648	24775	33565	725254	325513
	78.35	6.38	7.97	7.30	
590	907430	105256	57135	150220	1220041
	86.75	6.44	3.22	3.59	

N.B. $CO:H_2$ ratio = 1:3

Table 3.55

Activity of Os/MgOin Carbon Monoxide Hydrogenation

After Activation in Hydrogen/Helium Mixture ($CO:H_2$ = 1:3)

T/K	Products/counts (mol %)				
	CH_4	C_2H_4	C_2H_6	C_3	Total count
544	71454	14061	9527	25835	120877
	77.22	9.73	6.07	6.98	
563	154574	30673		35795	221042
	84.68	10.42		4.90	
595	739859	36139	43587	74670	894255
	91.64	2.86	3.19	2.31	
601	990970	34319	46286	82523	1154098
	93.41	2.07	2.58	1.94	
629	4366227	20240	103262	72574	4562403
	97.93	0.29	1.37	0.41	

Table 3.56

Effect of Varying $CO:H_2$ Feed Gas Ratio for CO Hydrogenation Over Os/MgO

Gas ratio	T/K	Products /counts (mol %)			
$CO:H_2$		CH_4	C_2H_4	C_2H_6	C_3
1:3	573	342179 82.82	83453 12.52		77016 4.66
1:2	574	203130 74.15	46242 10.80	24379 5.25	107363 9.80
1:1	573	154919 68.91	51332 14.61	13545 3.55	116271 12.93

Table 3.57

Effect of Varying $CO:H_2$ Partial Pressures for CO Hydrogenation Over Os/MgO at 575 K

Flow rate $cm^3 min^{-1}$			Products /counts (mol %)			
CO	H_2	He	CH_4	C_2H_4	C_2H_6	C_3
25	25	0	111039 73.58	33201 13.64		77173 12.78
20	25	5	135239 77.65	37072 13.20		63768 9.15
15	25	10	173522 80.56	44133 12.70		58043 6.74
10	25	15	230177 85.92	45380 10.50		38365 3.58
5	25	20	312047 90.31	26025 4,82	15119 2.58	31647 2.29
10	40	0	665537 90.18	49481 4.29	34310 2.74	82316 2.79
10	35	5	537990 90.18	43450 4.66	25207 2.49	63716 2.67
10	30	10	462329 89.26	49721 6.14	15251 1.74	59263 2.86
10	20	20	278500 86.73	51882 10.02		41712 3.25
10	10	30	133948 84.21	29439 11.47		27509 4.32

Table 3.58

Deactivation of Os/MgO at 575 K ($CO:H_2$ = 1:3)

Run time /hours	Products /counts (mol %)			
	CH_4	C_2H_4	C_2H_6	C_3
0.0	541530 82.97	108143 10.27		176316 6.76
2.0	398752 84.80	70563 9.30		110961 5.90
4.0	375730 85.83	66107 9.36		242146 4.81
4.9	363481 87.15	61186 9.10		62697 3.75
10.2	316998 87.35	52204 8.92		54158 3.73
22.0	296115 86.73	51334 9.32		53963 3.95
36.0	240666 85.78	44367 9.80		49506 4.42
46.0	234587 85.69	43214 9.79		49555 4.52

Table 3.59

Flow Chemisorption Studies of CO Uptake on Os/MgO

at 295 K and 1 atm

First series (after He/H_2 flush at 295 K)		Second series (after He/H_2 flush at 575 K)	
Dose no.	Uptake/counts	Dose no.	Uptake/counts
1	10227	1	41264
2	4526	2	8320
3	3862	3	2947
4	3055	4	1972
5	2287	5	1544
6	2106	6	1152
Total	26113*	Total	57199**

* Equivalent to 3.75 micromol CO

** Equivalent to 7.99 micromol CO

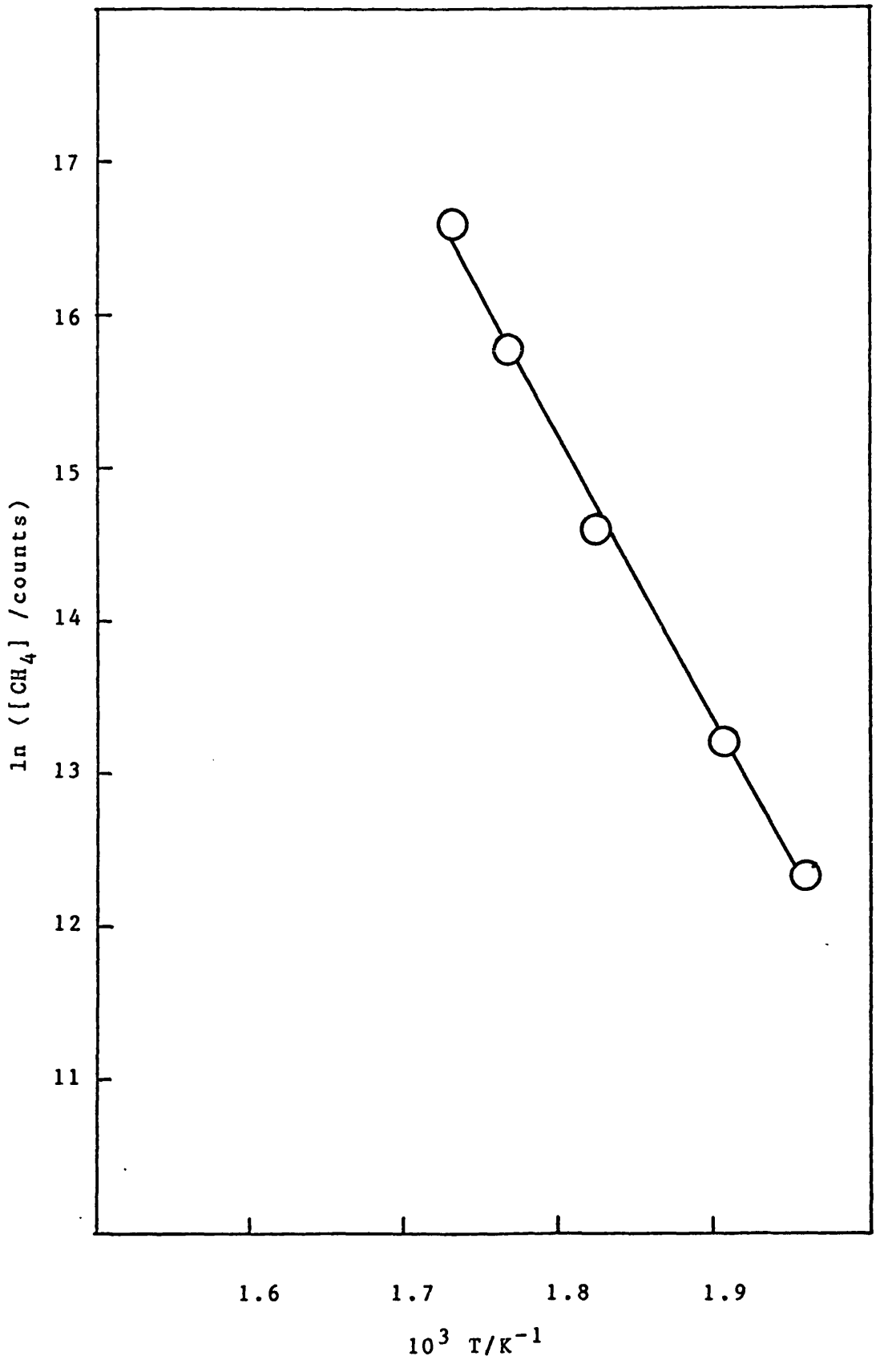

Fig. 3.21 Arrhenius Plot for Os/Al_2O_3

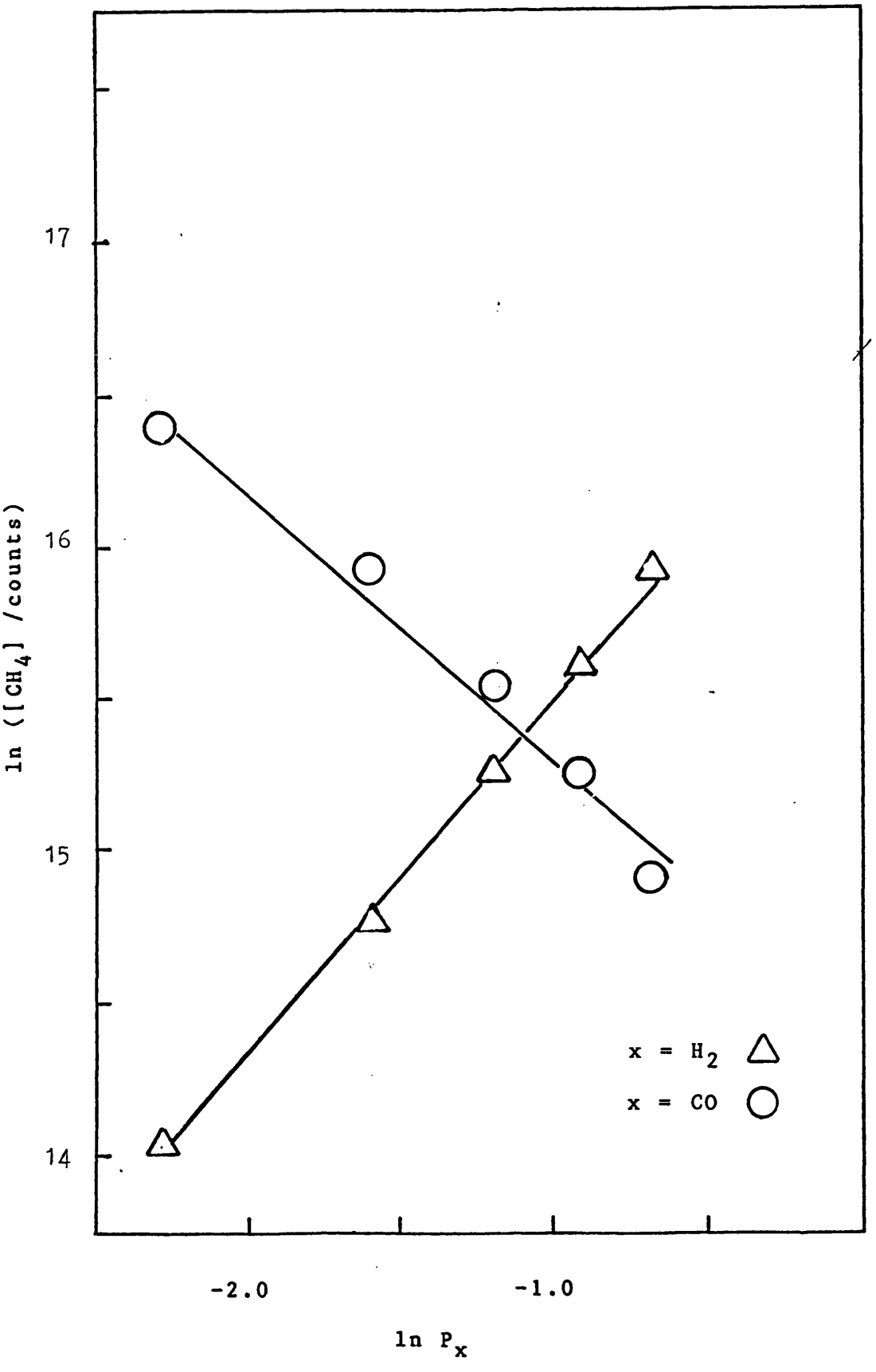

Fig. 3.22 Orders of Reaction for Methanation Over Os/Al_2O_3

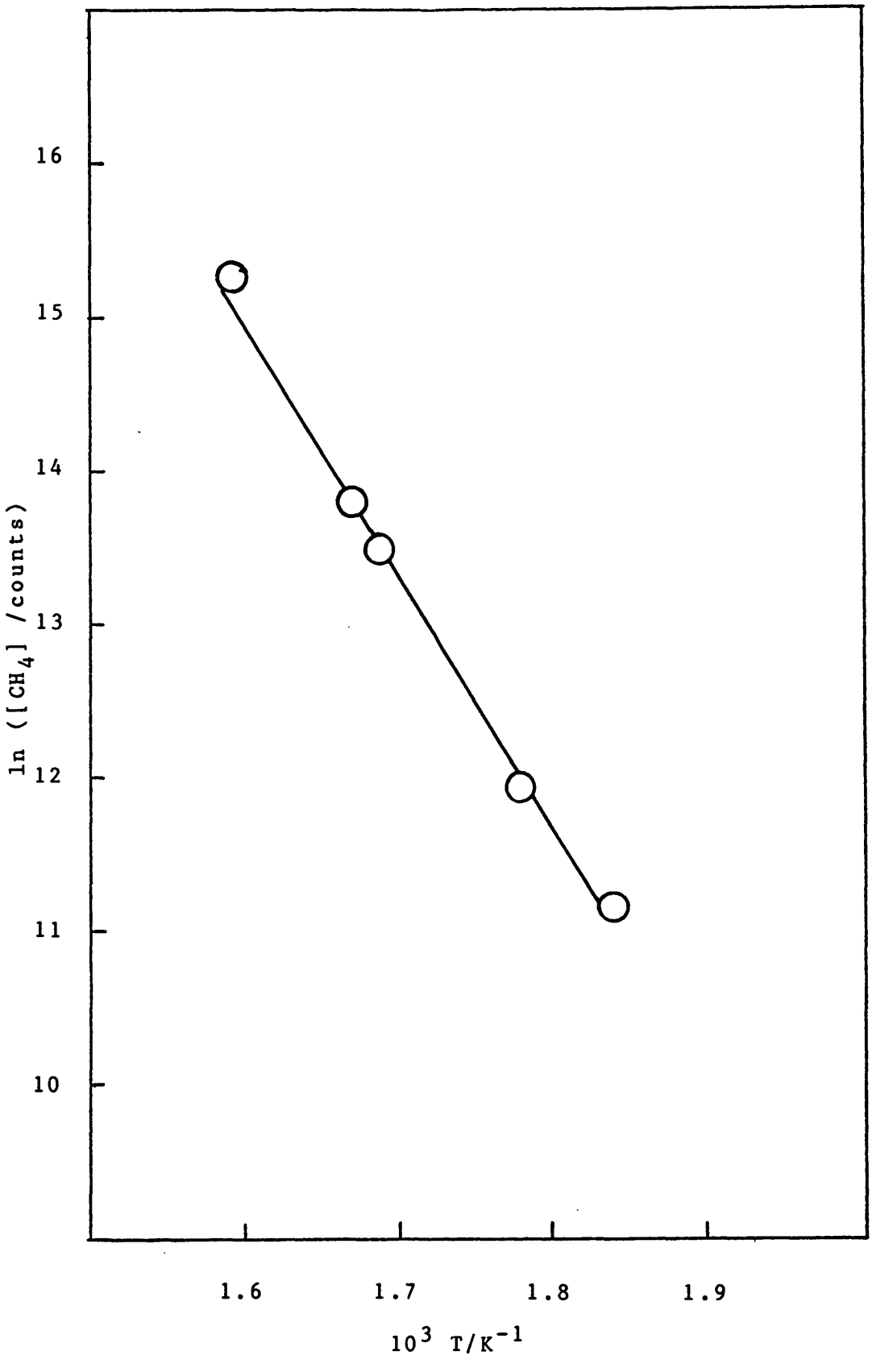

Fig. 3.23 Arrhenius Plot for Os/MgO

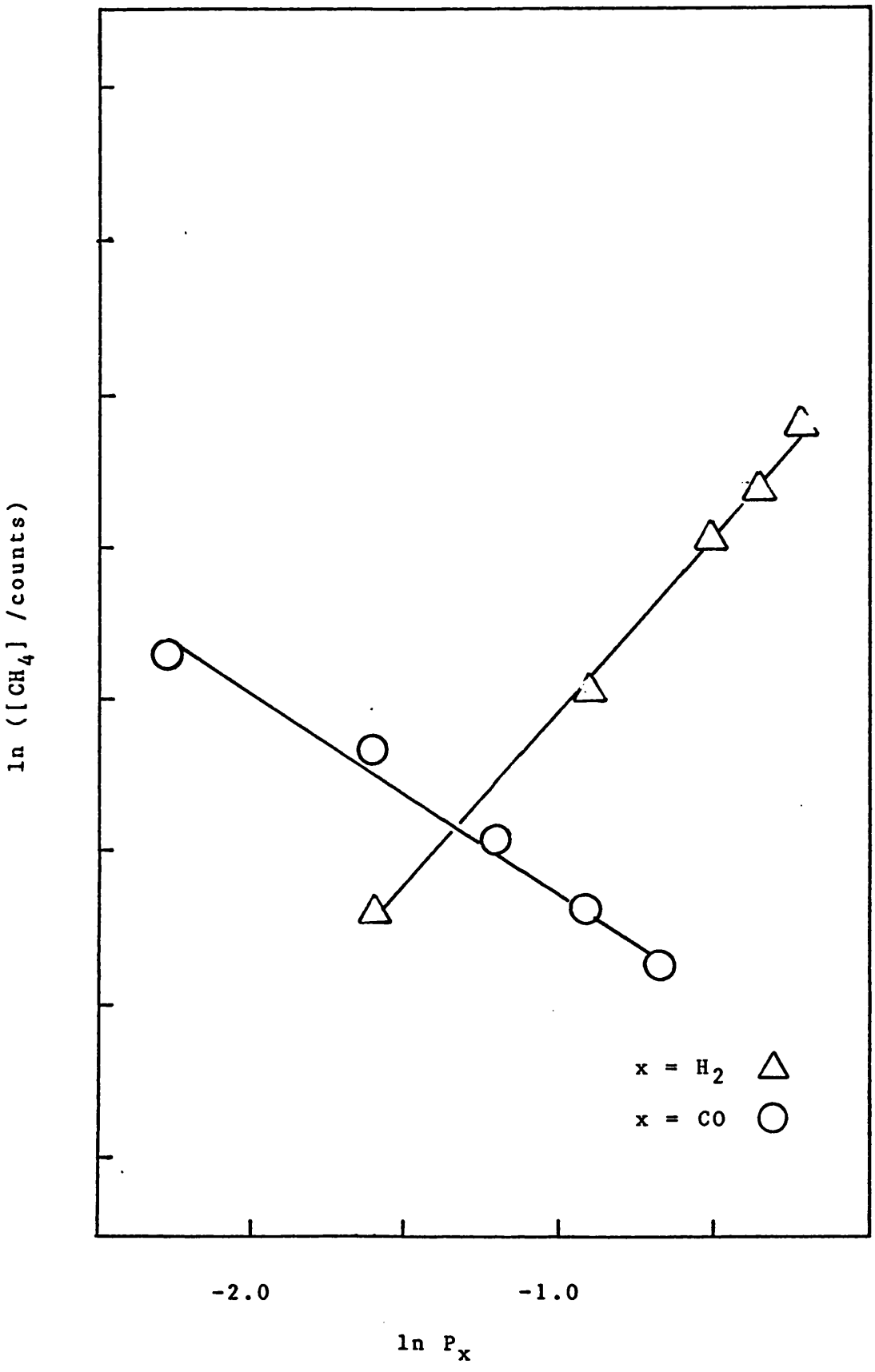

Fig. 3.24 Orders of Reaction for Methanation Over Os/MgO

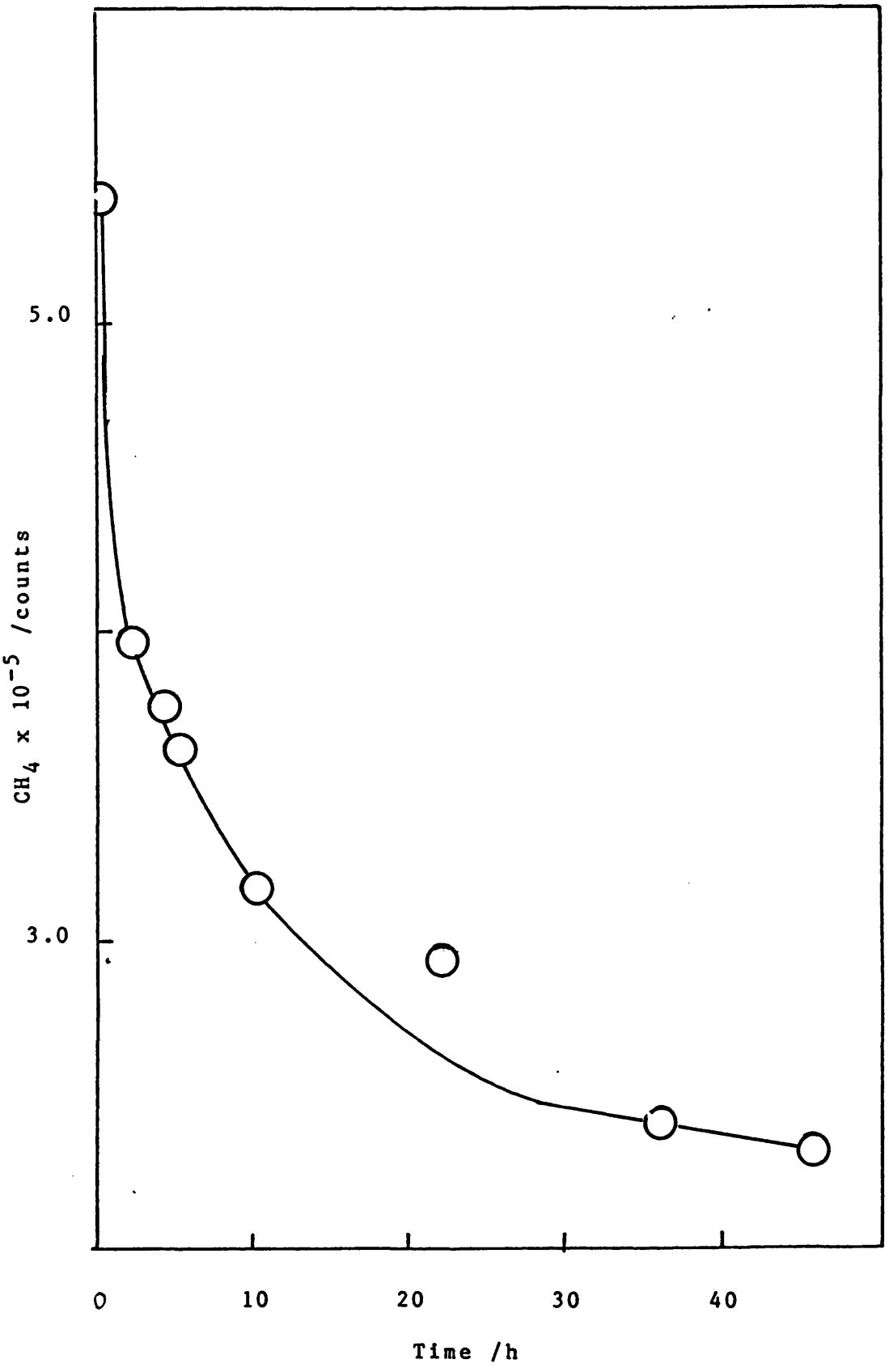

Fig. 3.25 Deactivation with Time of Os/MgO

3.5. Work carried out at I.C.I. Plc, Runcorn

Catalysts consisting of osmium impregnated on high surface area silica and alumina were studied. The preparation of the catalysts is described in Section 2.2.5. Prior to impregnation, the supports were treated in a vacuum at either 393 or 773 K. This treatment was carried out so as to alter the number of hydroxyl groups left on the surface of the support. This, it was assumed, would have an effect on the bonding of the osmium to the alumina and hence the catalytic activity.

Experiments were carried out using two reactor systems, namely a 10 atm flow reactor (Section 2.4.3.1) and a 100 atm reactor of the Berty type (Section 2.4.3.2). The experiments conducted in the 10 atm reactor will be described first.

3.5.1. Results obtained in the 10 atm reactor

In total three catalyst systems were studied in this reactor, namely 2% w/w Os/silica pretreated at 393 K, 2% w/w Os/silica pretreated at 773 K and 2% w/w Os/alumina pretreated at 393 K. The metal loadings in each case were later confirmed by analysis to be within the range 1.8-2.2% w/w. In all cases the method of catalyst preparation used was the dry pressing method (Section 2.2.5). Attempts to make these catalysts by the incipient wetness method failed to produce satisfactory osmium loadings on the support.

3.5.1.1. 2% Os/silica pretreated at 393 K

0.45 g of this catalyst was loaded into the reactor. Activation was similar to that used for the Os/MgO sample at Bath (Section 3.4.5.2). Nitrogen was flowed briefly over the sample and the temperature was raised to about 423 K. The nitrogen was then replaced with a 4:1 nitrogen:hydrogen mixture and the temperature was raised to about 575 K for 3 h.

After activation, CO hydrogenation runs were carried out at 473, 523 and 573 K at a total pressure of 10 atm and a $CO:H_2$ ratio of 1:1. The results of these experiments are shown in Table 3.60 where activity is quoted in moles per kilogram of catalyst per hour and selectivity is in mol %.

Table 3.60

CO Hydrogenation at 10 atm Over 2% Os/silica (393 K)

Temp. /K	Activity*	Products /mol%							
		CH_4	C_2H_4	C_2H_6	C_3H_6	C_3H_8	C_4	C_5	MeCHO
473	0.009	21.8	-	-	-	-	-	-	78.2
523	0.013	75.6	5.7	8.6	-	10.1	-	-	-
573	0.152	68.4	3.6	5.1	5.3	4.5	7.5	5.6	-

* Activity in moles of CO converted per kg of catalyst per hour

A flow chemisorption experiment with CO similar to those carried out at Bath on spinel catalysts was performed, the total uptake being 1.29 micromol.

Various analytical techniques were applied to

another sample of the same catalyst which had not been used in CO hydrogenation (but which had been activated). TEM indicated that the maximum metal particle size was ca 0.3 nm, and SIMS showed a small Os-Si peak. This peak was also observed when the "used" sample was tested with SIMS.

3.5.1.2. 2% Os/silica pretreated at 773 K

The weight of catalyst loaded was 0.39 g. After activation in the same manner as the previous catalyst the CO hydrogenation activity of the solid was tested at several temperatures. The $CO:H_2$ ratio was 1:1. Results are shown in Table 3.61.

Table 3.61

CO Hydrogenation at 10 atm Over 2% Os/silica (773 K)

Temp /K	Activity*	Products /mol%								
		CH_4	C_2H_4	C_2H_6	C_3H_6	C_3H_8	C_4	C_5	RCHO	ROH
473	0.578	65.8	9.7	8.4	9.8	1.5	3.1	0.3	1.1	-
518	0.539	79.1	2.8	8.4	2.3	2.3	1.4	1.0	1.3	1.3
523	0.563	78.6	2.9	9.0	2.8	2.3	1.3	1.8	-	1.3
573	0.672	76.3	2.8	9.0	3.4	2.7	2.0	1.8	-	2.0

* units as in Table 3.60

A flow chemisorption experiment with CO was carried out on the catalyst: the uptake was very small. This was taken to mean the particle size of the catalyst was large.

3.5.1.3. Os/alumina pretreated at 393 K

The weight of catalyst used was 0.65 g. The procedure used was the same as with previous samples. Results are shown in Table 3.62. A flow chemisorption experiment with CO was not carried out.

Table 3.62

CO Hydrogenation at 10 atm Over 2% Os/alumina (393 K)

Temp /K	Activity*	Products /mol%								
		CH_4	C_2H_4	C_2H_6	C_3H_6	C_3H_8	C_4	C_5	RCHO	ROH
467	1.36	92.3	1.0	3.4	1.3	0.7	0.7	0.4		0.2
518	1.89	93.2	0.7	2.6	1.1	0.6	0.7	0.4	0.3	0.3[a]
568	2.17	90.7	0.8	2.9	1.6	1.1	1.6	0.8	0.2	0.1[b]

* Activity units as in Table 3.60
a Also 0.1% of dimethyl ether
b Also 0.2% of dimethyl ether

3.5.2. Results Obtained in the 100 atm Reactor

Three catalysts were studied in the Berty reactor. Although the reactor was principally used at 100 atm, it was felt desirable in these experiments to obtain results at 10 atm also, in order to see clearly the effect of pressure on the CO hydrogenation reaction and to compare the results with those obtained in the (non-recirculating) 10 atm reactor. All the experiments were carried out using a $CO:H_2$ ratio of 1:1 and a flow rate of 800 $cm^3\ min^{-1}$. The activity is in the same units as in the previous section. In all cases the catalyst was mixed with silica chips in order to make up

the volume of material required to pack the reactor. Chemical analysis for osmium revealed that the $OsCl_3$-derived catalyst had an osmium loading of about 1.5% w/w, whereas the $Os_3(CO)_{12}$ catalysts were 2% w/w.

3.5.2.1. 2% Os/alumina pretreated at 393 K

This catalyst was one derived from $Os_3(CO)_{12}$ and alumina prepared by the dry pressing method. The catalyst was activated in a nitrogen-hydrogen mixture as described in the previous section. The weight of catalyst used was 7.1 g. CO hydrogenation was carried out at various temperatures: first at 10 atm and then at 100 atm and the results of these experiments are shown in Table 3.63. No other characterization was carried out.

3.5.2.2. 2% Os/alumina pretreated at 773 K

This solid was also one prepared by the dry-pressing method from $Os_3(CO)_{12}$ and alumina, with the alumina having been heated to 773 K in vacuum prior to pressing. 7.2 g of the catalyst was used. CO hydrogenation results at 10 and 100 atm are shown in Table 3.64.

3.5.2.3. 2% Os/alumina derived from $OsCl_3$

This catalyst was prepared by the incipient wetness method using $OsCl_3$ rather than $Os_3(CO)_{12}$ in order to determine if this different precursor had any effect on the nature of the osmium bonded to the surface and hence the catalytic activity. 7.4 g of the solid

was used and the results of CO hydrogenation experiments at 10 and 100 atm are shown in Table 3.65.

Table 3.63

CO Hydrogenation Over 2% Os/Alumina (393 K) in the Berty Reactor

Temp /K	Activity	Products /mol%							
		CH_4	C_2H_4	C_2H_6	C_3H_6	C_3H_8	C_4	C_5	DME*
Experiments at 10 atm									
503	0.087	36.2	4.2	9.1	13.0		16.1	18.6	2.7
523	0.080	32.7	4.5	6.0	8.0		20.4	20.9	7.1
548	0.253	37.8	5.2	5.9	6.2	7.7	16.0	15.2	4.3
573	0.709	45.6	4.7	6.3	8.1	5.8	13.4	10.8	1.6
Experiments at 100 atm									
498	0.004	61.6	38.4						
523	0.049	52.1	3.9	12.2	10.3		3.2		18.1
548	0.517	37.0	1.0	8.6	1.2	5.9	12.6	5.7	19.6
573	0.942	35.1	0.8	8.3	2.4	5.3	9.4	4.9	16.1

* DME = Dimethyl ether

In this table and in the two following, various minor products have been omitted for clarity. The mol % values shown refer to the total products. The activity is expressed as in Table 3.60.

Table 3.64

CO Hydrogenation Over 2% Os/Alumina (773 K) in the Berty Reactor

Temp /K	Activity	Products /mol%							
		CH_4	C_2H_4	C_2H_6	C_3H_6	C_3H_8	C_4	C_5	DME
Experiments at 10 atm									
498	0.034	29.0	Values unreliable						
523	0.131	39.3	5.4	6.6	7.3		20.3	16.0	4.8
548	0.238	41.5	5.5	6.3	6.7	5.0	13.3	13.2	5.0
573	0.752	37.4	4.6	5.3	6.8	5.0	10.5	10.4	1.7*
Experiments at 100 atm									
498	0.043	50.1	11.9		6.2		5.3		26.2
523	0.084	47.8	2.6	11.2	7.4		6.7		24.2
548	0.534	35.1	1.0	8.6	1.3	6.2	6.5	6.3	15.3*
573	1.417	33.4	0.8	8.1	3.2	5.9	6.1	5.2	11.2*

* CO_2 significant

Table 3.65

CO Hydrogenation Over 2% Os/alumina ex ($OsCl_3$) in the Berty Reactor

Temp /K	Activity	Products /mol%							
		CH_4	C_2H_4	C_2H_6	C_3H_6	C_3H_8	C_4	C_5	DME
Experiments at 10 atm									
498	0.015	26.9	4.2	5.6	Data not reliable				
523	0.045	30.6	5.8	7.0	2.1	7.2	15.2	17.6	14.4
548	0.205	45.2	4.5	5.6	7.9	5.3	11.4	13.3	3.6
573	0.458	54.2	4.9	5.6	8.1	4.1	9.2	9.1	2.2
Experiments at 100 atm									
498	0.019	38.7	2.9	12.5	20.1	8.7			17.1
523	0.046	41.9	3.2	12.3	8.4	10.5	10.7		12.7
548	0.324	32.3	2.8	8.6	6.4	7.2	9.0	9.3	1.3
573	1.163	35.1	1.6	9.0	5.3	5.8	6.3	5.6	3.6

4. DISCUSSION

4.1. The Cobalt-Magnesium Aluminate Spinel System

Surprisingly, in view of the great amount of work which has been described in the literature for the reaction of carbon monoxide and hydrogen to form hydrocarbons using transition metal catalysts, relatively little definitive work can be found relating to the use of supported cobalt in the absence of promoters. In particular, recent data where experimental conditions have been well controlled and characterisation has been attempted, are rare. Since the pioneering work of Fischer[13] over 50 years ago, much of the work carried out has concentrated on the the kinetics and mechanism of the methanation reaction.[5,26] However, recently both Vannice[31,101] and Reuel and Bartholomew[32,46] have carried out comprehensive investigations using cobalt supported on Al_2O_3, SiO_2, MgO and TiO_2 which have also investigated the formation of higher hydrocarbons.

In reviewing the data obtained in the present studies on reduced cobalt-containing spinels, comparison will be made chiefly with results obtained using conventionally supported cobalt catalysts.[31,32] Reference will also be made to results obtained by Highfield et al. on the reduced CoO-MgO system.[89]

Eight catalysts were studied with cobalt concentration in the range 5 to 20 mol %. Of these, four were not subject to acid washing after preparation and these were found by examination of the XRD pattern

to contain significant amounts of CoO-MgO phase. The four unwashed samples were 5CoSpinel 1, 20CoSpinel 1, 10CoSpinel 1 and 10CoSpinel 2.

4.1.1. Reduction of Cobalt-Containing Spinel

The results show that these catalysts are extremely resistant to reduction, and that when reduction takes place the quantities of metal produced are small. Table 4.1 summarizes reduction treatment used with the catalysts and also shows oxygen uptake values obtained after reduction in the static system. As can be seen, the reduction conditions used were very severe, indicating the high stability of the Co^{2+} ions in the spinel lattice. This meant that temperatures up to 400 K greater than those required for conventional catalyst[31] were required to effect measurable reduction. All the conditions shown in Table 4.1 represent the most severe temperatures and longest exposure times applied to the catalyst. Another noteworthy feature of the reduction of spinel solid solutions is the need for pretreatment in CO before exposure to hydrogen at high temperature. Exposure to hydrogen alone did not produce significant reduction even at very high temperatures and prior treatment in carbon monoxide was always needed. This is a particular feature of the reduction of Co-containing solid solutions.[50,89,100]

4.1.2. Oxygen Chemisorption Measurememts

Oxygen chemisorption data in Table 4.1 are expressed in units of micromol g^{-1} in order that broad

comparison can be made with CO chemisorption data quoted in the literature in these units. CO chemisorption measurements were also carried out in the present work, but are not cited in the results section as the values tended to be rather variable. In general, CO uptake at ca 295 K gave values between 25% and 50% of the corresponding oxygen value. Hydrogen adsorption was not sytematically studied in view of the complications arising from the process being activated.[30] A value of 16 micromol g-1 for CO adsorption on a fresh 2% Co/Al2O3 catalyst is reported by Vannice.[31] This is to be compared with values of 15 to 43 micromol g^{-1} for oxygen chemisorption in the present work. Assuming an adsorption stoichiometry of 1 CO molecule per cobalt site but 1 atom of oxygen per cobalt site, the oxygen uptake on Vannice's catalyst would be 8 micromol g^{-1}. This indicates that the cobalt metal areas are broadly similar for the two systems, but greater for the reduced spinel.

4.1.3. Dispersion and Degree of Reduction

In order to discuss the nature of the surface cobalt it is necessary to use the concept of dispersion. Dispersion for conventional supported catalysts is usually defined by the equation below[31,32]

$$D = M_s/M_t \qquad (13)$$

where:

D is the dispersion

M_s is the number of surface metal atoms (from chemisorption measurements)

M_t is the total number of metal atoms in the sample

This definition of dispersion henceforth referred to as D_c is relevant to conventional catalysts, where all the active metal is available on the surface of the support and the dispersion gives a rough measure of the average particle size present.

The situation with the catalyst derived from the oxide solid solutions of the present work is rather different. Initially all the cobalt is trapped within the lattice of the support. In the case of the spinel systems of interest, the cobalt is either in the octahedral or tetrahedral sites of the spinel structure. The population of cobalt in each type of site has been investigated by Angeletti et al.[86] and it would appear from their results that the majority of the cobalt occupies tetrahedral sites. Reduction causes the cobalt to be removed from some of these sites to form metallic clusters on the surface. The surface of these clusters is then available for catalysis. Evidence for the above was initially developed with MgO-based systems[50] but similar experimental evidence has been found to exist for the spinel system. Thus after the initial extremely severe reduction, oxygen chemisorption

Table 4.1

Reduction of Spinel Solid Solutions and Oxygen Uptake at Room Temperature

Catalyst	Reduction in static system	Oxygen* uptake	Reduction in flow system
5CoSpinel 1	Not carried out	–	CO 875 K, 20 h H_2 875 K, 12 h
5CoSpinel 2	CO to 920 K, 1 h H_2 to 1005 K, 6 h	19.5	H_2 625 K, 12 h
10CoSpinel 1	H_2 to 1000 K no uptake measured	-	Not carried out
10CoSpinel 2	No reduction- CO+H_2 at 575 K	–	Not carried out
10CoSpinel 3	CO to 990 K, 4 h H_2 to 1070 K, 8 h	42.8	H_2 725 K, 12 h
15CoSpinel	CO to 933 K, 17 h H_2 to 971 K, 20 h	32.3	H_2 615 K, 12 h
20CoSpinel 1	Not carried out	-	CO 875 K, 12 h H_2 895 K, 12 h
20CoSpinel 2	CO to 952 K, 20 h H_2 to 980 K, 12 h	15.2	H_2 675 K, 12 h

* Oxygen uptake in micromol per gram of catalyst at at room temperature after reduction in static system

is observed to a limit at room temperature and then further O_2 uptake occurs on raising the temperature to about 550 K. Subsequent reduction in hydrogen can be carried out at very much lower temperatures than the initial reduction. Highfield et al.[50] proposed that O_2 chemisorption at room temperature is chemisorption/ oxidation of the surface of the particles produced

during the high temperature reduction and the further oxygen uptake up to about 650 K (in their case) is due to oxidation of the interior of the particles and isolated atoms in the matrix. In the course of this work a correlation was found between oxygen uptake to about 650 K and the capability for subsequent uptake of hydrogen (1 O_2:2 H_2) at about the same temperature. For this reason, using the conventional measure of dispersion D_c can be misleading as, depending on the severity of the reduction, a substantial proportion of the cobalt is unavailable as it remains as cobalt ions within the spinel lattice. Hence D_c is an underestimate of the true dispersion. To overcome this, another measurement of dispersion was proposed [50] which is more relevant to solid-solution-derived catalysts. This will be referred to as D_{ss} and is defined as

$$D_{ss} = M_s/M_r \qquad (14)$$

$$= \frac{\text{Oxygen uptake at room temperature}}{\text{Total oxygen uptake to 550 K}}$$

where D_{ss} is the dispersion for a supported metal catalyst derived from a solid solution

M_s is the number of surface atoms

M_r is the number of atoms of cobalt reduced out of the solid solution

Table 4.2 shows the respective values of D_c and D_{ss} for the washed spinel samples free of MgO phase, using the chemisorption data reported in Section 3.2. In order to make comparison with conventional catalysts, the effective w/w loading of the catalysts (weight of

reduced metal x 100/total weight of catalyst) after reduction has been calculated.

Initially it was thought that the stabilization of the cobalt in the precursor solid solution would be beneficial in enabling very small amounts of highly dispersed surface cobalt to be produced by controlled reduction. In this way, the possible effect of particle size on catalysis could then be studied. Unfortunately it appears that, owing to the high temperatures needed for reduction, the process, once initiated, was difficult to control. Hence a relatively large proportion of the total cobalt was removed from the solid solution (Table 4.2). The consequence of this is that the catalysts studied had metal loadings of the same order of magnitude as those obtained with conventionally supported catalysts. This is in contrast to the MgO-based systems, which will be discussed later, where smaller amounts of reduction and hence smaller effective metal loadings were observed.

Table 4.2

Dispersion Values and Degree of Reduction of CoSpinels

Catalyst	% of total cobalt reduced	D_c	D_{ss}	Loading w/w%
5CoSpinel 2	82.4	0.110	0.134	1.67
10CoSpinel 3	35.6	0.130	0.365	1.46
15Cospinel	21.0	0.063	0.302	1.26
20CoSpinel 2	9.3	0.022	0.243	0.74

In order to place the above results into context it may be noted that Vannice[31] has published data for a 2% Co/Al_2O_3 catalyst where the dispersion (D_c) was measured by CO chemisorption to be 0.08. As can be seen from Table 4.2, this falls within the range found for the spinel-derived catalysts. However, if the assumptions made in the calculation of D_{ss} are valid, then the true dispersion of the cobalt metal is some four to five times greater.

Finally, it can be seen from the table that the largest effective loading of metal (supported on the oxide-spinel) was found when the concentration of the cobalt ions in the original solid solution was lowest. There is in fact a general trend observable in Table 4.2, although the extent of cobalt reduction must in reality also be a function of the highest temperature and period of reduction treatment.

4.1.4. Kinetics of CO Hydrogenation Over Reduced Co-Spinels

Table 4.3 contains the activation energy and order of reaction data collated from the results in Section 3.4. The data were gathered using the flow reactor under differential operating conditions. The value of the activation energy for methanation over the MgO-free samples is generally lower than the literature values for conventional supported Co catalysts[31,32] or for catalysts derived from MgO solid solutions.[89] Thus, Vannice[31] quotes a value of 112 kJ mol^{-1} for 2% Co/Al_2O_3

and Bartholomew[32] quotes 143 kJ mol^{-1} for 3%Co/Al_2O_3. Typical results obtained for reduced CoO-MgO systems gave values around 150 kJ mol^{-1}.[72]

To eliminate the possibility that the lower values might be influenced by diffusional limitations, experiments were often repeated at different space velocities and with different reactor packings. The results were found to be reproducible and independent of these variables.

Agrawal, Katzer and Manogue[49] report changes in the activation energy for methanation over a Co/Al_2O_3 catalyst with time and deduce that this is due to bulk carburization of the cobalt and the growth of multilayer graphitic deposits. Their activation energy values for methanation in the carburized state were 67 ± 8 kJ mol^{-1}. It seems unlikely that an explanation involving carburization could be the whole answer to the lower values in the present work, as the values observed by Agrawal et al. were found only after using the catalyst for long periods at much higher temperatures than those used in this study. Nevertheless, some effect of this kind may be present since deactivation and carbon lay-down were noted.

Order of reaction data for all the spinel catalysts studied are also shown in Table 4.3. Comparing the results with conventional catalysts[31,32] shows the order in CO to be very similar but the order in hydrogen for the washed spinel catalysts to be significantly higher.

4.1.5. Turnover Frequencies

Turnover frequencies have been calculated using the assumption that the metal surface available for catalysis in the flow system was the same as that measured by oxygen chemisorption in the static system. This assumption, however, is unlikely to be completely

Table 4.3

Activation Energies and Orders of Reaction for Methanation Over Spinel Catalysts

Catalyst	Orders of reaction		Activation energy kJ mol^{-1}
	CO	H_2	
5CoSpinel 1	-0.6	1.1	152
5CoSpinel 2*	-	-	75
10CoSpinel 3*	-0.6	1.5	87
15CoSpinel*	-0.5	1.5	110
20CoSpinel 1	-0.8	1.2	152
20CoSpinel 2*	-0.2	1.6	83
2% Co/Al_2O_3**	-0.5	1.2	112

* Samples washed free of MgO phase

** Data of Vannice[31]

true for the following reasons:

(1) it is likely that some decrease in the metal surface area would have occurred under catalysis conditions;

(2) results calculated using oxygen uptake assume monolayer coverage of the available metal, and it is possible that the coverage is greater than this.

The values cited are therefore the minimum possible and are quoted so that a comparison of the activity with that of conventional catalysts may be made.

Table 4.4 shows the values calculated. Inspection of literature values[31,32] for methanation over supported cobalt catalysts shows the values for the spinel-derived catalysts to be very low by comparison. For example, Vannice quotes a value of 0.026 s^{-1} at 548 K, whereas the most active catalyst studied (15CoSpinel) gave only 0.008 s^{-1} at 575 K. No particular trends seem evident for the spinel-derived catalysts. In particular, the catalyst with the largest apparent dispersion (10CoSpinel) gave the lowest specfic activity but 15CoSpinel with the next largest dispersion (D_{ss}) had the largest activity. The relatively low reduction temperature used in the activation of 15CoSpinel may be related to its subsequent large specific activity.

It is possible that the assumptions made in the calculation of these turnover frequencies causes greater errors than imagined. There is some evidence for this in the very low values of uptake obtained when flow chemisorption was carried out on samples after transfer to the flow reactor, and in the relatively high rates of

Table 4.4

Turnover Frequencies for Methanation in CO Hydrogenation over Spinel Catalysts

Catalyst	Temp/K	$N(CH4)/s^{-1}$
5CoSpinel	565	0.0037
10CoSpinel	575	0.0012
15CoSpinel	575	0.0081
20CoSpinel	575	0.0020

catalyst deactivation seen during catalytic testing. However, it is unlikely that these factors could account for the factor of up to 20 times lower activity in comparison with alumina-supported cobalt. It must be concluded that the activity of cobalt supported in this way is significantly less active than conventionally supported material.

4.1.6. Products of CO Hydrogenation

In all cases when CO hydrogenation was performed over these catalysts at temperatures around 575 K the major product (in mol % terms) was always methane, as expected.

The effect of increasing temperature on the product distribution was broadly that as the temperature was increased the quantity of non-methane products decreased, as is the case with conventional cobalt

catalysts.[31,32] Table 4.5 shows the C_1 to C_3 product selectivity for all the spinel catalysts investigated in the flow system at ca 560 K. In order to compare these figures to equivalent values for conventional catalysts it is important to note that these values are given in mol % units. Products of carbon number 4 and greater were no doubt produced but normally were not recognised by the analytical system which operated isothermally. C_4 peaks, for example, were already very broad in the GC analysis and were integrated only rarely. They were

Table 4.5

Products of CO Hydrogenation Over CoSpinels

Catalyst	Temp /K	Products mol %			
		CH_4	C_2H_4	C_2H_6	C_3
5CoSpinel 1	559	88.7	8.7		2.6
5CoSpinel 2*	564	68.3	20.5		11.1
10CoSpinel 3*	557	68.1	19.9		11.9
15CoSpinel*	561	89.7	7.9		2.2
20CoSpinel 1	555	78.4	15.2		6.4
20CoSpinel 2*	557	55.1	27.7		17.7

* Washed free of MgO phase

always very minor contributors (in mol % terms) to the overall selectivity.

Considering Table 4.5, it is generally true that catalysts which display large activity tend to be predominantly methane producers and this is borne out with the 15CoSpinel sample which has the lowest C2 and C3 product selectivity at this temperature but has the highest methane turnover frequency (Table 4.4). Also from Table 4.5 it can be clearly seen that the washed samples of spinel catalysts display a greater tendency to produce non-methane products when compared with the unwashed samples of the same concentration. This is taken as evidence of the superiority of the spinel system in this respect when compared to the MgO system which contaminates the unwashed samples. Comparing the results with the data of Vannice[31] for conventionally supported cobalt, the spinel-based catalyst is clearly better than conventional Co/alumina in producing non-methane hydrocarbons. This is especially emphasized if it is recalled that the results quoted for the spinel relate to a higher operating temperature which favours C_1 product. For the Vannice 2% Co/Al_2O_3 catalyst, the methane figure at 548 K is 83 mol %, the C_2 value being approximately 9 mol % and C_3 8 mol %.

The results in Table 4.5 refer to studies carried out under differential conditions in the flow reactor. By reference to Table 3.34 (Section 3.2) it can be seen that the product distributions obtained under static conditions are broadly similar, although direct comparison

is difficult as all the results in Table 3.29 utilized a $CO:H_2$ ratio of 1:3, whereas in the static experiments other ratios were used.

When the $CO:H_2$ ratio was changed from the normally used value of 1:3 to either 1:1 or 1:2, a substantial increase in the amount of C_2 and C_3 hydrocarbons was seen (Section 3.4). This feature is commonly found with Fischer-Tropsch catalysts and the experiments in Section 3.4 confirm that the present catalysts behave conventionally in this respect.

4.1.7. Deactivation in the Flow Reactor

Deactivation experiments were carried out on the washed catalysts under the reaction conditions of 575 K and $CO:H_2$ = 1:3. In order to be able to make comparisons, the percentage deactivation during reaction over a subsequent 4 h period was chosen as a standard observation. The results are shown in Table 4.6 for the spinel catalysts studied for deactivation in this way.

Table 4.6

Deactivation of CoSpinel Catalysts

Catalyst	Deactivation during 4 h /%
5CoSpinel 1	14.5
10CoSpinel 3	24.5
15CoSpinel	20.3

The table shows that the rate of deactivation of these catalysts is quite high. Highfield and Stone[89] found a rate of deactivation of 15-20% for CoO-MgO catalysts studied in the same way. Agrawal et al.[49] made a detailed study of deactivation over a Co/Al_2O_3 catalyst but used a CO:H2 ratio of 1:25. Using this system, two distinct rates of deactivation were noted, namely a very high initial rate and a lower one after some 30 h under reaction conditions at 675 K. The rate of deactivation referred to in Table 4.6 is taken to correspond to the latter, as a very high initial rate of deactivation was also noted in the present work prior to any measurements being recorded (Section 3.4) for all the catalysts studied.

4.1.8. Summary and Conclusions

Cobalt-Spinel solid solutions stabilize the Co^{2+} ion to such an extent that, in order to reduce it out of the solid solution, very high temperatures (of the order of 1000 K) have to be used. Although dispersion measurements indicate that quite highly dispersed metal may be present, there is little correlation between this measurement and the observed product distribution. As with the CoO-MgO system, reduction in hydrogen is facilitated by a pre-treatment in CO which, although not in itself producing an active catalyst, appears to activate the surface towards hydrogen reduction.

The products of CO hydrogenation are similar to those produced over conventional catalysts, although a

higher activity to non-methane products is observed. The activation energy for methanation is markedly lower compared with Co/alumina and although the order of reaction for CO is similar, the order for H_2 is significantly higher. Specific activities over the spinel-derived catalysts are considerably lower than values obtained with conventional supported catalysts.

Future work with these catalysts must be aimed at more systematic control of reduction experiments, and characterization of the catalyst surface before and after use, using the whole spectrum of modern analytical techniques, should be applied.

4.2. The NiO-MgO System

NiO-MgO has been extensively reported in the literature as a catalyst where the cations of the transition metal are the active sites. Catalytic reactions studied include the oxidation of CO[78,79] and the decomposition of nitrous oxide.[64] The reduced system, where nickel atoms are the catalytically active sites, have been much less investigated.[50]

The experiments carried out on NiO-MgO during this study (Sections 3.1 and 3.3) continued the work initiated by Dr J.G. Highfield. It was largly confined to studies where the nickel ion concentration in the solid solution was small (3 mol %). A very limited amount of work was also carried out on the 10 mol % NiO-MgO system in the first flow reactor.

4.2.1. 3NiO-MgO

4.2.1.1. Reduction Behaviour and Oxygen Chemisorption

After standardization and characterization of the extent of Ni^{3+} formation (normally small), reduction of the solid solution was carried out using hydrogen at temperatures between 800 and 900 K. These temperatures were in the same region as those previously used to reduce 5NiO-MgO.[89] In contrast to cobalt-containing systems, pre-treatment in CO did not appear to be needed. Uptakes of hydrogen shown in the results section (Table 3.4) indicate by a simple calculation that between 5 and 10% of the nickel in the solid solution was reduced. However, measurement of the metal present using oxygen at room temperature and then at higher temperatures (in the same manner as that used for spinel samples discussed in Section 4.1) indicated a much lower extent of reduction in the region of 2% of the total nickel. This is equivalent to an effective loading of about 0.055 w/w% for a conventional catalyst.

The lack of correlation between the hydrogen uptake in the reduction process and the oxygen uptake afterwards (evident from Tables 3.2 and 3.3) appears to be a feature of the reduction of solid solutions. It was present also when the cobalt spinel solid solutions were reduced, although not to such a marked extent. This is presumably due to a hydrogen spillover on to the support, causing surface hydroxylation to occur. Notwithstanding this, it is difficult to explain why the catalyst which had the largest hydrogen uptake

(3NiO-MgO 1) should have the smallest oxygen uptake at both the temperatures used.

Measurement of the dispersion of the catalyst was made using the method described in Section 4.1. The value of D_{ss} is shown in Table 4.7

The dispersion figures are only a guide[50] but do show moderate increase in the metal particle size after exposure to oxygen and re-reduction. This is logical as, at the temperatures used, there is bound to be some mobility of metal atoms on the surface. By comparison, the dispersion measured in the same way for spinel samples, although generally seen to decrease, does not fall by the same amount (typically 5%).

Table 4.7

Dispersion of 3NiO-MgO from Oxygen Uptake Measurements

	D_{ss}	
	3NiO-MgO 1	3NiO-MgO 2
After high temp. reduction	0.36	0.37
After oxidation and lower temp. re-reduction in hydrogen	0.23	0.27

4.2.1.2. Catalytic Activity of 3NiO-MgO

Ethane hydrogenolysis was carried out on both samples. The rate was much larger for 3NiO-MgO 2,

presumably due to its larger metal surface area as measured by oxygen chemisorption. 3NiO-MgO 2 was also more active in CO hydrogenation but in both cases methane was the only significant product. This is to be expected as nickel is primarily a methanation rather than a Fischer-Tropsch catalyst, and the result is in accord with previously studied examples of the same system.[89]

To sum up, the 3NiO-MgO system behaves in a broadly similar manner to other nickel/MgO systems which have been studied. It appears more difficult to reduce than similar samples of higher nickel concentration and can only be regarded as a methanation catalyst.

4.2.2. 10 NiO-MgO

Only one sample of this catalyst was studied in the first flow system. The kinetic parameters established were in good agreement with previous work and literature values,[32,102] although the activation energy for methanation was slightly higher than published values.

The deactivation of the catalyst was studied at 575 K ($CO:H_2$ = 1:2) and over 4 h was calculated as 22%, making the deactivation of this sample very similar to the rate observed for both other MgO and spinel-based systems.

4.3. The CoO-MgO system

Experimental work on the CoO-MgO system was confined to a study of 3CoO-MgO in the first static system and some reduction and catalytic experiments on

10 CoO-MgO. As was the case with the nickel system (Section 4.2.) the experiments were a continuation of work carried out by Dr J.G. Highfield.

4.3.1. 3CoO-MgO

4.3.1.1. Reduction Behaviour and Oxygen Chemisorption

Studies of the 3CoO-MgO system were more complicated than those of the equivalent NiO-MgO system. This was due to the relatively large uptakes of oxygen on the unreduced solid solution caused by the formation of Co^{3+} species.[103] This effect is much greater in the case of CoO-MgO than is the equivalent formation of Ni^{3+} in NiO-MgO systems because of the greater stability of the Co^{3+} ion. For reasons which must be connected with the ionic structure of the oxide, the effect with CoO-MgO is also much greater than with CoSpinel (Section 4.1). Because of the ease with which unreduced residual Co^{2+} ions are re-oxidized by oxygen to Co^{3+} ions, it was difficult to apply the technique of oxygen chemisorption/ oxidation accurately to measure the size of the metal surface area and dispersion: the uptake of oxygen on unreduced cobalt ions formed a very large proportion of the total uptake. The experimental position was further complicated by the fact that, in common with previous low concentration CoO-MgO solid solutions studied[89], reduction in hydrogen alone was ineffective and it was found that, even after pretreatment in CO, reduction in hydrogen would only occur at very high temperatures.

It is difficult to estimate the extent of reduction

from reductant uptake values as two gases are involved, and it is clear that not all the CO taken up partakes in genuine reduction (due to the Boudouard reaction). Even where genuine reduction does occur, some of the reduced metal atoms produced are inaccessible to oxygen occupying positions below the surface of the lattice.

However, it is clear from the results that reduction of the Co^{2+} ions is slight and the metal loading of the catalyst must be even smaller for 3CoO-MgO than it is in the NiO-MgO system studied. For example, after allowing for the uptake of oxygen on the solid solution (to form Co^{3+} ions), the uptake of oxygen on 3CoO-MgO 1 was only 0.005 micromol m^{-2} (Section 3.1.2.1) and although this value is subject to a large error, it does show that a very small amount of metal was formed. The amount was three to six times less than the equivalent uptakes for 3NiO-MgO. For the reasons outlined above, dispersion measurements could not be confidently made for the 3CoO-MgO system.

4.3.1.2. Catalytic Activity of 3CoO-MgO

Activity in ethane hydrogenolysis showed a broadly similar behaviour to the 3NiO-MgO system, except that 3CoO-MgO 3 gave a very low value commensurate with its very small degree of reduction.

The initial rate in CO hydrogenation was also similar to the corresponding NiO-MgO catalysts, the only noteworthy feature being that the catalyst mentioned above as having a low activity in ethane hydrogenolysis

showed similar CO hydrogenation rates to the other catalyst tested.

The products of the CO hydrogenation reaction contained larger percentages of C_2 and C_3 products than in the equivalent nickel case. This would be expected as cobalt has a better selectivity to non-methane products than nickel. The total percentage of higher hydrocarbons was nevertheless small, probably due to the severity of the initial high temperature reduction giving rise to large particles of cobalt, which seem to be more methane-selective.

To sum up, the 3CoO-MgO system was difficult to reduce and to characterize by oxygen chemisorption. Products of CO hydrogenation showed methane to be the major product with very small amounts of higher hydrocarbons.

4.3.2. 10CoO-MgO

This higher concentration sample of CoO-MgO was studied in order that comparison of its reduction and catalytic behaviour could be made with 3CoO-MgO and also with the CoSpinel-derived catalysts.

It was found possible to effect reduction of divalent cobalt using only hydrogen at 823 K over many hours. This confirmed that higher concentration CoO-MgO solid solutions do not require pretreatment in CO, a fact which had been observed in earlier work.[89]

Oxygen chemisorption results lead to dispersion values (D_{ss}) of 0.33 prior to catalytic experiments and

0.35 after them. The very small difference between these figures indicates a very low rate of sintering of the metallic particles during catalysis.

CO hydrogenation experiments using different $CO:H_2$ ratios show clearly the increase in higher hydrocarbon products as the ratio nears unity. Both this and the increased production of carbon dioxide are normal features of conventionally supported cobalt catalysts.[31]

4.4. Osmium-Containing Catalysts

Osmium-containing catalysts conventionally supported on Al_2O_3, SiO_2 and MgO were investigated at pressures in the range 1-100 atm. The main aim of the work carried out at I.C.I. was to discover how different support pretreatments affected CO hydrogenation product selectivity. The experiments at Bath on Os/MgO were carried out both to compare results with the other osmium catalysts and to provide data on a catalyst other than cobalt at 1 atm.

4.4.1. Os/alumina

Os/alumina was investigated at I.C.I. Runcorn in both a 10 atm flow reactor and a 10-100 atm recycle reactor of the Berty type. Osmium in the form of $Os_3(CO)_{12}$ was impregnated on to the support using the dry-pressing method (Section 2.2.5), as attempts using the more conventional incipient wetness technique were unsuccessful. The alumina surface was pretreated by heating in vacuum at either 393 or 773 K prior to osmium impregnation. Specimen results for each alumina-based

catalyst derived from data in Section 3.5. are shown in Table 4.8. Results obtained at ca 570 K are shown as data and are available for all the catalysts at this temperature.

Several conclusions can be drawn from the data. It appears that the overall activity of each catalyst increases with pressure, while from examination of the results in Section 3.5, a decrease in olefin selectivity and an increase in paraffin selectivity is seen. For example, catalyst (2) showed an increase in overall activity of 32% when the pressure was raised from 10 to 100 atm. At the same time, although total C_2-C_4 products fell, the ethane selectivity increased by 32% and propane, although falling in absolute amount, became favoured over propene. Notwithstanding this, it is difficult to see why a 2% Os/alumina catalyst (pretreated at 393 K) tested in the 10 atm laboratory reactor should have a much higher specific activity than a similar sample tested at 10 atm in the Berty reactor. The only obvious explanation is that the active surface area of the former catalyst was larger (differences in space velocity etc being accounted for in the way the activity was calculated) in spite of the two catalysts having been prepared and activated under the same closely controlled conditions. The higher activity sample has the larger activity for methane production, a feature of other CO hydrogenation catalysts.

The activity and selectivity of both the catalysts pre-treated at 393 or 773 K are very similar and hence

Table 4.8

Comparison of CO Hydrogenation Results Over Os/alumina Catalysts at Temperatures Near 570 K

Catalyst[a] pre treatment	Pressure[b] /atm	Temp /K	Activity[c]	Products /mol %			
				C_1	C_2	C_3	C_4
393 K (1)	10 (L)	568	2.17	90.7	3.7	2.7	1.6
393 K (2)	10 (B)	573	0.71	45.6	11.0	13.9	13.4
393 K (2)	100 (B)	573	0.94	35.1[d]	9.1	7.7	9.4
773 K (3)	10 (B)	573	0.75	37.4[d]	9.9	11.8	10.5
773 K (3)	100 (B)	573	1.42	33.4[d]	8.9	9.1	6.1

a: all catalysts 2% Os/alumina, figure in brackets indicates sample number.

b: (L) = 10 atm reactor, (B) = Berty reactor

c: activity expressed in units of CO converted per kilogram of catalyst per hour

d: significant amounts of dimethyl ether also seen

for this catalyst system, catalyst pretreatment appears not to be an important factor in catalytic behaviour. At 100 atm the activity of the sample pretreated at 775 K is larger than the 393 K treated sample by a factor of 1.5 but the product selectivity is similar.

Owing to the lack of surface area data on the catalysts, it is difficult to make any accurate comparisons of activity for these Os carbonyl-derived catalysts. Also most published data on Os-based

catalysts have been directed at identifying the catalytically active site.[37-40,104] Catalytic work has mostly been carried out at low pressure (1 atm). Knozinger et al.[40] have investigated a 0.34 % w/w $Os_3(CO)_{12}$-derived catalyst supported on alumina operated at 1 atm ($CO:H_2$ = 1:3, 600 K). 81% of the products were methane, the rest being composed of C_2 (16%) and C_3 (3%), although in another paper of which Knozinger was a co-author[38], more C_2 was seen when operating a similar catalyst.

4.4.2. Os/silica

Os/silica was investigated in much the same way as the Os/alumina discussed in Section 4.4.1. but no experiments were carried out at 100 atm as the Berty reactor was not available. Table 4.9 shows a comparison of catalytic results obtained at 573 K and 10 atm for samples pretreated at 393 K and 773 K respectively. The data are shown in full in Section 3.5.

Table 4.9

Comparison of CO Hydrogenation Results Over Os/silica Catalysts at 573 K

Catalyst[a] pre treatment	Pressure[b] /atm	Temp /K	Activity[c]	Products /mol %			
				C_1	C_2	C_3	C_4
393 K (1)	10 (L)	573	0.15	68.4	8.7	9.8	7.5
773 K (2)	10 (L)	573	0.67	76.3	11.8	6.1	2.0

a, b and c as in Table 4.8

In this case a definite increase in activity can be seen in the sample pre-treated at 773 K, the activity being about four times the value for the 393 K sample. As is normally seen, the more active sample has a greater methane selectivity. At the start of this work it was thought possible that a higher temperature of pretreatment might be beneficial in producing catalysts of high activity by stablizing chemisorbed osmium (by dehydroxylation) and reducing aggregation under reaction conditions. From the limited amount of work done this would appear to be the case, but more work is required before a definite statement can be made.

It is of interest to compare results obtained for osmium supported on alumina and silica in the 10 atm reactor. From comparison of the values it would appear that the alumina-supported catalyst was more active when both catalysts were prepared by the dry-pressing technique. Wells, Jackson et al.[105-107] found the reverse to be true for similar osmium catalysts prepared by a wet impregnation technique, and proposed that the order of activity on three oxide supports was in the order $SiO_2 > TiO_2 > Al_2O_3$.[92-94]

Activation energies for the reactions over silica and alumina-supported catalysts have not been calculated as the raw rate data for methanation were not produced by the analytical system used at I.C.I. Runcorn. It would be possible to calculate the necessary values by using a combination of selectivity and activity data but large errors would be inevitable. Furthermore, only three or

four temperatures were used for catalytic experiments and experimental runs were not often repeated.

4.4.3. $OsCl_3$-derived catalysts

One Os/alumina catalyst was prepared by conventional wet impregnation using $OsCl_3$ as a precursor. The catalytic work on this catalyst was carried out by Mr A. Simpson at I.C.I. Runcorn. The results obtained (Table 3.30 in Section 3.5) are similar to those obtained for alumina-supported catalysts derived from osmium carbonyl.

4.4.4. Os/alumina and Os/magnesia at 1 atm

Os/alumina and Os/magnesia catalysts were prepared in Bath by a wet impregnation technique for testing at 1 atm. It was not possible to carry out characterization of the active surface, and hence the calculation of turnover frequencies was not possible. However, kinetic parameters and product selectivities were established.

Os/alumina

At 566 K and 1 atm the catalyst produced mostly methane. Although for the reason mentioned specific activities cannot be determined, the activity in terms of the weight of catalyst used was comparable to the more active CoSpinel catalysts studied. As osmium catalysts have been reported in the literature to have turnover frequencies in the range 1-20 x 10^{-3} s^{-1} [37,38] comparable to those observed in the present work for CoSpinel, this would appear reasonable.

Orders of reaction for CO and H_2 were found to be similar to those obtained for other CO-hydrogenation catalysts, although the activation energy for methanation at 153 kJ mol^{-1} was higher than other reported values, Knozinger et al. [38] have quoted a value of 110 kJ mol^{-1} for a similar catalyst.

Os/Magnesia

This catalyst was less active than the alumina-based one and produced a higher percentage of non-methane products in CO hydrogenation (15 mol % at 563 K).

Kinetic parameters were established and were found to be generally similar to those obtained for the alumina-supported catalyst, although the activation energy for methanation is closer to literature values at 134 kJ mol^{-1}.

4.4.5. Summary of Osmium Behaviour

Although less active than other Fischer-Tropsch catalysts, the osmium catalysts studied appear to have activity similar to the Cobalt-Spinel solid-solution-derived catalysts. At 1 atm the major product is methane and at this pressure the osmium catalysts are inferior to the Cobalt-Spinel ones at comparable temperatures. At higher pressures significant quantities of higher hydrocarbons were seen and under these conditions it would be interesting to study the solid-solution derived catalysts to compare their performance with the osmium systems.

In order to confirm any pretreatment or precursor

effects more work is necessary on these systems. In particular it will be necessary to carry out comprehensive spectroscopic characterization of catalysts prior to and after catalytic studies. The method of preparing these catalysts by the incipient wetness technique requires further investigation.

REFERENCES

1. P.H. Spitz, Chemtech, 7, 295 (1977).
2. I. Wender, Catal. Rev.-Sci. Eng., 14, 97 (1976).
3. F.S. Stone, in "Frontiers of Chemistry (IUPAC)", (ed. K.J. Laidler), p.317, Pergamon, Oxford, 1982.
4. J.J. Berzelius (1836), cited by D.A. Dowden, Endeavour, 23, 69 (1965)
5. G.A. Mills and F.W. Steffgen, Catalysis Reviews, 8, 159, (1973).
6. P.J. Denny and D.A. Whan, in "Catalysis", Vol. 2, p.46, The Chemical Society, London, 1978.
7. M.A. Vannice, Catal. Rev.-Sci. Eng., 14, 153, (1976).
8. M.A. Vannice, J. Catal., 44, 152, (1976).
9. S.Z. Ozdogan, P.D. Gochis and J.L. Falconer, J. Catal., 83, 257, (1983).
10. E.C. Kruissink, L.L van Reijen and J.R.H. Ross, J. Chem. Soc., Faraday Trans. 1, 77, 649 (1981).
11. L.E. Alzamora, J.R.H. Ross, E.C. Kruissink and L.L. van Reijen, J. Chem. Soc., Faraday Trans. 1, 77, 665 (1981)
12. C.C. Kao, S.C. Tsai and Y.W. Chung, J. Catal., 73, 136 (1982).
13. F. Fischer and H. Tropsch, Brennst. Chem., 7, 97, (1926).
14. S.R. Craxford and E.K. Rideal, J. Chem. Soc., p.1604, (1939).
15. S.R. Craxford, Trans. Faraday Soc., 42, 576 (1946).

16. R.B. Anderson, "The Fischer-Tropsch Synthesis", Ch. 4, p.100 and Ch. 5, p. 174, Academic Press, New York,1984.

17. H. Pichler, Adv. Catal., 4, 272 (1952).

18. G.M. Kozub, M.T. Ruzov and V.M. Vlasenko, Kinet. Katal. 6, 244, (1965).

19. M.E. Dry, T. Shingles, L.J. Boshoff and G.J. Oosthuizen, J. Catal., 15, 190 (1969).

20. T. van Herwijnen, H. van Doesburg and W.A. de Jong, J. Catal., 28, 391 (1973).

21. M.A. Vannice, J. Catal, 37, 462 (1975).

22. P. Schoubye, J. Catal. 14, 238 (1969).

23. H.H. Storch, N. Golumbic and R.B. Anderson, "The Fischer-Tropsch and Related Synthesis", Wiley, New York, 1951.

24. K. Kishi and M.W. Roberts, J. Chem. Soc., Faraday Trans. 1, 71, 1715 (1975).

25. R.W. Joyner and M.W. Roberts, J. Chem. Soc., Faraday Trans. 1, 70, 1819 (1974).

26. V. Ponec, Catal. Rev.- Sci. Eng., 18, 151 (1978).

27. M. Araki and V. Ponec, J. Catal., 44, 439 (1976).

28. G. Wedler, H. Papp and G. Schroll, J. Catal., 38, 153, (1975).

29. A. Palazov, G. Kadinov, Ch. Bonev and D. Shopov, J. Catal., 74, 44 (1982).

30. J.M. Zowtiak and C.H. Bartholomew, J. Catal., 83, 107 (1983).

31. M.A. Vannice, J. Catal., 37, 449, (1975).

32. R.C. Reuel and C.H. Bartholomew, J. Catal., 85, 78 (1984).

33. Y.T. Shah and A.J. Perrotta, Ind. Eng. Chem., Prod. Res. Dev., 15, 123 (1976).

34. R.B. Anderson, in "Catalysis" (ed. P.H. Emmett), Vol. 4, Van Nostrand-Reinhold, Princeton, New Jersey, 1956.

35. C.S. Kellner and A.T. Bell, J. Catal., 75, 251 (1982).

36. T. Iizuka, Y. Tanaka and K. Tanabe, J. Catal., 76, 1 (1982).

37. M. Deeba, J.P. Scott, R. Barth and B.C. Gates, J. Catal., 71, 373 (1981).

38. H. Knözinger, Y. Zhao, B. Tesche, R. Barth, R. Epstein, B.C. Gates and J.P. Scott, Faraday Disc. Chem. Soc., 72, 53 (1981).

39. R. Psaro, R. Ugo and G.M. Zanderighi, J. Organometal. Chem., 213, 215 (1981).

40. E.O. Odebunmi, Y. Zhao, H. Knözinger, B. Tesche, W.H. Manogue, B.C. Gates and J. Hulse, J. Catal. 86, 95 (1984)

41. M.E. Dry, Chemtech, 12, 744 (1982).

42. M.A. Vannice and R.L. Garten, J. Catal., 56, 236 (1979).

43. M.A. Vannice and R.L. Garten, J. Catal., 66, 242 (1980).

44. C.H. Bartholomew, R.B. Pannell and J.L. Butler, J. Catal., 65, 335 (1980).

45. R.L. Palmer and D.A. Vroom, J. Catal., 50, 244 (1977).

46. R.C. Reuel and C.H. Bartholomew, J. Catal., 85, 63 (1984).

47. S.H. Moon and K.E. Yoon, Applied Catal., 16, 289 (1985).

48. D. Vanhove, Z. Zhuyong, L. Makambo and M. Blanchard, Applied Catal., 9, 327 (1984).

49. P.K. Agrawal, J.R. Katzer and W.H. Manogue, J. Catal., 69, 312 (1981).

50. J.G. Highfield, A. Bossi and F.S. Stone, in "Preparation of Catalysts III" (ed. G. Poncelet, P. Grange and P.A. Jacobs), p.181, Elsevier, Amsterdam, 1983.

51. A.T. Bell, Catal. Rev.- Sci. Eng., 23, 203 (1981).

52. P. Biloen and W.M.H. Sachtler, Adv. Catal., 30, 165 (1981).

53. G.A. Somorjai, Catal. Rev.- Sci. Eng., 23, 189 (1981).

54. Ya.T. Eidus, Russian Chem. Rev., 36, 339 (1967).

55. C.K. Rofer-DePoorter, Chem. Rev., 81, 447 (1981).

56. H. Schulz, Pure and Applied Chem., p.2225, (1979).

57. W.A.A. van Barneveld and V. Ponec, J. Catal., 51, 426, (1978).

58. C.H. Bartholomew and C.K. Vance, J. Catal., 91, 78 (1985).

59. F. Solymosi, I. Tombacz and M. Kocsis, J. Catal., 75, 78 (1982).

60. A. Outi, I. Rautavuoma and H.S. van der Baan, Applied Catal., 1, 247 (1981).

61. H.H. Nijs and P.A. Jacobs, J. Catal., 66, 401 (1980).

62. J. Klose and M. Baerns, J. Catal., 85, 105 (1984).

63. R.W. Joyner, J. Catal., 50, 176 (1977).

64. "A New Dictionary of Chemistry", (ed. Mackenzie Hall), Longmans, London, 1964.

65. F.S. Stone, in "Chemical and Physical Aspects of Catalytic Oxidation" (ed. J.L. Portefaix and F. Figueras), p.437, Editions du C.N.R.S., Paris, 1980.

66. J.C. Vickerman, in "Catalysis", Vol. 2, p.107, Chemical Society, London, 1978.

67. A. Cimino, M. Lo Jacono, P. Porta and M. Valigi, Z. Phys. Chem., N. F., 55, 14 (1967).

68. A. Cimino, M. Lo Jacono, P. Porta and M. Valigi, Z. Phys. Chem., N. F. 70, 166 (1970).

69. R.V. Bunina and I.S. Sazonova, React. Kinet. Catal. Lett., 3, 89 (1975).

70. Z. Kluz and M. Jagiello, Z. Phys. Chem., N.F., 122, 117 (1980).

71. Z. Kluz, J. Stoch and T. Czeppe, Z. Phys. Chem., N.F., 134, 125 (1983).

72. A. Cimino, Materials Chem. Phys., 13, 221 (1985).

73. A. Cimino, B.A. De Angelis and G. Minelli, Surf. Interface Anal., 5, 150 (1983).

74. A.P. Hagan, M.G. Lofthouse, F.S. Stone and M.A. Trevethan, in "Preparation of Catalysts II, (ed. G. Poncelet, P. Grange and P.A. Jacobs), p.417, Elsevier, Amsterdam, 1979.

75. K. Dyrek and Z. Sojka, J. Chem. Soc., Faraday Trans. 1, 78, 3177 (1982).

76. A. Cimino, M. Schiavello and F.S. Stone, Disc. Faraday Soc., 41, 350 (1966).

77. A. Cimino and F. Pepe, J. Catal., 25, 362 (1972).

78. V. Indovina, A. Cimino and F. Pepe, Gazzetta Chim. Italiana, 110, 13 (1980).

79. Z. Kluz and A. Wojtaszczyk, Z. Phys. Chem. N.F. 111, 225 (1978).

80. F. Pepe and F.S. Stone, J. Catal., 56, 160 (1979).

81. O.I. Goncharova and T.M. Yurieva, React. Kinet. and Catal. Lett., 15, 73 (1980).

82. V.V. Popovskii, G.K. Boreskov, V.S. Muzykantov, V.A. Sazonov, G.I. Panov, V.A. Roshchin, I.M. Plyasova and V.V. Malakov, Kinet. Katal., 13, 727 (1972).

83. H.H. Kung, J. Catal., 73, 387 (1982).

84. P. Pomonis and J.C. Vickerman, J. Catal., 55, 88 (1978).

85. P. Porta, F.S. Stone and R.G. Turner, J. Solid State Chem., 11, 135 (1974).

86. C. Angeletti, F. Pepe and P. Porta, J. Chem. Soc., Faraday Trans. 1, 73, 1972 (1977).

87. C. Angeletti, F. Pepe and P. Porta, J. Chem. Soc., Faraday Trans. 1, 73, 1595 (1977).

88. A. Cimino and M. Schiavello, J. Catal., 20, 202 (1971).

89. J.G. Highfield and F.S. Stone, unpublished data.

90. R.J. Matyi, L.H. Schwartz and J.B. Butt, Catal. Rev.-Sci Eng., 29, 41 (1987).

91. V. Indovina, A. Cimino, M. Inversi and F. Pepe, J. Catal., 58, 396 (1979).

92. C. Morterra, G. Ghiotti, F. Boccuzzi and S. Coluccia, J. Catal., 51, 299 (1978).

93. A.C.C. Tseung and J.R. Goldstein, J. Mater. Sci., 7, 1383 (1972).

94. E.G. Christoffel, Catal. Rev.-Sci. Eng., 24, 159 (1982).

95. H.L. Gruber, J. Phys. Chem., 66, 48 (1962).

96. H.L. Gruber, Anal. Chem., 34, 1828 (1962).

97. J.M. Berty, Chem. Eng. Prog., 70, 78 (1974).

98. J.M. Berty, J.O. Hambrick, T.R. Mallone and D.S. Ullock, "Symposium on Advances in High Pressure Technology", New Orleans, Louisiana (1969).

99. J.M. Berty, Catal. Rev.-Sci. Eng., 20, 75 (1979).

100. A.J. Rennison and F.S. Stone, 11th Annual Research Meeting, The Institution of Chemical Engineers, University of Bath, 1984

101. M.A. Vannice, J. Catal., 50, 228 (1977).

102. P. Biloen, J.N. Helle and W.M.H. Sachtler, J. Catal., 58, 95 (1979).

103. A.P. Hagan, Ph.D. Thesis, Bristol, 1974.

104. R. Psaro, C. Dossi and R. Ugo, J. Molec. Catal., 21, 331 (1983).

105. G. Collier, D.J. Hunt, S.D. Jackson, R.B. Moyes, I.A. Pickering, P.B. Wells, A.F. Simpson and R. Whymam, J. Catal., 80, 154 (1983).

106. D.J. Hunt, S.D. Jackson, R.B. Moyes, P.B. Wells and R. Whyman, J. Catal., 86, 333 (1984).

107. S.D. Jackson, R.B. Moyes, P.B. Wells and R. Whyman, J. Catal., 86, 342 (1984).

APPENDIX

Computer Program for Mass Spectrometric Analysis

```
REM Mass Spec Analysis Program (Condensed)
REM Versio
REM By A.J
CLS
REM Input
DIM f(12),                                                    2),o(12),a(100),z(50)
a=0
FOR j=12 T
PRINT"Mass
INPUT "Len
a=a+a(j)
NEXT j
FOR j=24 T
PRINT "mas
INPUT "len
a=a+a(j)
NEXT j
FOR j=37 T
PRINT"mass
INPUT "len
a=a+a(j)
NEXT j
FOR j=55 TO 56
PRINT "mass no";j
INPUT "length of line in mm";a(j)
FOR j=55 TO 56
PRINT "mass no";j
INPUT "length of line in mm";a(j)
a=a+a(j)
NEXT j
f(3)=f(1)*0.217
a(29)=a(29)-f(3)
f(4)=f(1)
a(28)=a(28)-f(4)
f(5)=f(1)*0.352
a(27)=a(27)-f(5)
f(6)=f(1)*0.219
a(26)=a(26)-f(6)
f(7)=f(1)*0.047
a(25)=a(25)-f(7)
f(8)=f(1)*0.068
a(15)=a(15)-f(8)
f(9)=f(1)*0.042
a(14)=a(14)-f(9)
f(10)=f(2)+f(3)+f(4)+f(5)+f(6)+f(7)+f(8)+f(9)
REM above gives total contribution for ethane
g(1)=a(26)*1.605
g(2)=g(1)
a(28)=a(28)-g(2)
g(3)=g(1)*0.648
a(27)=a(27)-g(3)
g(4)=a(26)
a(26)=0
g(5)=a(25)
a(25)=0
g(6)=a(24)
a(24)=0
g(7)=g(1)*0.063
a(14)=a(14)-g(7)
g(8)=a(13)
a(13)=0
g(9)=g(1)*0.021
a(12)=a(12)-g(9)
g(10)=g(2)+g(3)+g(4)+g(5)+g(6)+g(7)+g(8)+g(9)
REM above gives total contribution for ethene
h(1)=a(29)
h(2)=h(1)
a(29)=0
```

```
h(3)=h(1)*0.591
)=a(28)-h(3)
h(4)=h(1)*0.394
a(27)=a(27)-h(4)
h(5)=h(1)*0.062
a(15)=a(15)-h(5)
h(6)=h(1)*0.290
a(44)=a(44)-h(6)
h(10)=h(2)+h(3)+h(4)+h(5)+h(6)
REM above for prppane
i(1)=a(42)*1.477
i(2)=a(42)
a(42)=0
i(3)=i(1)
a(41)=a(41)-i(3)
i(4)=i(1)*0.289
a(40)=a(40)-i(4)
i(5)=i(1)*0.711
a(39)=a(39)-i(5)
i(6)=i(1)*0.193
a(38)=a(38)-i(6)
i(7)=i(1)*0.136
a(37)=a(37)-i(7)
i(8)=a(27)
a(27)=0
i(9)=i(1)*0.054
a(15)=a(15)-i(9)
i(10)=i(2)+i(3)+i(4)+i(5)+i(6)+i(7)+i(8)+i(9)
REM above gives total line length for propene
j(1)=a(56)*2.227
j(2)=a(56)
a(56)=0
j(3)=j(1)*0.162
a(55)=a(55)-j(3)
j(4)=j(1)
a(41)=a(41)-j(4)
j(5)=j(1)*0.473
a(39)=a(39)-j(5)
j(10)=j(1)+j(2)+j(3)+j(4)
REM above gives total line length for isobutene
k(1)=a(55)
a(55)=0
k(10)=k(1)
REM above an approx for c5
l(1)=a(32)
a(32)=0
l(2)=l(1)*0.009
a(16)=a(16)-l(2)
l(10)=l(1)+l(2)
REM above gives line length for oxygen
m(1)=a(44)
a(44)=0
m(2)=m(1)*0.082
a(28)=a(28)-m(2)
m(3)=m(1)*0.094
a(16)=a(16)-m(3)
m(4)=a(12)
a(12)=0
m(10)=m(1)+m(2)+m(3)+m(4)
REM above gives line length for carbon dioxide
n(1)=a(16)
a(16)=0
n(2)=a(15)
a(15)=0
n(10)=n(1)+n(2)
REM above for methane
DIM p(12),q(12)
o(1)=a(28)
a(28)=0
o(2)=a(14)
a(14)=0
o(10)=o(1)+o(2)
REM above for nitrogen
p(1)=a(18)
```

```
a(18)=0
2)=a(17)
a(17)=0
p(lq(1)=f(10)*100/a
REMq(2)=g(10)*100/a
q(lq(3)=h(10)*100/a
q(2q(4)=i(10)*100/a
q(3q(5)=j(10)*100/a
q(4q(6)=k(10)*100/a
q(5q(7)=l(10)*100/a
q(6q(8)=m(10)*100/a
q(7q(9)=n(10)*100/a
q(8q(10)=o(10)*100/a
q(9q(11)=p(10)*100/a
q(1LPRINT "Results o
q(11)=p(10)*100/a
LPRINT "Results of Analysis of Mass Spec"
LPRINT "********************************"
LPRINT
LPRINT "Ethane";q(1)
LPRINT "Ethene";q(2)
LPRINT "Propane";q(3)
LPRINT "Propene";q(4)
LPRINT "Butene";q(5)
LPRINT "C5    ";q(6)
LPRINT "Oxygen";q(7)
LPRINT "Carbon Dioxide";q(8)
LPRINT "Methane";q(9)
LPRINT "Nitrogen";q(10)
LPRINT "Water";q(11)
LPRINT
LPRINT
q=q(1)+q(2)+q(3)+q(4)+q(5)+q(6)+q(7)+q(8)+q(9)+q(10)+q(11)
LPRINT "Fraction of lines analysed ";q
```